

VIBRATION ANALYSIS OF PCBS AND ELECTRONIC COMPONENTS

A THESIS SUBMITTED TO  
THE GRADUATE SCHOOL OF NATURAL AND APPLIED SCIENCES  
OF  
MIDDLE EAST TECHNICAL UNIVERSITY

BY

BANU AYTEKİN

IN PARTIAL FULFILLMENT OF THE REQUIREMENTS  
FOR  
THE DEGREE OF MASTER OF SCIENCE  
IN  
MECHANICAL ENGINEERING

APRIL 2008

Approval of the thesis:

**VIBRATION ANALYSIS OF PCBS AND ELECTRONIC COMPONENTS**

submitted by **BANU AYTEKİN** in partial fulfillment of requirements for the degree of **Master of Science in Mechanical Engineering Department, Middle East Technical University** by,

Prof. Dr. Canan Özgen  
Dean, Graduate School of **Natural and Applied Sciences**

\_\_\_\_\_

Prof. Dr. S. Kemal İder  
Head of Department, **Mechanical Engineering**

\_\_\_\_\_

Prof. Dr. H. Nevzat Özgüven  
Supervisor, **Mechanical Engineering Dept., METU**

\_\_\_\_\_

**Examining Committee Members**

Prof. Dr. Y. Samim Ünlüsoy  
Mechanical Engineering Dept., METU

\_\_\_\_\_

Prof. Dr. H. Nevzat Özgüven  
Mechanical Engineering Dept., METU

\_\_\_\_\_

Prof. Dr. Mehmet Çalışkan  
Mechanical Engineering Dept., METU

\_\_\_\_\_

Asst. Prof. Dr. Yiğit Yazıcıoğlu  
Mechanical Engineering Dept., METU

\_\_\_\_\_

Dr. Mutlu D. Cömert  
TÜBİTAK-SAGE

\_\_\_\_\_

**Date:**

\_\_\_\_\_

**I hereby declare that all information in this document has been obtained and presented in accordance with academic rules and ethical conduct. I also declare that, as required by these rules and conduct, I have fully cited and referenced all material and results that are not original to this work.**

Name, Last name : Banu Aytekin

Signature :

## **ABSTRACT**

### **VIBRATION ANALYSIS OF PCBS AND ELECTRONIC COMPONENTS**

Aytekin, Banu

M.S., Department of Mechanical Engineering

Supervisor: Prof. Dr. H. Nevzat Özgüven

April 2008, 118 Pages

In this thesis, vibration analyses of electronic assemblies that consist of an electronic box, printed circuit board and electronic components are presented. A detailed vibration analysis of a real electronic assembly is performed by finite element methods and vibration tests. Effects of component addition and component modeling are investigated by finite element analysis in detail. Results are compared in order to identify the most efficient, reliable and suitable method depending on the type of problem. Experimental results for the vibration of an electronic box, PCB and components are presented and discussed. Furthermore, an analytical model that represents a printed circuit board and electronic component is suggested for fixed and simply supported boundary conditions of the PCB. Different types of electronic components are modeled analytically to observe different dynamic characteristics. The validity of the analytical model is computationally checked by comparing results with those of finite element solution.

Keywords: Electronic Assembly, Printed Circuit Board, Electronic System Vibration

## ÖZ

### ELEKTRONİK KARTLARIN VE PARÇALARIN TİTREŞİM ANALİZİ

Aytekin, Banu

Yüksek Lisans, Makina Mühendisliği Bölümü

Tez Yöneticisi : Prof. Dr. H. Nevzat ÖZGÜVEN

Nisan 2008, 118 Sayfa

Bu çalışmada; kart kutusu, elektronik kart ve elektronik parçaların oluşturduğu bir elektronik bütünün titreşim analizleri gerçekleştirilmiştir. Gerçek bir sistemde kullanılan elektronik bütünün sonlu eleman yöntemi ve titreşim testleri ile yapılan ayrıntılı titreşim analizleri sunulmuştur. Kart üzerine elektronik parça eklenmesinin ve bu parçaların modellenmesinin titreşim karakteristiğine etkileri sonlu elemanlar analizleri ile detaylı şekilde incelenmiştir. Elde edilen sonuçlar en etkin, güvenilir ve uygun çözüm yöntemini problem tiplerine göre belirleyebilmek amacıyla kıyaslanmıştır. Kart kutusu, elektronik kart ve elektronik parçalar için gerçekleştirilen titreşim testleri sunulmuş ve sonuçlar değerlendirilmiştir. Bu çalışmaların sonrasında, belirli sınır koşullarına sahip elektronik kartı ve üzerine yerleştirilmiş elektronik parçayı temsil eden analitik bir yöntem sunulmuştur. Değişik özelliklerdeki elektronik parçalar modellenerek dinamik davranışları elde edilmiştir. Analitik modelin geçerliliği, sonlu eleman çözümlerinin sonuçları kullanılarak doğrulanmıştır.

Anahtar Kelimeler: Elektronik Bütünlere, Elektronik Kartlar, Elektronik Sistemlerin Titreşimi

To My Gorgeous Mother

## ACKNOWLEDGMENTS

The author wishes to express her deepest gratitude to her supervisor Prof. Dr. Nevzat H. Özgüven for his excellent supervision, guidance, advice, criticism, encouragements and insight throughout the research.

The author would like to express her appreciation to Mümtaz Afşın Esi for his guidance and unlimited help during the research.

The author would like to thank to her colleagues in TUBITAK-SAGE, especially to Mehmet Sinan Hasanoğlu and Ethem Bozkurt for their support.

The author would also like to express her gratefulness to her friends Çiğdem, Filiz, Nevra, Özge, Serdar and İlke for their support throughout the research.

The author would like to express her gratitude to Tolga Tekşen for his faith in me, patience, consideration and great support during the research.

The author would like to thank her family, especially her mother Naciye Aytekin for her support and patience throughout the research.

The facilities and support provided by TÜBİTAK-SAGE are kindly appreciated.

Domestic Master of Science Scholarship provided for the author by the Scientific and Technological Research Council of Turkey (TUBİTAK) is gratefully acknowledged.

## TABLE OF CONTENTS

|   |      |
|---|------|
| ABSTRACT .....  | iv   |
| ÖZ .....  | v    |
| ACKNOWLEDGMENTS .....   | vii  |
| TABLE OF CONTENTS .....   | viii |
| LIST OF TABLES .....  | xi   |
| LIST OF FIGURES .....   | xiii |
| LIST OF SYMBOLS AND ABBREVIATIONS .....   | xvi  |
| CHAPTERS  |      |
| 1. INTRODUCTION .....   | 1    |
| 1.1 Printed Circuit Board .....   | 1    |
| 1.1.1 PCB Usage in Industry .....   | 1    |
| 1.1.2 Printed Circuit Board Materials .....   | 2    |
| 1.1.3 Printed Circuit Board Assembly Elements .....                                 | 4    |
| 1.1.4 Mounting of Printed Circuit Boards .....                                      | 4    |
| 1.2 Electronic Component Mounting .....   | 8    |
| 1.3 Failure Modes of Electronic Devices .....                                       | 9    |
| 1.4 Vibration of Electronic Assemblies .....  | 10   |
| 1.4.1 Failure of Electronic Assemblies due to Vibration .....                       | 10   |
| 1.5 Objective of the Study .....  | 12   |
| 1.6 Scope of Thesis .....   | 13   |
| 2. LITERATURE REVIEW .....  | 15   |
| 3. FINITE ELEMENT VIBRATION ANALYSES OF ELECTRONIC BOX<br>AND PCB .....             | 23   |
| 3.1 Finite Element Vibration Analysis of Electronic Box .....                       | 24   |
| 3.1.1 Finite Element Vibration Analysis of Base of Electronic Box ...               | 26   |
| 3.1.2 Finite Element Vibration Analysis of Electronic Box with Front<br>Cover ..... | 27   |

|         |   |    |
|---------|---|----|
| 3.1.3   | Finite Element Vibration Analysis of Electronic Box with Front and Top Covers ..... | 29 |
| 3.2     | Finite Element Vibration Analysis of Printed Circuit Board.....                     | 33 |
| 3.2.1   | Analysis of the Connector Mounted Edges .....                                       | 35 |
| 3.2.2   | Printed Circuit Board with Components Added .....                                   | 43 |
| 3.2.3   | Analysis of PCB Mounted in Electronic Box .....                                     | 48 |
| 3.3     | Finite Element Vibration Analysis of Electronic Assembly.....                       | 50 |
| 4.      | EXPERIMENTAL ANALYSIS.....  | 55 |
| 4.1     | Experimental Setup.....   | 55 |
| 4.2     | Experiment 1 .....  | 61 |
| 4.3     | Experiment 2.....   | 62 |
| 4.4     | Experiment 3 .....  | 63 |
| 4.5     | Experiment 4.....   | 65 |
| 4.6     | Experiment 5.....   | 66 |
| 4.7     | Experiment 6.....   | 68 |
| 4.8     | Comparison of Finite Element and Experimental Results.....                          | 70 |
| 5.      | ANALYTICAL MODEL .....  | 75 |
| 5.1     | Electronic Box Vibration as a Rigid Body .....                                      | 75 |
| 5.2     | Printed Circuit Board Vibration.....  | 76 |
| 5.2.1   | The Natural Frequency of a Plate .....  | 76 |
| 5.2.2   | Sandwich Plates .....   | 77 |
| 5.2.3   | PCB Geometry and Material Properties.....   | 78 |
| 5.2.4   | Discrete Modeling of PCB.....   | 81 |
| 5.2.4.1 | PCB with Fixed Edges .....  | 81 |
| 5.2.4.2 | PCB with Simply Supported Edges .....   | 83 |
| 5.3     | Discrete Modeling of Electronic Component .....                                     | 88 |
| 5.3.1   | Case Study I-An Oscillator .....  | 89 |
| 5.3.2   | Case Study II-An Integrated Circuit .....   | 94 |
| 5.4     | Random Vibration Analysis of the Analytical Model .....                             | 98 |
| 5.4.1   | Transmission of Random Vibration.....   | 99 |

|   |     |
|---|-----|
| 5.5 Validation of the Model .....         | 103 |
| 6. SUMMARY AND CONCLUSIONS .....          | 108 |
| 6.1 Finite Element Modeling .....         | 108 |
| 6.2 Experimental Study .....              | 109 |
| 6.3 Analytical Model .....                | 110 |
| 6.4 Design Guidelines .....               | 112 |
| 6.5 Suggestions for Future Research ..... | 113 |
| REFERENCES .....                          | 114 |

## LIST OF TABLES

|  |    |
|--|----|
| Table 1. PCB laminate materials and common applications [4].....   | 3  |
| Table 2. Electronic box dimensions.....  | 25 |
| Table 3. First two natural frequencies of the base.....  | 26 |
| Table 4. First two natural frequencies of the box with front cover.....  | 28 |
| Table 5. Natural frequencies of the box with its covers.....   | 30 |
| Table 6. PCB dimensions.....   | 34 |
| Table 7. PCB dimensions-without connectors.....  | 39 |
| Table 8. Natural frequencies of the actual and assumed models.....   | 40 |
| Table 9. First mode comparison with real and assumed configurations.....   | 41 |
| Table 10. Second mode comparison with real and assumed configurations.....   | 42 |
| Table 11. Component masses.....  | 45 |
| Table 12. Natural frequencies and mode shapes of component added PCB.....  | 46 |
| Table 13. Natural frequencies of the PCB and box assembly.....   | 49 |
| Table 14. First natural frequencies of PCB configurations.....   | 51 |
| Table 15. Natural frequencies and mode shapes of electronic assembly with different component modeling approaches..... | 52 |
| Table 16. Transmissibility of the fixture at natural frequencies.....  | 58 |
| Table 17. Summary of sine sweep testing conditions.....  | 58 |
| Table 18. Summary of sine sweep testing configurations.....  | 59 |
| Table 19. Transmissibility of the top cover at natural frequencies - Experiment 4...                                   | 66 |
| Table 20. Transmissibility of the largest component -Experiment 5.....   | 67 |
| Table 21. Transmissibility of component and PCB at natural frequencies-Experiment 6.....                               | 70 |
| Table 22. Natural frequencies and mode shapes of the test item with different component modeling approaches.....       | 72 |
| Table 23. PCB dimensions.....  | 80 |
| Table 24. Material properties of PCB laminas.....  | 80 |

|  |     |
|--|-----|
| Table 25. First natural frequency and vibration parameter of PCB with fixed edges  | 83  |
| Table 26. The equivalent stiffness, equivalent mass and first natural frequency of PCB with simply supported edges ..... | 87  |
| Table 27. Analytical and finite element solution comparison of PCB natural frequencies .....                             | 88  |
| Table 28. Oscillator properties .....  | 90  |
| Table 29. Oscillator properties .....  | 90  |
| Table 30. Natural frequency values for integrated circuit.....   | 92  |
| Table 31. Natural frequency values for oscillator and PCB system .....   | 93  |
| Table 32. First natural frequency values for integrated circuit and PCB system obtained by lumped mass model.....        | 93  |
| Table 33. Lead wire properties.....  | 95  |
| Table 34. Spring constant for IC's lead wire .....   | 96  |
| Table 35. Natural frequency values for integrated circuit.....   | 97  |
| Table 36. Natural frequency result of analytical model.....  | 102 |
| Table 37. Natural frequency comparison between analytical and finite element solution.....                               | 106 |
| Table 38. Acceleration PSD comparison between analytical and finite element solution.....                                | 106 |

## LIST OF FIGURES

|   |    |
|---|----|
| Figure 1. An example of a a) PCB [2] b) PCB assembly [3].....   | 1  |
| Figure 2. An example of an electronic box-1 [5].....  | 5  |
| Figure 3. An example of an electronic box-2 [6].....  | 5  |
| Figure 4. Card-lok retainer [7] .....   | 5  |
| Figure 5. PCB mounting elements [8] .....   | 6  |
| Figure 6. PCB mounting elements [9] .....   | 6  |
| Figure 7. PCB mounting elements [10] .....  | 6  |
| Figure 8. PCB mounting elements [11] .....  | 7  |
| Figure 9. An example of a backplane [12].....   | 7  |
| Figure 10. Through-hole mounting.....   | 8  |
| Figure 11. Types of surface mounting .....  | 8  |
| Figure 12. Failure mode distribution [13].....  | 9  |
| Figure 13. Ruptured lead wires due to fatigue [15] .....  | 11 |
| Figure 14. Solder joint fatigue failure [16] .....  | 11 |
| Figure 15. Solder joint crack initiation [16].....  | 12 |
| Figure 16. Dynamic model of vibration - isolated electronic box containing PCB [20].....                | 17 |
| Figure 17. Model of CCGA on PCB [38] .....  | 21 |
| Figure 18. Electronic box components and assembly.....  | 24 |
| Figure 19. First mode shape of the base of the electronic box.....                                      | 27 |
| Figure 20. First mode shape of the base with front cover.....   | 28 |
| Figure 21. a) Second mode shape of the base with front cover b) Same mode with front cover hidden ..... | 29 |
| Figure 22. a) First mode shape b) Second mode shape of the base with front and top covers .....         | 31 |
| Figure 23. a) Third mode shape b) Fourth mode shape of the base with front and top covers .....         | 31 |
| Figure 24. Fifth mode shape of the base with front and top covers.....                                  | 32 |

|   |    |
|---|----|
| Figure 25. PCB connection points-top view .....   | 32 |
| Figure 26. PCB geometry.....  | 33 |
| Figure 27. PCB layers .....   | 34 |
| Figure 28. Connector.....   | 35 |
| Figure 29. PCB Connection Points .....  | 36 |
| Figure 30. Displacement of PCB through path-1.....  | 37 |
| Figure 31. Displacement of PCB through path-2.....  | 37 |
| Figure 32. Displacement of PCB through path-3.....  | 38 |
| Figure 33. Assumed configurations of PCB without connectors.....  | 39 |
| Figure 34. Schematic view of components on the PCB.....   | 45 |
| Figure 35. Second mode shape of the lumped model at 1905 Hz.....  | 47 |
| Figure 36. Fourth mode shape of the assembly-contour plot in z direction (front and top cover hidden).....                  | 50 |
| Figure 37. a) Second (1631 Hz) and b) third (1748 Hz) mode shapes of the PCB with lumped components (top cover hidden)..... | 53 |
| Figure 38. Shakers and slip table [41].....   | 56 |
| Figure 39. LMS <sup>®</sup> SCADAS III data acquisition hardware [41] .....   | 56 |
| Figure 40. Transmissibility of the fixture .....  | 57 |
| Figure 41. Transmissibility of the base of the box (Experiment 1) .....   | 61 |
| Figure 42. Transmissibility of the box (Experiment 2).....  | 63 |
| Figure 43. Transmissibility of base of the box (Experiment 3) .....   | 64 |
| Figure 44. Transmissibility of the top cover (Experiment 4).....  | 65 |
| Figure 45. Transmissibility of the largest component (Experiment 5) .....   | 67 |
| Figure 46. Transmissibility of the PCB and the largest component (Experiment 6) .   | 69 |
| Figure 47. a) Second (1621 Hz) and b) third (1732 Hz) mode shapes of the PCB with lumped components in electronic box.....  | 73 |
| Figure 48. Sandwich plate [42].....   | 77 |
| Figure 49. PCB layers .....   | 79 |
| Figure 50. PCB geometry.....  | 79 |
| Figure 51. Point Load on the PCB with Fixed Edges .....   | 82 |

|  |     |
|--|-----|
| Figure 52. Point Load on the PCB with Simply Supported Edges .....   | 84  |
| Figure 53. Oscillator front view .....   | 89  |
| Figure 54. Three dof model of oscillator .....   | 91  |
| Figure 55. Discrete model of PCB and oscillator .....  | 92  |
| Figure 56. Integrated Circuit Top View [28] .....  | 94  |
| Figure 57. Lead wire geometry of the integrated circuit [44] .....   | 95  |
| Figure 58. Three dof model of integrated circuit .....   | 96  |
| Figure 59. Side view of lead wire deflection for large components .....  | 98  |
| Figure 60. Random vibration input .....  | 99  |
| Figure 61. PCB and component 2 dof model .....   | 100 |
| Figure 62. Random vibration response of oscillator bonded over fixed PCB .....   | 102 |
| Figure 63. Random vibration response of oscillator bonded over simply supported PCB .....                                | 103 |
| Figure 64. Finite element model of oscillator bonded over PCB .....  | 104 |
| Figure 65. Oscillator response comparison of analytical model and finite element solution for fixed PCB .....            | 104 |
| Figure 66. Oscillator response comparison of analytical model and finite element solution for simply supported PCB ..... | 105 |

## LIST OF SYMBOLS AND ABBREVIATIONS

|             |   |
|-------------|---|
| c           | : Damping constant                                  |
| CEM-1       | : Composite Epoxy Material 1                        |
| CEM-3       | : Composite Epoxy Material 3                        |
| [C]         | : Damping matrix                                    |
| CCGA        | : Ceramic Column Grid Array                         |
| dof         | : Degree of freedom                                 |
| D           | : Flexural Rigidity                                 |
| E           | : Young's Modulus                                   |
| f           | : Frequency in Hz                                   |
| F           | : Fixed end   |
| FR-2        | : Flame Resistant 2                                 |
| FR-3        | : Flame Resistant 3                                 |
| FR-4        | : Flame Retardant 4                                 |
| g           | : grams   |
| GI          | : Glass filled polyimide                            |
| GT          | : Glass filled Teflon                               |
| $H(\omega)$ | : Frequency response function                       |
| I           | : Area moment of inertia                            |
| IPC         | : Interconnecting and Packaging Electronic Circuits |
| k           | : Spring constant                                   |
| [K]         | : Stiffness matrix                                  |

|             |                                  |
|-------------|----------------------------------|
| $m$         | : Mass                           |
| $[M]$       | : Mass matrix                    |
| PCB         | : Printed Circuit Board          |
| PSD         | : Power Spectral Density         |
| PWB         | : Printed Wiring Board           |
| SS          | : Simply supported edge          |
| $S(\omega)$ | : Spectral density               |
| $T$         | : Kinetic energy                 |
| $w$         | : Deflection of a plate          |
| $\nu$       | : Poisson's ratio                |
| $\gamma$    | : Mass per unit area             |
| $\mu$       | : Density                        |
| $\omega$    | : Frequency in radian per second |
| $\delta$    | : Deflection of a beam           |
| $\epsilon$  | : Strain                         |
| $\sigma$    | : Stress                         |

# CHAPTER 1

## INTRODUCTION

### 1.1 Printed Circuit Board

Printed circuit board (PCB), which is also referred as printed wiring board (PWB), is used primarily to create a connection between components, such as resistors, integrated circuits, and connectors [1]. It becomes an electrical circuit when components are attached and soldered to it, which then is called printed circuit board assembly (Figure 1).



a)



b)

Figure 1. An example of a a) PCB [2] b) PCB assembly [3]

#### 1.1.1 PCB Usage in Industry

Serious use of printed circuit assemblies began shortly before the end of World War II. One of the first applications for these assemblies was in a radio set. Another type

of circuit board was designed for use in proximity fuzes. By the end of the war, these were being produced successfully in very large quantities [4].

In today's world, all high technology devices contain printed circuit boards. Their sizes, shapes, properties and endurances vary depending on where they are utilized. Standards developed by the Institute for Interconnecting and Packaging Electronic Circuits (IPC) identify the following three classes of electronic products in which printed circuit board assemblies are used [4]:

- Class 1: General products, including consumer items, computers and peripherals, and some military systems.
- Class 2: Dedicated service products, including communication equipment, business machinery, industrial controls, instruments, and military systems, where extended life and reliable service is needed.
- Class 3: High-reliability products, including equipment and systems where continuous performance or performance on demand is essential.

### **1.1.2 Printed Circuit Board Materials**

A printed circuit board is a composite structure. Many types of copper-clad materials are available, but the ones used most commonly for PCBs are FR-4, FR-2, FR-3, CEM-1, CEM-3, GI and GT. Table 1 contains basic features of various laminate materials [4]:

Table 1. PCB laminate materials and common applications [4]

| Type  | Construction   | Applications   |
|-------|--|--|
| FR-4  | Multiple layers of woven glass cloth impregnated with epoxy resin; fire retardant              | Widely used in computers, industrial controls, telecommunications and military/space systems |
| FR-3  | Multiple layers of paper impregnated with flame-retardant epoxy resin                          | Found in consumer products such as computers, TVs, and audio equipment                       |
| FR-2  | Multiple layers of paper impregnated with flame-retardant phenolic resin                       | Mainly used in consumer electronics such as games, radios and calculators                    |
| CEM-1 | Glass cloth impregnated with epoxy on outer surfaces of paper core impregnated with epoxy      | Used extensively in industrial electronics, smoke detectors and for automotive devices       |
| CEM-3 | Glass cloth impregnated with epoxy on outer surfaces of fiberglass core impregnated with epoxy | Used in appliances, automobiles and commercial communication equipment                       |
| GI    | Multiple layers of woven glass cloth impregnated with polyimide resin                          | Used in products exposed to high-temperature environments                                    |
| GT    | Glass fabric base with Teflon resin  | Applied where low dielectric constant is needed for high-frequency circuits.                 |

### **1.1.3 Printed Circuit Board Assembly Elements**

Printed circuit board assemblies are commonly composed of a similar set of basic elements. These are [4]

- Electronic components that perform the intended circuit functions
- A printed circuit board that supports components and provides interconnections between them
- One or more connectors that are used as an electrical interface between the printed circuit board assembly and the rest of the system
- Mechanical parts for mounting parts and hardware to the board, attaching PCB to the system, providing thermal paths and supporting and stiffening the assembly

### **1.1.4 Mounting of Printed Circuit Boards**

PCBs are very sensitive to environmental conditions. Depending on the device type in which a PCB is utilized, different requirements come into existence such as mechanical integrity of a system, durability against thermal loading and prevention of electromagnetic interference (EMI). In order to meet such requirements PCBs are mounted onto frames or into box-like structures.

Electronic boxes are usually composed of one or more covers and a body where printed circuit boards are mounted. Examples of an electronic box are given in Figure 2-3.



Figure 2. An example of an electronic box-1 [5]



Figure 3. An example of an electronic box-2 [6]

PCBs are usually connected to an electronic box by screws or card-lok retainers. Screws occupy less space on a PCB compared to card-lok retainers. However, more rigid connections are often provided by card-lok retainers especially for larger PCBs. An example of a card-lok retainer is given in Figure 4.

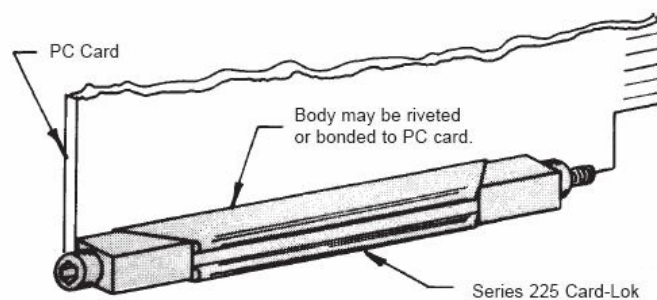


Figure 4. Card-lok retainer [7]

There are also many products to increase rigidity of a PCB mounted with screws. These additional mechanical parts are designed for absorbing mechanical loads applied to PCB connection points. Some examples of PCB mounting elements are given in Figures 5-8.

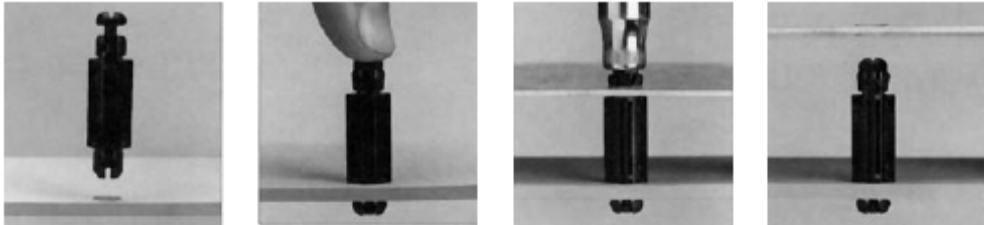


Figure 5. PCB mounting elements [8]



Figure 6. PCB mounting elements [9]



Figure 7. PCB mounting elements [10]



Figure 8. PCB mounting elements [11]

Another important issue about printed circuit boards is connectors. PCBs contain connectors at one or more edges for power and data transmission. Commonly, there are two ways of connector mounting, one of which is mounting a connector directly into the holes on a chassis and the other is using backplanes. A backplane is a printed circuit board with connectors that are used for plugging in other PCBs of a system (Figure 9).

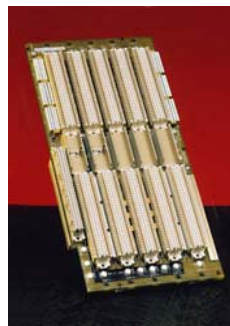


Figure 9. An example of a backplane [12]

To conclude, in electronic box design; type of connector mountings, covers and connections are important factors that identify the rigidity of an electronic box and a printed circuit board.

## 1.2 Electronic Component Mounting

Electronic component mounting can be classified in two groups; (i) through-hole mounting (Figure 10) and (ii) surface mount technology (Figure 11).

In through-hole mounting, holes on PCBs are used to connect components to PCBs. Lead wires are placed into these holes and soldered. In surface mount technology, electronic components are attached directly to the surface of a printed circuit board. Since lead wires are not placed in the holes, both surfaces of the PCB can be used for component mounting.

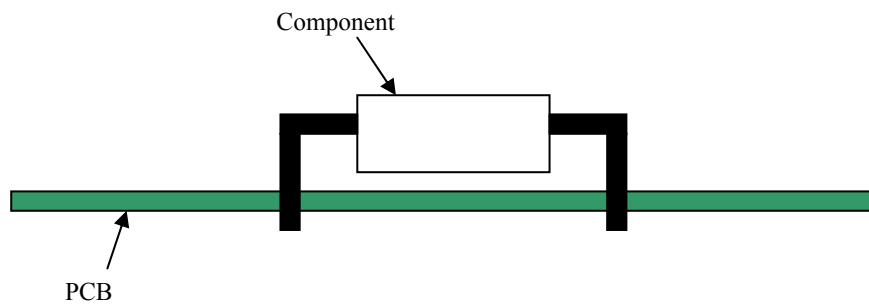


Figure 10. Through-hole mounting

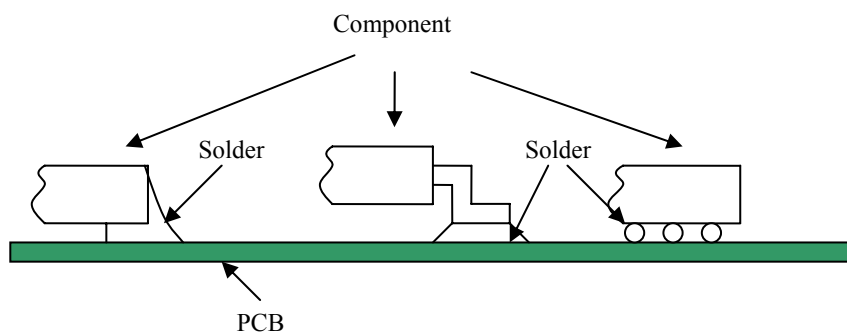


Figure 11. Types of surface mounting

### 1.3 Failure Modes of Electronic Devices

Electronic devices which are used in control, guidance and communication systems are one of the most important parts of modern avionic systems. Common aim in the aerospace industry is to design and produce systems which possess a usage life of at least 20 years with high reliability levels. The complex and fragile structure of electronic systems necessitates special study in order to meet the expectations of the aerospace industry.

Electronic systems are composed of many different materials and interfaces which make system very complex. In addition to complexity, systems are subjected to various environmental conditions during storage, handling, transportation and operation. Therefore, various failure modes such as mechanical, thermal and electrical are encountered in electronic systems.

A study on hardware failure rates of military aircraft electronic systems utilized in the US, shows that 40% of failures are found in electrical connectors, 30% are found in cables and harnesses, 20% are related to electronic components and 10% are due to other factors [13]. Another study based on environmental failure rates shows that thermal, vibrational, humid and dusty environments are the major reasons of environmental failures [13]. Distribution of these failures is shown in Figure 12.

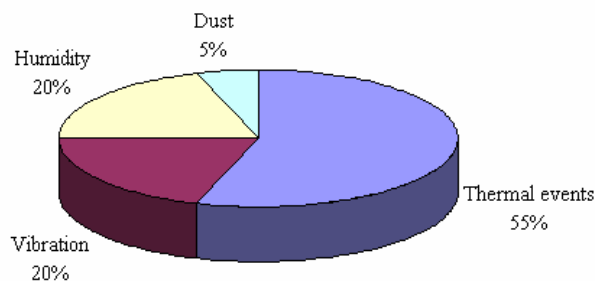


Figure 12. Failure mode distribution [13]

## **1.4 Vibration of Electronic Assemblies**

It is a well known fact that vibration is one of the most important loading conditions in electronic systems. The life cycle of avionic systems includes vibration loading at different life phases such as transportation, handling, captive carry flight and free flight. As mentioned in the previous section, electronic assemblies are formed by electronic components attached to the PCBs which are mounted into the electronic boxes. Therefore, vibration analysis of an electronic system is usually handled in three main levels: (i) electronic box, (ii) printed circuit board, and (iii) electronic components. One has to analyze dynamics of a complete system and interactions between each level in order to obtain a complete system model which then leads to the solution of vibration problem.

Dynamic analysis of electronic systems under vibration loading can be performed by three different approaches: (i) analytical methods, (ii) finite element analyses and (iii) experimental studies. However, common practice in industry is to employ finite element methods. This trend is due to the complexity of today's electronic assemblies. The sophisticated structure of systems makes analytical modeling difficult and sometimes even impossible. Therefore, engineers tend to prefer finite element analysis instead of dealing with complicated formulations. Definitely, conducting experiments is indispensable in order to validate computational results. They also lead to improvement of finite element techniques.

### **1.4.1 Failure of Electronic Assemblies due to Vibration**

Excessive deformations and accelerations of PCBs result in damage to mounted components, solder joints and electrical interfaces, as well as the circuit board itself.

Failure mechanisms due to vibration can be specified as follows [14]

- Lead wire fatigue failure (Figure 13)
- Connector contact fretting corrosion
- Structural fatigue failure
- Solder joint fatigue failure (Figure 14)
- Excessive deflection
- Loose hardware

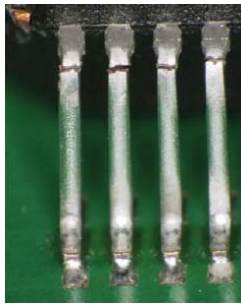


Figure 13. Ruptured lead wires due to fatigue [15]

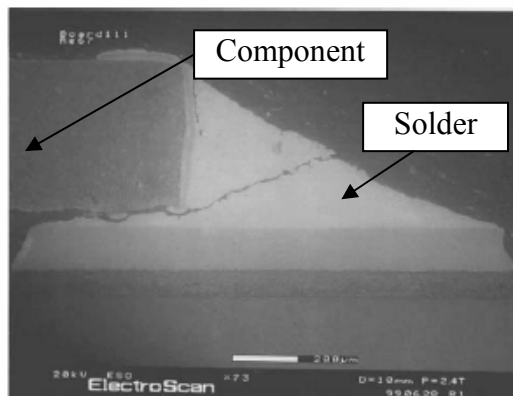


Figure 14. Solder joint fatigue failure [16]

Soldering is inevitable during mounting processes of electronic components over printed circuit boards. High solder reliability is required since failures of solder joints and lead wires directly result in failure of systems.

Main failure mode of solder joints under vibration loading is fatigue failure. High cycle fatigue causes crack growth in solder joints (Figure 15) and excessive stresses in lead wires.

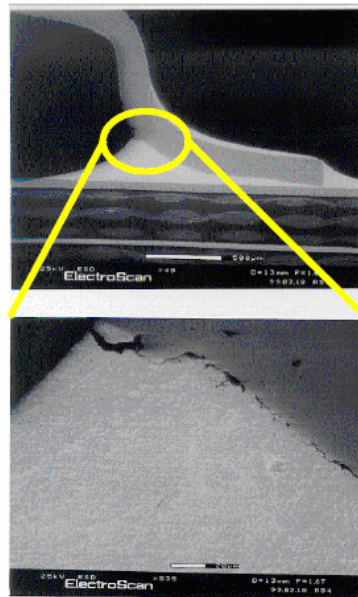


Figure 15. Solder joint crack initiation [16]

## 1.5 Objective of the Study

In this thesis, firstly it is aimed to understand the dynamic behavior of an electronic assembly and individual parts of this assembly under vibratory loading. It is also intended to apply aforementioned solution methods in order to identify efficiency of these approaches for possible problem types since vibration is a case dependent phenomenon for electronic structures. The motivation of this work is to provide a

useful guidance to present the most suitable method to be utilized in vibration analysis.

One of the major objectives of the study is to develop an analytical model for common printed circuit board configurations and electronic components in order to predict dynamics of the assembly and effects of component placement under vibration loading. The reason for analytical modeling is to develop simple and reliable approaches to perform vibration analysis of electronic assemblies during preliminary design process, vibration isolation design and life calculations.

## **1.6 Scope of Thesis**

The outline of the thesis is as follows:

In Chapter 2, previous studies on vibration of electronic assemblies are reviewed. Analysis of problems related to vibration in electronic assemblies varies depending on the purpose of the study. Therefore one can find various studies on the subject such as printed circuit board vibration, solder joint fatigue due to vibration and vibration isolation of electronic assemblies. These studies are presented briefly in Chapter 2.

In Chapter 3, finite element analysis of the selected electronic box and the printed circuit board is presented in details. The electronic box is examined by considering effect of connector holes on the box and covers attached to the box. Also effect of printed circuit board placement inside the box is investigated in detail. Boundary conditions of the printed circuit board are also analyzed. In addition to these studies, the printed circuit board is modeled with and without components. Effect of component addition onto a PCB is investigated in terms of mass addition, component type, lead wire properties and location of addition.

In Chapter 4, the vibration tests of the electronic box are presented as a case study. Sinusoidal sweep tests are performed and natural frequency results are compared to finite element solutions.

The analytical model representing a printed circuit board and an electronic component is presented in Chapter 5. The analytical model is constructed for rectangular printed circuit boards which are simply supported or fixed at all edges. Calculation of equivalent vibration parameters are explained in detail. Two degree of freedom model is introduced. Modal analysis and random vibration analysis results are presented. In order to validate the analytical model, constructed finite element model is utilized and analyses results are compared.

In Chapter 6, brief summary of the work done is given with conclusions and discussions. Finally, suggestions for further studies are made.

## CHAPTER 2

### LITERATURE REVIEW

There are several studies related to different vibration problems occurring in electronic systems. These researches have different objectives such as understanding the vibration phenomenon in electronic systems, vibration isolation, life prediction of solder joints and reliability calculations. Review of these studies is presented in this section.

Steinberg [17] presented analytical methods for analyzing vibration in electronic assemblies. He concluded that failures in electronic equipment mostly depend on mechanical loading and these mechanical failures are mainly observed in component lead wires and solder joints [17]. He introduced an empirical formula to estimate transmissibility (Q) of chassis and PCB which is given as [17]

$$Q = c\sqrt{f_n} \quad (2.1)$$

where c is a constant which has values between 0.5-2 depending on excitation amplitude and natural frequency, and  $f_n$  is the first natural frequency (Hz) of the relevant structure. Another transmissibility (Q) equation Steinberg formulated is as follows [13]:

$$Q = A \left( \frac{f_n}{G_{in}^{0.6}} \right)^{0.76} \quad (2.2)$$

where A is a constant which is equal to 1 for beam types of structure with end restraints, 0.5 for plate and PCB structures with various parameter restraints, 0.25 for enclosures or boxes with lengths two or more times greater than the height and with

various end restraints,  $f_n$  is the natural frequency in Hz, and  $G_{in}$  is the acceleration input. Another empirical formula developed by Steinberg is used to estimate maximum PCB displacement ( $Z$ ) in order to have 10 million stress cycles under harmonic vibration loading which is given as [13,17]

$$Z = \frac{0.00022 \cdot B}{c \cdot h \cdot r \sqrt{L}} \quad (2.3)$$

where  $B$  is the length of PCB edge parallel to component (inch),  $L$  is the length of electronic component (inch),  $h$  is the height or thickness of PCB (inch),  $C$  is a constant for different types of components, and  $r$  is the relative position factor for components. Steinberg used these formulations after constructing a lumped mass model to simulate electronic equipment.

McKeown [18] studied vibration problems in electronic equipment by considering the whole system in three levels: component, module and chassis levels. He reviewed available vibration analysis methods for each level. He also stressed out importance of modal testing to avoid inherent assumptions and simplifications included in analytical techniques. He suggested some useful approaches in finite element modeling related to component, board and chassis. He recommended to model leads by using beam elements, and components by using solid elements. He mentioned that the components are usually modeled by smearing the component mass over the printed circuit board. He also noted that this assumption will fail if the component significantly influences stiffness, and when this is the case the component must be modeled separately. He pointed out possible reasons for finite element solution inconsistencies with test results, which are listed as (i) boundary conditions do not match the actual situation, (ii) material types improperly assigned, (iii) total mass of the model does not match total system mass, and (iv) frequency range of the analysis does not match the input environment.

Veprík [19] studied vibration isolation of electronic assemblies and described the vibration of such systems as follows:

*“In spite the fact that electronic box is a complex, sometimes non-linear, dynamic structure containing sensitive internal components, the design for vibration isolation normally relies on the traditional simplified linear model of flexurally suspended body.”*

Consequently, he used a 2 degree-of-freedom mass, spring and damper system for solving vibration isolation problems regarding electronic box [19,20] (Figure 16).

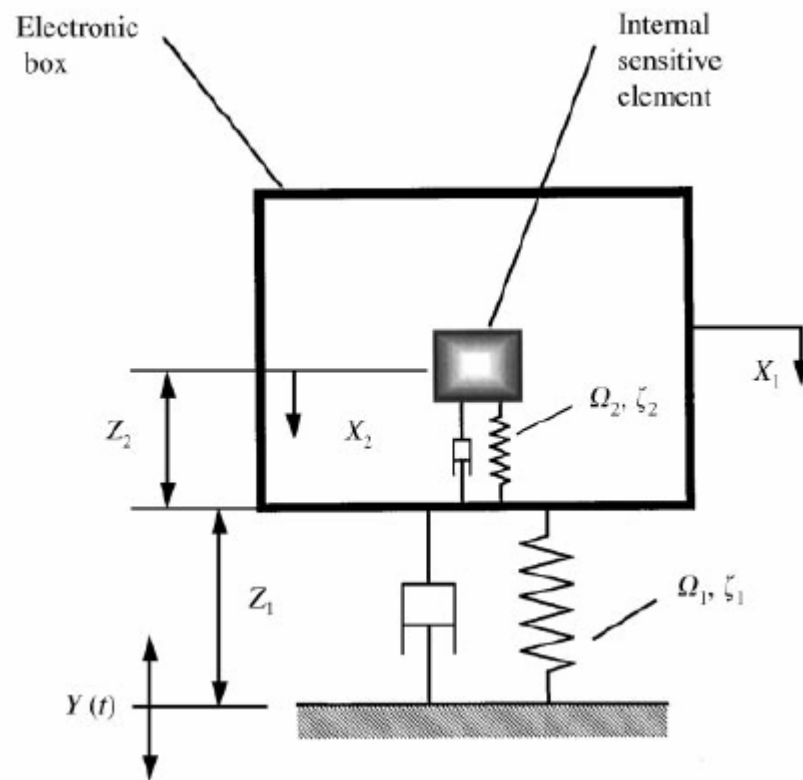


Figure 16. Dynamic model of vibration-isolated electronic box containing PCB [20]

Veprík and Babitsky [19,20] focused on the dynamic response of the printed circuit board in order to perform vibration isolation of electronic boxes. This approach provided an improvement in protection of the electronic box from harmonic and

random vibration compared to traditional approaches where isolation is based on compromising damping and stiffness properties of mounts.

Ho, Veprík and Babitsky [21] also studied ruggedizing of printed circuit board. They designed a miniature wideband dynamic absorber and showed that this absorber can suppress the dynamic response of the system theoretically and experimentally. In this study the printed circuit board was modeled as a multi degree of freedom system since higher modes were also important in this analysis.

Esser and Huston [22] who worked on active mass damping of printed circuit boards, assumed PCB as a lumped mass. In that model they did not consider the continuous vibration modes since they were only interested in the first mode of the PCB.

Jung et al. [23] performed structural vibration analysis of an electronic equipment and they obtained results by using analytical modeling, finite element modeling and testing. In their analytical model they treated PCB as a 1 dof structure. They solved the problem by using Steinberg's formulations for natural frequency and maximum desired displacement.

Zampino [24] studied finite element modeling of a rectangular electronic box containing a PCB. He predicted the response of this assembly to random vibration. He also investigated the possibility of a PCB and the box having a coupled mode, and examined modes shapes in order to see if there is a critical condition of PCB touching the box due to dynamic deflections.

Cifuentes and Kalbag [25] studied optimization of support locations of a PCB which influences the natural frequency values of PCB. They employed finite element modeling in their solutions. Cifuentes [26] also carried out studies to identify issues that affect the dynamic behavior of PCB. He came up with four issues which are (i) the validity of estimates based on the first mode of vibration, (ii) geometric nonlinearities, (iii) component location on the board, and (iv) mass and stiffness values.

Pitarresi [27] dealt with modeling issues of PCBs. He used different finite element modeling approaches and compared obtained results with experimental outcomes.

Aglietti and Schwingshackl [28] emphasized the importance of structural dynamic analysis in electronic equipments. They considered three requirements (i) withstanding the required random vibration spectrum, (ii) avoiding coupling, (iii) withstanding launch loads at low frequencies. They performed analysis by finite element modeling and experiments.

Xie et al. [29] studied finite element modeling of a PCB and performed modal and random vibration analysis.

Suhir [30] studied component vibrations in the vibration analysis of electronic equipments. He derived a formula which gives the natural frequency of a heavy electronic component mounted to a circuit board with a plated through-hole.

Liguore and Followell [31] studied the fatigue in solder joints due to vibration. They investigated the effect of component location, component size and component type (leadless vs leaded). Results showed that smaller components mounted at regions whose vibration responses were higher, had longer fatigue lives compared to larger components mounted on a lower amplitude areas. Also, test results of three different sizes of components revealed that fatigue life is logarithmically inversely proportional to the diagonal length of the component. Another important observation is the higher durability of leaded components under vibration loading compared to leadless components.

Schaller [32] emphasized the wide capabilities of finite element modeling in analyzing dynamic behavior of microelectronic components. However he pointed out the difficulty in obtaining accurate material properties and boundary conditions related to the system. Therefore he remarked the value of laboratory testing. He modeled component lead wires as stiffness components or beam elements. He added the effects of components by increasing the board's modulus of elasticity and density

in those regions. He analyzed the wedge locks and connectors and modeled them as torsional springs and springs, respectively.

Chiang et al. [33] pointed out the importance of electronic box in electronic systems since the box filters environmental loads such as vibration and shock. Therefore, the simulation program they developed for reliability calculations of an electronic system differs from other commercial software by including electronic box effects.

He and Fulton [34] applied nonlinear laminate theory to a simply supported printed circuit board in order to obtain equation of motion for free and forced vibrations. They compared the linear and nonlinear results and concluded that under heavy loads with relatively large amplitude deflection, nonlinear analysis yields more reasonable results than the linear theory does. Therefore they suggested including nonlinear effect in dynamic analysis.

Veilleux [35] dealt with controlling the destructive resonant amplitude of printed circuit boards in electronic systems. He compared isolation, extensional damping and shear damping techniques for decreasing resonant amplitude value. He conducted his study by performing vibration tests and showed that shear damping techniques offer the best solution for vibration control.

Lau and Keely [36] investigated the lead dynamics with and without solder joints. They employed finite element analysis to obtain natural frequencies, and verified their results by vibration tests using a Laser Doppler Vibrometer. Results showed that the fundamental frequency of the soldered lead is at least five times higher than the unsoldered lead. This showed the importance of solder joint quality in fatigue life of a component.

Ham and Lee [37] also investigated the effect of vibration on lead wire fatigue life. By constructing a fatigue test set-up, they applied a constant frequency vibration load and measured the electrical resistance in the lead. Depending on these measurements, they obtained the component's fatigue life. Their study showed that thermal loading

is not the only reason for lead fatigue; vibration is also an important issue in an electronic system's fatigue life.

Perkins and Sitaraman [38] investigated the effect of an electronic component on the vibration characteristics of an electronic system. They performed vibration experiments, developed an analytical model to observe the effect of solder joint stiffness and mass of the component on the natural frequencies and mode shapes of the system (Figure 17).

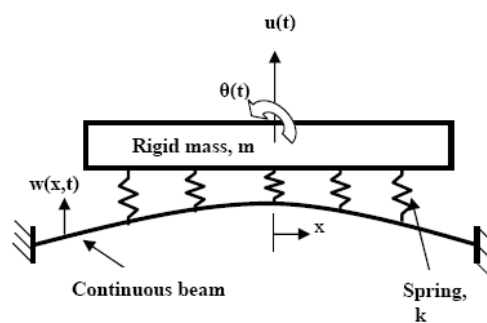


Figure 17. Model of CCGA on PCB [38]

They also predicted failure locations and behavior of the failed solder joints by finite element analysis. Their results showed that attaching component on the printed circuit board leads to a decrease in natural frequency due to added mass; however it provides a localized stiffness to the PCB. They also observed that solders close to the clamped boundaries experience the greatest bending and fail first.

Yang et al. [39] pointed out the importance of high-cycle fatigue induced by vibration. They also studied the effect of added components on the dynamic properties of the system. They developed finite element models and performed vibration tests. In finite element analyses they tried four different approaches for component and solder modeling: (i) component was modeled as a distributed mass on PCB, (ii) component was modeled as a concentrated mass on PCB, (iii)

component was modeled as a solid part and solder joints were modeled as springs, and (iv) component was modeled as a solid part and solder joints were modeled as beams. Results showed that component attachment increases the modal frequencies of the PCB but mode shapes remain constant. They concluded that, in finite element modeling, components should be modeled as solid parts and solders should be modeled as springs or beam elements.

Genç [40] studied vibration fatigue life of specific types of capacitors such as axial leaded tantalum and aluminum capacitors. CirVibe Software was utilized for finite element modeling. Modal and transmissibility tests were performed and outputs of these tests were used in fatigue analysis. Main consideration in this study was to estimate fatigue life therefore accelerated life tests were carried out. Tests results were fitted to Weibull distribution curves in order to estimate life. Another important study was the sensitivity analysis of important parameters which affected component life. In sensitivity analysis, the effects of printed circuit board geometry, Young's modulus, S-N curve, component orientation, lead wire geometry and component geometry were investigated by simulations.

## **CHAPTER 3**

### **FINITE ELEMENT VIBRATION ANALYSES OF ELECTRONIC BOX AND PCB**

In this chapter, finite element models developed for vibration analysis of an electronic box, PCB and critical electronic components will be presented. In order to study system vibrations, a real electronic assembly is taken as a case study. This system is used in a research and development project which is conducted in TUBİTAK-SAGE. The system will be introduced in this section and then the results obtained will be given in detail. In finite element modeling ANSYS® is used.

In this study, firstly individual models were developed in order to understand dynamic behaviors of the electronic box, printed circuit board and electronic components. After inspecting individual models, combined models were developed. These models provide the analysis of the whole assembly. Additional analyses were performed in order to verify assumptions made for defining boundary conditions at the edges of the PCB where connectors are attached.

Finite element models are developed based on some basic assumptions. These are given as follows:

- The electronic component itself is assumed to be rigid.
- Lead wires of an electronic component are assumed to be a beam structure and modeled with beam elements.
- The printed circuit board is a composite structure and modeled with shell elements. Each layer of the printed circuit board is assumed to be isotropic.
- The electronic box is assumed to be mounted on a rigid base.

- Connectors are assumed as rigidly connected to the cover and to the electronic box.
- Solder stiffness effects are ignored.

### 3.1 Finite Element Vibration Analysis of Electronic Box

The geometry of the electronic box used in this study is shown in Figure 18. Electronic box is composed of three parts; base, front cover and top cover. Base of the box is attached to the main structure from four points with cap screws. Front and top covers are also attached to the base with four cap screws. There are four connection points inside the base which are used for printed circuit board connection. There are two holes for connectors; one of them is on the back side of the base and the other is on the front cover.

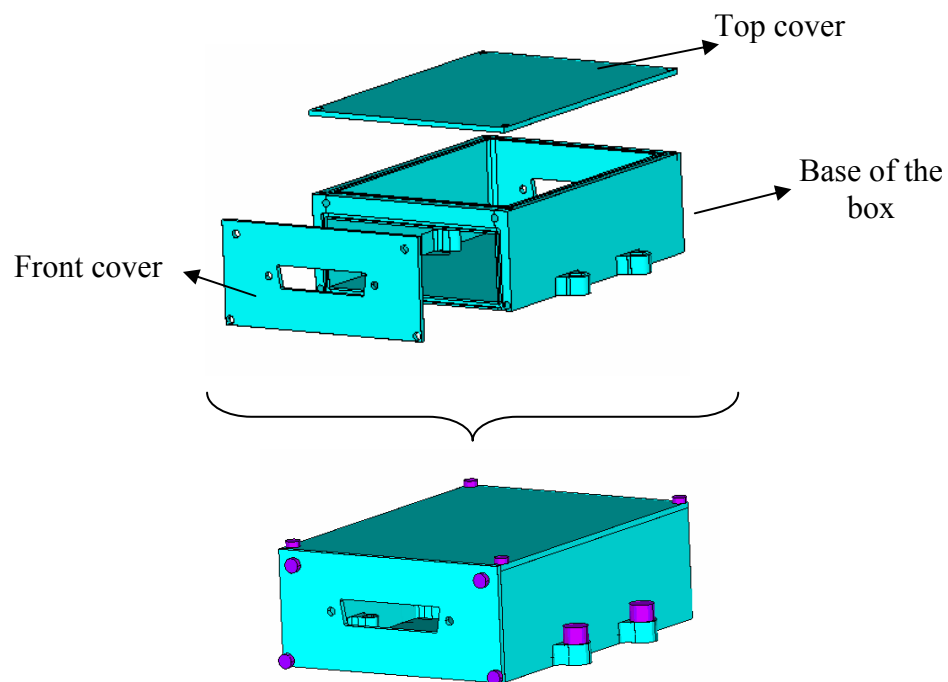


Figure 18. Electronic box components and assembly

The dimensions of the covers and base of the box are given in Table 2. The box is made of aluminum with mass density  $\rho = 2650 \text{ kg/m}^3$ , Young's Modulus  $E = 72 \text{ GPa}$  and Poisson's ratio  $\nu = 0.3$ . The material of cap screws is steel with mass density  $\rho = 7900 \text{ kg/m}^3$ , Young's Modulus  $E = 210 \text{ GPa}$  and Poisson's ratio  $\nu = 0.3$ .

Table 2. Electronic box dimensions

| <b>Base</b>        |               |                  |
|--------------------|---------------|------------------|
| <i>Width</i>       | <i>Height</i> | <i>Length</i>    |
| 87 mm              | 38 mm         | 119 mm           |
| <b>Front Cover</b> |               |                  |
| <i>Width</i>       | <i>Height</i> | <i>Thickness</i> |
| 87 mm              | 40 mm         | 2 mm             |
| <b>Top Cover</b>   |               |                  |
| <i>Width</i>       | <i>Length</i> | <i>Thickness</i> |
| 87 mm              | 119 mm        | 2 mm             |

Finite element analysis of the electronic box was made for three cases which are (i) base of the box, (ii) base with front covers and (iii) base with front and top covers. Natural frequencies and the mode shapes were obtained in ANSYS<sup>®</sup>. Solid element SOLID92 of ANSYS<sup>®</sup> was used for modeling the box components. Cap screws were also modeled with SOLID92 element of ANSYS<sup>®</sup>. The analyses are presented in the following sections.

### 3.1.1 Finite Element Vibration Analysis of Base of Electronic Box

Dynamic behavior of electronic box under vibration loading is important since excitation is transmitted to the printed circuit board by passing through electronic box. In this study, base of the box is fixed from four points through which external forces are transmitted.

Finite element vibration analysis of the base is performed to obtain natural frequencies and mode shapes in order to observe dynamics of the base under vibration loading. Two lowest natural frequencies of the box obtained by finite element model are tabulated in Table 3.

Table 3. First two natural frequencies of the base

| Mode | Frequency [Hz] |
|------|----------------|
| 1    | 2220           |
| 2    | 2304           |

Modal analysis results showed that in the frequency range of 20-2000 Hz, which is a commonly used range of interest for aerospace systems, there are no natural frequencies of the box. Although, even the lowest two modes of the base are not in the range of interest, dynamic behavior of the box itself will give an idea on how to analyze similar structures. Therefore mode shapes are examined and vibration characteristics are defined. Results demonstrate that the first natural frequency is dominated by the bottom part of the base, which is a plate like structure clamped through three edges (Figure 19). In higher modes, one can see the effect of side walls and bottom part which vibrate in a manner resembling plate vibrations.

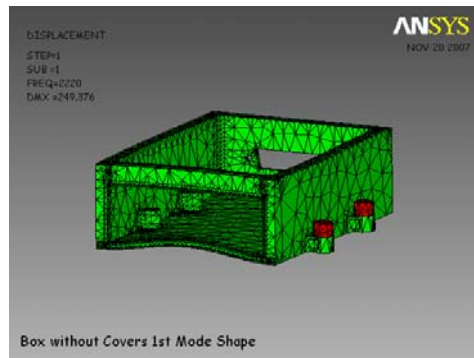


Figure 19. First mode shape of the base of the electronic box

Finite element solution exhibits that base of the electronic box does not show a rigid body behavior, and for that reason it will not be appropriate to model similar structures as a lumped mass.

### 3.1.2 Finite Element Vibration Analysis of Electronic Box with Front Cover

Covers are unavoidable components of electronic boxes. There should be at least one cover which is used for closing the open side of the box left for printed circuit board mounting. Covers usually contain holes where connectors are fixed. Structurally, covers resemble a plate with a hole and a common way to connect them to the base of the box is using screws. Therefore, they are usually more sensitive to vibration compared to the base of the box. This behavior is becoming more important if cover contains connectors, because in that case vibration of the cover will directly affect printed circuit board boundary condition.

In order to understand the effect of the cover on the system dynamics, finite element vibration analysis of the electronic box with its front cover is carried out. The front cover is connected to the base from four points with cap screws. This cover has a

hole for connector placement. This connector, which is connected to the cover with two cap screws, provides power and data transmission.

First two natural frequencies of the box obtained by finite element model are tabulated in Table 4.

Table 4. First two natural frequencies of the box with front cover

| Mode | Frequency [Hz] |
|------|----------------|
| 1    | 1405           |
| 2    | 2099           |

Mode shapes of the assembly composed of base and the front cover show that first natural frequency is dominated by the vibrations of the front cover (Figure 20). This result is expected because the cover is a plate like structure with a hole and fixed at four corners which makes it more flexible than the base.

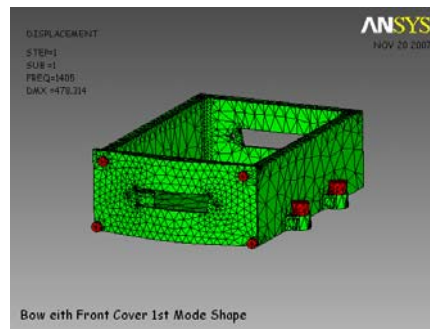


Figure 20. First mode shape of the base with front cover

Second mode of the assembly is dominated by both base and cover vibrations (Figure 21). In the previous analysis which is performed to find the vibration modes of the

base; a natural frequency of 2220 Hz was obtained. In this analysis 2099 Hz is found for the same mode. This is due to added mass which belongs to front cover.

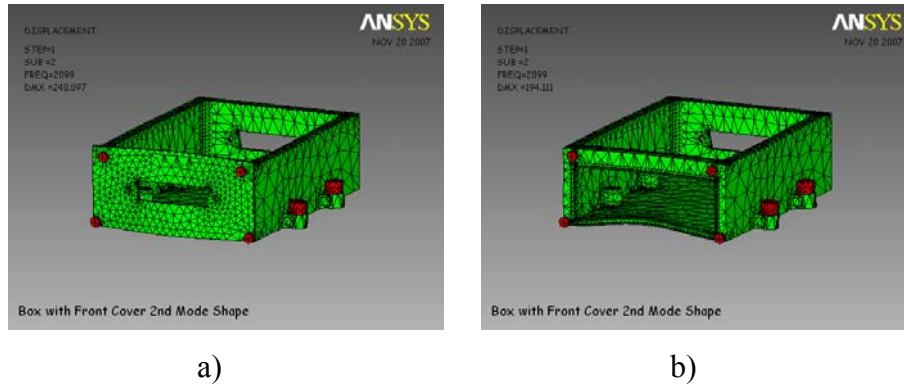


Figure 21. a) Second mode shape of the base with front cover b) Same mode with front cover hidden

This analysis revealed that there is one mode which is in the frequency range of interest. This mode is related with front cover vibration and it is very important since there is a connector attached to the front cover. Therefore special attention must be given to front cover vibrations during the vibration analyses of the assembly.

### 3.1.3 Finite Element Vibration Analysis of Electronic Box with Front and Top Covers

Finite element vibration analysis of the box with front and top covers is performed in ANSYS®. Natural frequencies and mode shapes are presented in this section. Top cover is attached to the base from corner points with four cap screws. It is expected to have the vibration modes of the cover in lower frequencies compared to those of

the base and front cover, since the top cover is a thin plate prone to transverse vibrations.

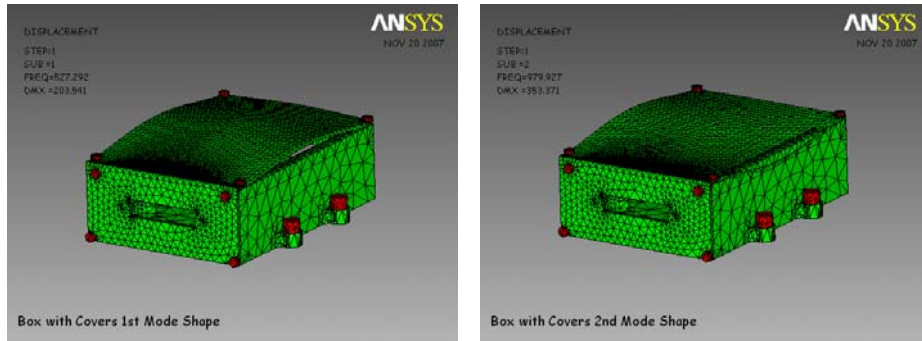
Natural frequencies of the box obtained by finite element model are tabulated in Table 5. Finite element vibration analysis results revealed that five of the modes are below 2000 Hz.

Further inspection on mode shapes show that all of these modes are related to the covers, and base of the box, and they are still not in the frequency range of 20-2000 Hz.

Table 5. Natural frequencies of the box with its covers

| Mode | Frequency [Hz] |
|------|----------------|
| 1    | 527            |
| 2    | 980            |
| 3    | 1217           |
| 4    | 1406           |
| 5    | 1437           |
| 6    | 2014           |

First three modes of the assembly are the plate vibration modes of the top cover. (Figure 22a-22b-23a).

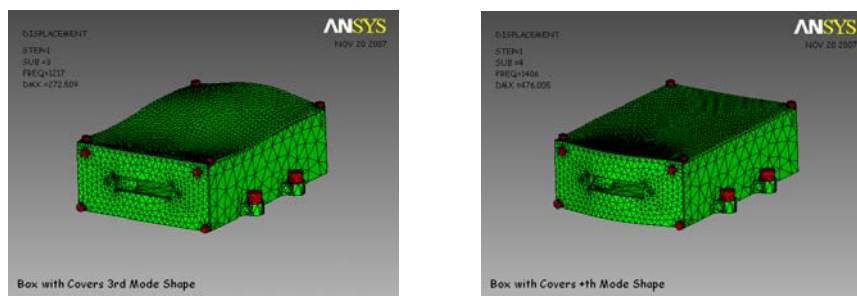


a)

b)

Figure 22. a) First mode shape b) Second mode shape of the base with front and top covers

In the fourth mode front cover vibrations dominate the system vibrations and the natural frequency is observed at 1406 Hz (Figure 23b). This mode is observed at 1405 Hz in the previous vibration analysis, which is performed for electronic box with front covers. It can be concluded from these results that addition of top cover has no effect on the dynamics of the front cover at this mode. This was anticipated since there is no physical connection between these two structures.



a)

b)

Figure 23. a) Third mode shape b) Fourth mode shape of the base with front and top covers

Fifth mode shape of the box, which is at the frequency of 1437 Hz, is dominated by top cover vibrations (Figure 24).

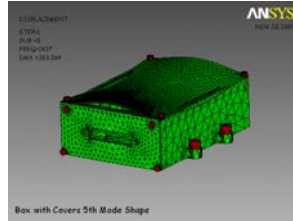


Figure 24. Fifth mode shape of the base with front and top covers

Cover vibration can change the dynamics of the base. Severity of cover vibration depends on cover mass, geometry, mounting type, excitation frequency and amplitude. If the base is affected from cover vibration modes significantly, then this may change the rigidity of PCB mounting locations on the base (Figure 25). As a result, rigid mounting of the PCB cannot be provided. Therefore, cover vibration modes are important and their effect on the base should be considered during design.

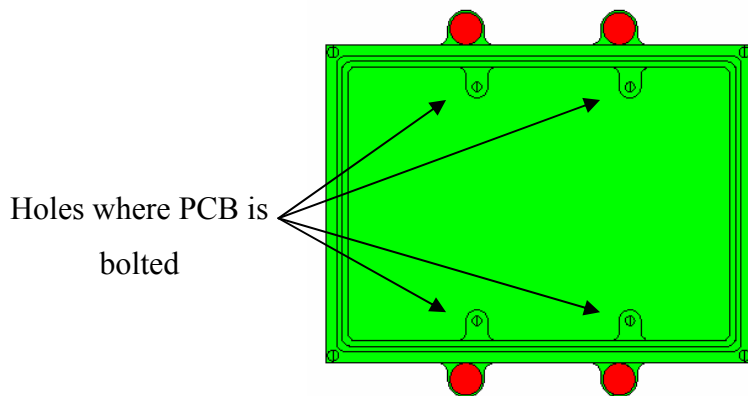


Figure 25. PCB connection points-top view

### 3.2 Finite Element Vibration Analysis of Printed Circuit Board

The geometry of the printed circuit board used in this study is shown in Figure 26. The PCB is mounted with four screws into the electronic box and it has two connectors at two opposite edges.

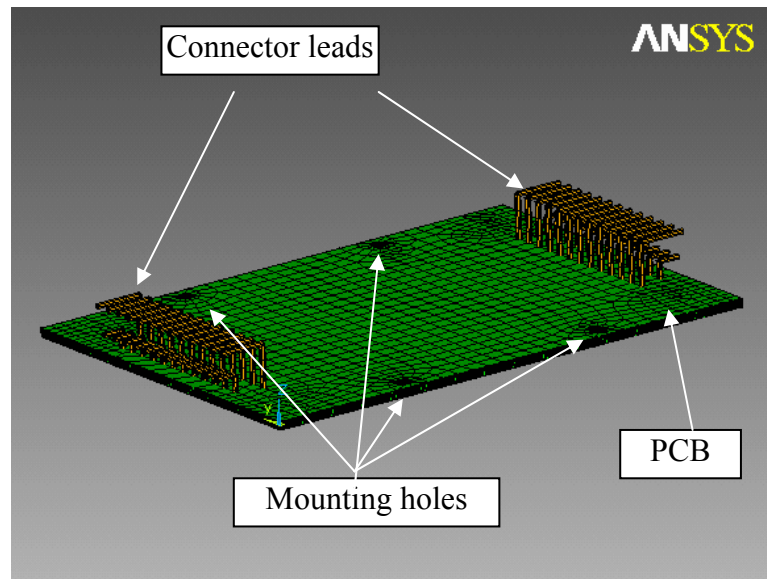


Figure 26. PCB geometry

The PCB is a 7 layered composite plate composed of copper with mass density  $\rho = 8900 \text{ kg/m}^3$ , Young's Modulus  $E = 107.9 \text{ GPa}$ , Poisson's ratio  $\nu = 0.3$  and FR-4 with mass density  $\rho = 1900 \text{ kg/m}^3$ , Young's Modulus  $E = 18.9 \text{ GPa}$ , Poisson's ratio  $\nu = 0.3$ . Cross sectional view of the PCB is shown in Figure 27.

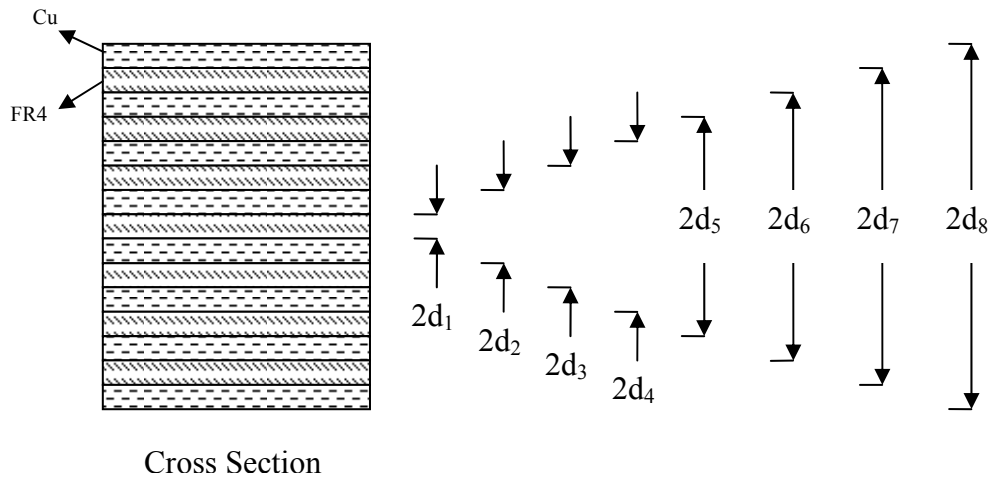


Figure 27. PCB layers

The geometric properties of the printed circuit board are given in Table 6.

Table 6. PCB dimensions

|  |                           |       |
|--|---------------------------|-------|
|  | a [mm]                    | 100   |
|  | b [mm]                    | 70    |
|  | $2d_8$ [mm]               | 1.60  |
|  | Cu layer thickness [mm]   | 0.035 |
|  | FR-4 layer thickness [mm] | 0.189 |

Finite element model of the printed circuit board is constructed in ANSYS<sup>®</sup> by using shell element SHELL99.

### 3.2.1 Analysis of the Connector Mounted Edges

Printed circuit board vibration depends on material properties, number of layers, dimensions and boundary conditions. If these properties are not defined correctly, results may be affected considerably. However, it is not always so easy to specify an effective boundary conditions at the connector mounted edge. Boundary conditions at a connector mounted edge depend on the connector length/edge length ratio, material type and geometry of connector leads and type of connector mounting to the box and printed circuit board.

In finite element modeling, it is possible to model and analyze connectors. However, it is very difficult and time consuming. Therefore, in this study it is aimed to specify connector edge boundary condition. If it is possible to identify such a boundary condition, finite element modeling effort will reduced and in similar problem types the identified conditions can be used.

In order to specify boundary conditions in this study, connector mounted edges are analyzed by using finite element modeling. Connector lead wires are modeled with beam element BEAM188 of ANSYS<sup>®</sup>. Connectors are taken to be rigid since they are attached to the box rigidly (Figure 28).

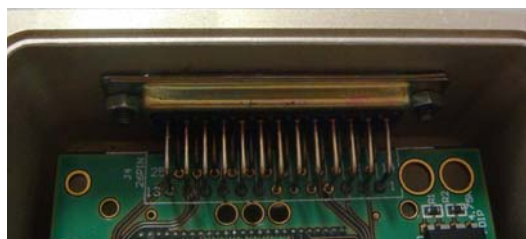


Figure 28. Connector

PCB is fixed at four points where screws are mounted. After complete finite element model is developed, first of all modal analysis is performed in order to obtain natural frequencies. Then, random vibration analysis is performed and amount of displacement is compared at the end of connector lead wires to predict the PCB behavior. Random vibration profile applied to the system is a white noise between 5-2000 Hz. Three paths which are shown in Figure 29 are chosen to study dynamic behavior in the connector region.

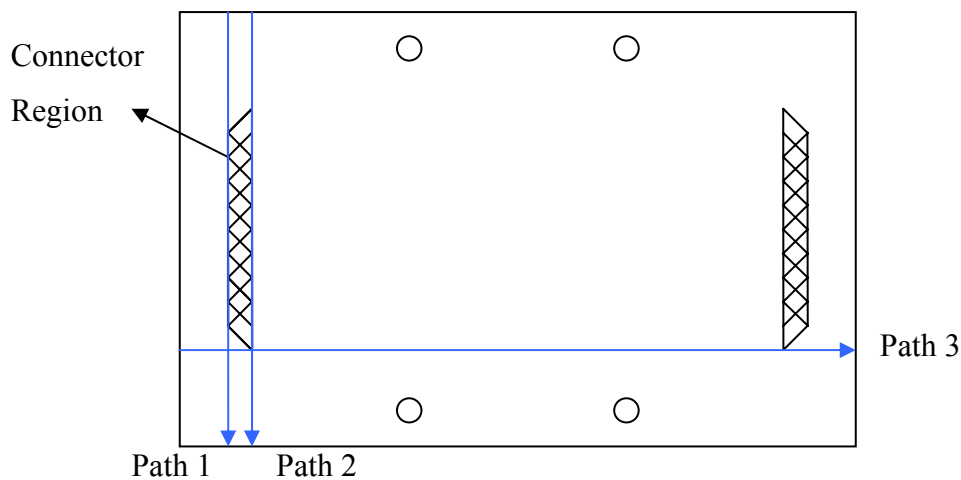


Figure 29. PCB Connection Points

The displacement variation along path 1 is shown in Figure 30. The maximum displacement in the connector region occurs at the outer lead wires. When compared to the maximum displacement on the path, the displacement of the outer pins may be assumed to be zero. However, angular displacements can not be ignored since the amount of angular displacement change of PCB at the connector pins is comparable with the other regions of the PCB.

Displacement through path 2 is shown in Figure 31. It is seen from the graph that maximum displacements in the connector region are not comparable to those in path 1. Therefore, on that path displacements can not assumed to be negligible.

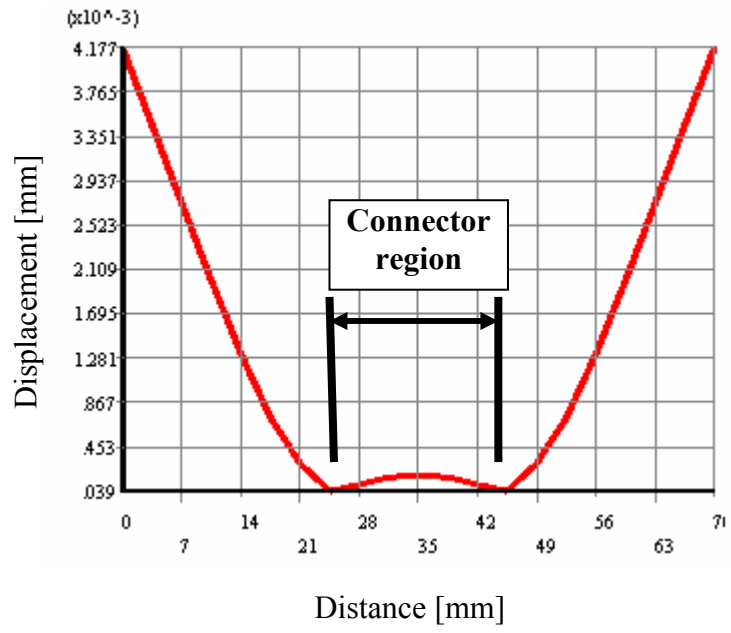


Figure 30. Displacement of PCB through path-1

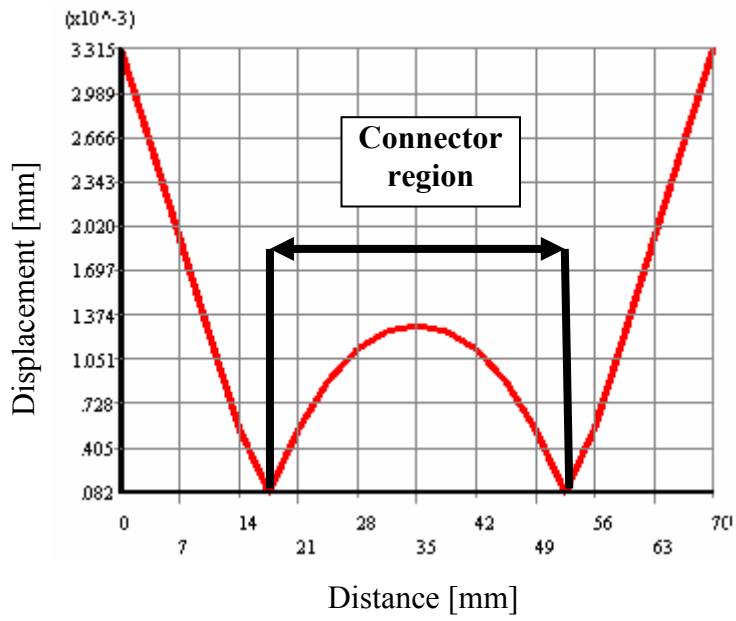


Figure 31. Displacement of PCB through path-2

Displacement through path 3 is shown in Figure 32. The graph shows that minimum displacement occurs at the connector pin. Therefore, this point can be assumed to be fixed. However, due to the angular displacements of the PCB at the pin, the connector edge cannot be assumed to be fixed.

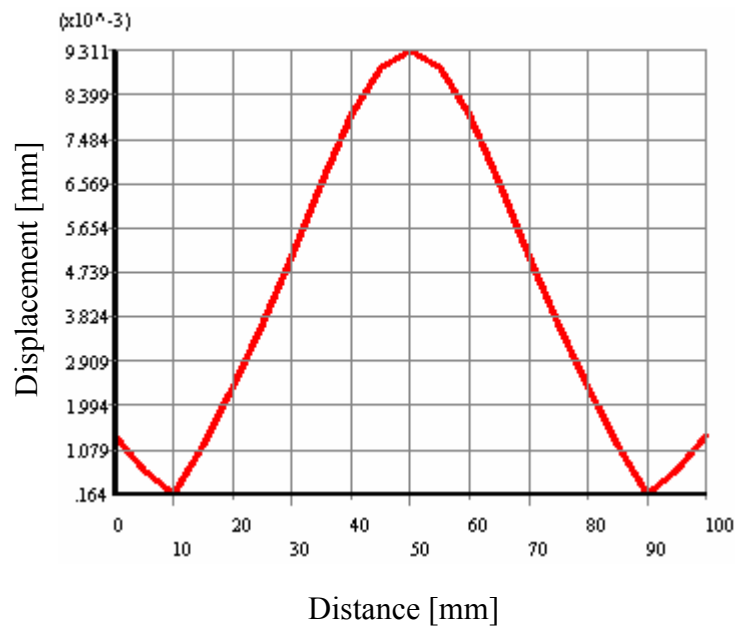


Figure 32. Displacement of PCB through path-3

From these results, it is difficult to define a specific boundary condition for the connector edge. However, if an assumption is to be made, it will be simply supported condition. If simply supported edge condition can be assumed, then another important decision should be made on where to apply simply supported condition. In this study, based on the displacement curve of the path-3, inner pins which are on path-2 are assumed to be simply supported. The outer part of the PCB which contains path 1 is not considered. In order to determine the best boundary conditions representing the actual system two alternatives based on two different assumptions are analyzed. In one of them entire edge is assumed to be simply supported and in the other only the region which has connectors is assumed to be simply supported. These models are shown in Figure 33.

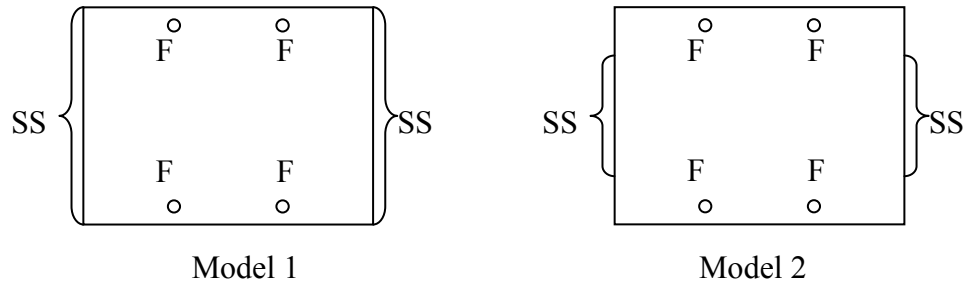


Figure 33. Assumed configurations of PCB without connectors

Finite element models are developed based on these assumptions and solved for natural frequency and mode shapes. The dimensions of the PCB which are used in the finite element vibration analysis are given in Table 7.

Table 7. PCB dimensions-without connectors

|  |        |      |
|--|--------|------|
|  | a [mm] | 80   |
|  | b [mm] | 70   |
|  | h [mm] | 1.60 |

Natural frequency results of the actual connector model and those of the assumed models are given in Table 8. The differences of the natural frequencies from the actual model are represented in percentages.

Results show that the first natural frequency values of the assumed configurations are very close to the natural frequency of the actual model. On the other hand, second and third natural frequencies are not so close. Although these natural frequencies are above 2000 Hz, in case of using any of the two simplified models care should be

taken, because when a component is added to the PCB, depending on the location and dimensions of the added component, vibration characteristics of the PCB can be altered and at least the second mode may be in the frequency range of interest. Therefore, at least the second mode of the PCB in the assumed model should be close to the actual value.

Table 8. Natural frequencies of the actual and assumed models

|   | <i>Actual model</i> | <i>Model 1</i> |                | <i>Model 2</i> |                |
|---|---------------------|----------------|----------------|----------------|----------------|
|   | $f_n$ [Hz]          | $f_n$ [Hz]     | Difference (%) | $f_n$ [Hz]     | Difference (%) |
| 1 | 1378                | 1374           | 0.29           | 1345           | 2.40           |
| 2 | 2398                | 2644           | 10.3           | 2604           | 8.59           |
| 3 | 2559                | 2960           | 15.7           | 2943           | 15.0           |

First natural frequency values show that configuration 1 is closer to the exact model solution. However, to have a final decision for the boundary condition, corresponding mode shapes of three configurations are compared.

In Table 9 mode shapes associated with the first mode are presented. Figures represent displacement contours in z direction. Despite the fact that the second configuration gives higher differences in natural frequencies its mode shape resembles those of the exact configuration.

Table 9. First mode comparison with real and assumed configurations

| <i>PCB model w connectors</i>  |  |
|--|--|
| $f_1=1378$ Hz  |  |
| <i>Configuration 1-PCB edges with connectors modeled as simply supported edges</i>     |  |
| $f_1=1374$ Hz  |  |
| <i>Configuration 2-PCB edges with connectors modeled as partially simply supported</i> |  |
| $f_1=1345$ Hz  |  |

Table 10. Second mode comparison with real and assumed configurations

| <i>PCB model w connectors</i>  |  |
|--|--|
| $f_2=2398$ Hz  |  |
| <i>Configuration 1-PCB edges with connectors modeled as simply supported edges</i>     |  |
| $f_2=2644$ Hz  |  |
| <i>Configuration 2-PCB edges with connectors modeled as partially simply supported</i> |  |
| $f_2=2604$ Hz  |  |

In Table 10 mode shapes associated with the second mode are presented. From these figures it is seen that both configurations fail in representing the exact model. Since these modes are above 2000 Hz, this result will not affect this analysis. However as discussed above, this mode should not be ignored and checked after possible component addition.

As a result, from natural frequency and mode shape analyses it is concluded that the second assumed model represents the exact model better in the first mode with slight differences both in natural frequency and mode shape. However, both models fail in representing higher modes. Also, to define a specific boundary condition for the connector mounted edge turns out to be more difficult than modeling the actual connector model. Hence, it is concluded that one should model the actual connector.

Therefore, in this case study, the simplified model is not used since higher modes of the printed circuit board may become critical after component addition.

During analyses of connectors, it is also revealed that they act like elastic supports and it is not so suitable to treat connectors as rigid mountings.

### **3.2.2 Printed Circuit Board with Components Added**

PCBs usually have a number of components. It is impractical and time consuming to pay attention to every electronic component in terms of vibration. Therefore, it is very critical to determine important components which will affect PCB dynamics. Decision of influential electronic components can be made by following some basic steps. First of all, bare PCB dynamics should be specified and understood completely. Once PCB vibration behavior is known, one can be aware of most and least vibrating parts of a board at its natural frequencies. Then, reliable interpretation of component addition effect can be made depending on its location. In addition to component location, it is critical to consider component mass. Mounting heavier

components on a board will result in more significant change in dynamics compared to lighter ones. Besides mass properties, size of components is also important for PCB dynamics. Larger components can result in stiffened regions on PCB if surface mount technology is employed for adding components on PCB.

The other crucial issue about component addition is the modeling approach in finite element modeling. There are various ways in finite element modeling of electronic components. The simplest approach is putting the component at a single point as a lumped mass. Another approach is distributing component mass over the region where it is bonded. In addition to these methods, more complex solutions are performed by modeling lead wires as spring or beam elements. Also there are various studies on modeling techniques of solder joints.

In this section, three different approaches are followed to model an electronic component and PCB assembly: (i) lumped mass model, (ii) merged component model and (iii) lead wire modeling.

Finite element models are developed by using shell element SHELL99 for the PCB. Lumped mass modeling is performed by utilizing mass element MASS21. Component bodies are created by solid elements SOLID92 with increased modulus of elasticity to obtain rigid behavior. Lead wires are modeled with beam elements BEAM188.

The components which need to be modeled are determined based on their locations, masses and sizes. Schematic view of electronic components used in this study is given in Figure 34. Component masses are given in Table 11.

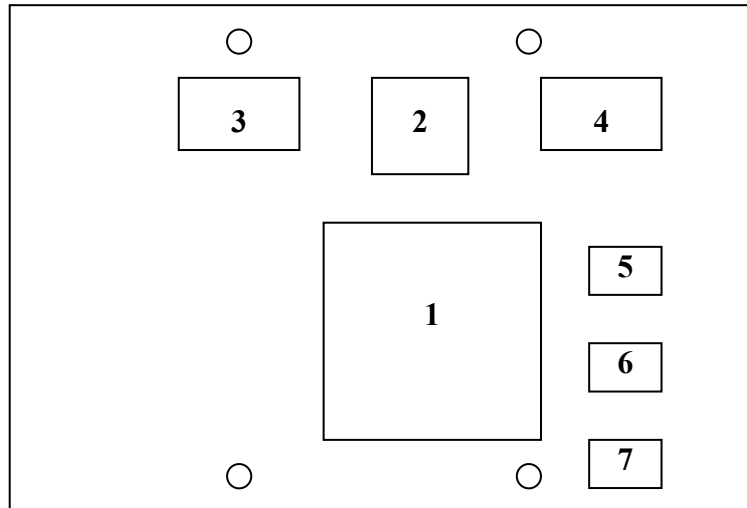


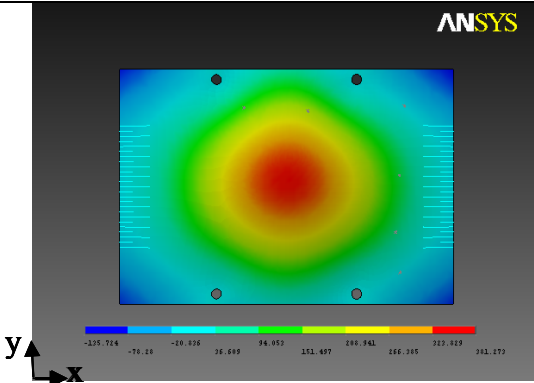
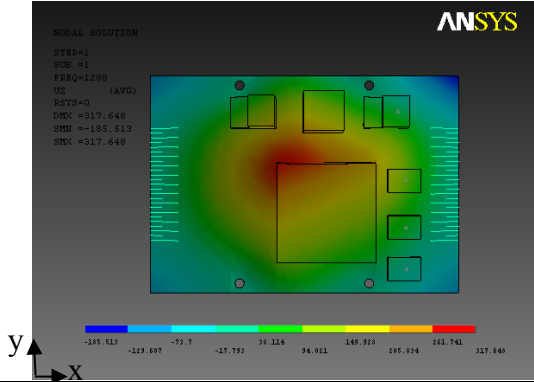
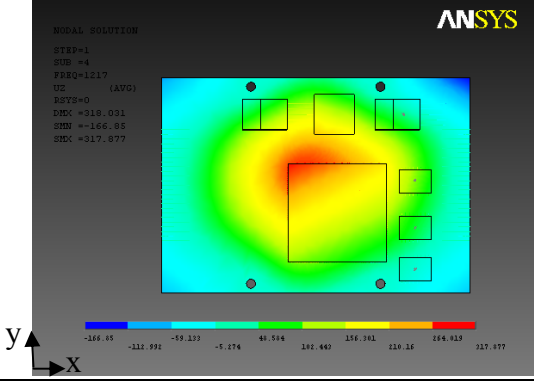
Figure 34. Schematic view of components on the PCB

Table 11. Component masses

| Component # | Mass (g) |
|-------------|----------|
| 1           | 7.31     |
| 2           | 1.95     |
| 3           | 1.98     |
| 4           | 2.05     |
| 5           | 0.88     |
| 6           | 0.88     |
| 7           | 0.88     |

Natural frequencies and mode shapes are obtained for the three different models considered; namely lumped mass model, merged component model and lead wired component model. The natural frequencies and mode shapes obtained by using these models are given in Table 12.

Table 12. Natural frequencies and mode shapes of component added PCB

| <b>Lumped mass model: Components are modeled as lumped masses</b> |  |
|---|--|
| $f_1 = 1294 \text{ Hz}$   |    |
| <b>Merged model: Component bodies are merged to PCB</b>           |  |
| $f_1 = 1287 \text{ Hz}$   |   |
| <b>Lead wired model: Components are modeled exactly</b>           |  |
| $f_1 = 1217 \text{ Hz}$   |  |

Finite element solution showed that lumped mass model has the highest natural frequency of all and lead wired model has the lowest. These results are reasonable because although mass addition is considered in all models, component vibration is

not included in the lumped mass model, and only component body vibration is included in the merged model.

Natural frequency difference with lead wired model is 6.3 % for lumped mass model, and 5.8% for merged model. It can be concluded from these results that the effect of component attachment flexibility is not very significant and a component may be assumed to be rigidly connected to the PCB in simple models.

The study of the mode shapes show that lumped mass model has relatively different shape whereas merged and lead wired models yield very similar mode shapes. This was an expected result, since lumped modeling of components will consider only the mass increase but will disregard the stiffening effect of components.

Another important result obtained from finite element analysis is that the lumped model has its second mode in the range of 20-2000 Hz (Figure 35), whereas the remaining models only have one mode in this frequency range.

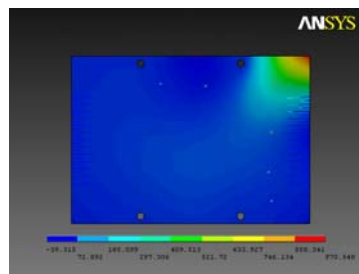


Figure 35. Second mode shape of the lumped model at 1905 Hz

Consequently, it can be concluded that merge component modeling can be used in the analysis. Merge model approach will provide computational time saving and will be simpler when compared with lead wire modeling.

### 3.2.3 Analysis of PCB Mounted in Electronic Box

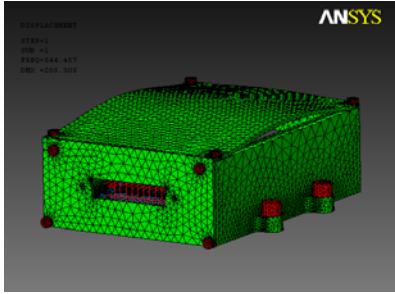
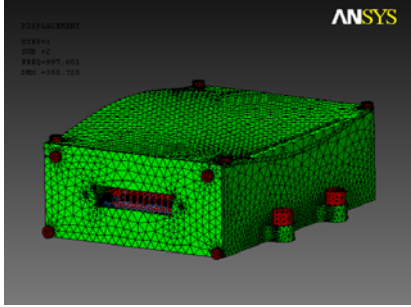
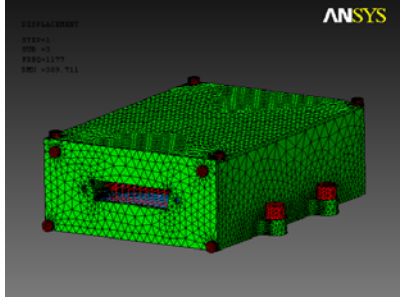
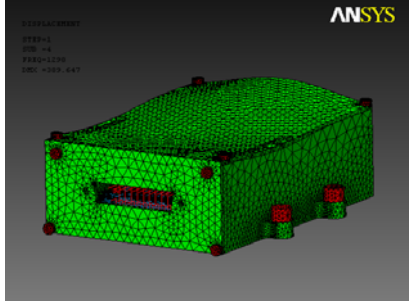
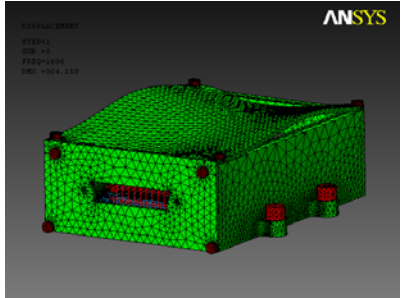
So far, connector effects on boundary conditions and effects of component addition effects on PCB dynamics are studied. Now, it is aimed to analyze PCB behavior inside the box, observe the effects of mounting and investigate whether electronic box vibration contributes to PCB dynamics. For this purpose, finite element model of the PCB and the electronic box is constructed in ANSYS<sup>®</sup>. Natural frequencies and associated mode shapes are obtained.

In this analysis, connector body is assumed to be rigidly mounted to the box which reflects the actual situation better. This assumption does not only affect the boundary conditions of the PCB, but also those of the front cover where the connector is attached. In order to represent the connection better, the front cover is assumed to be fixed at the mounting points of the connector, which makes front cover and therefore the box more rigid. A factor which will affect electronic box vibration is the addition of PCB into the box. However, since natural frequencies of the base of the box and PCB are far away from each other only mass addition could affect dynamics of the box, but this is also unlikely since PCB is a very light structure compared to the base of the box.

Natural frequency and mode shape results are tabulated in Table 13. Except the fourth vibration mode, all the modes are related to the top cover. If these frequencies are compared with the results of the previous analyses of the box, it is seen that previous results are not altered significantly. Therefore, it can be concluded that PCB has almost no effect on top cover dynamics.

The third mode is related to printed circuit board vibration. It is observed that the electronic box has no deflection at that mode therefore it can be concluded that PCB and the box is uncoupled in the frequency range of interest.

Table 13. Natural frequencies of the PCB and box assembly

|   |  |
|---|--|
| <p><i>First mode at <math>f_n=545</math> Hz</i></p>   |    |
| <p><i>Second mode at <math>f_n=998</math> Hz</i></p>  |    |
| <p><i>Third mode at <math>f_n=1177</math> Hz</i></p>  |   |
| <p><i>Fourth mode at <math>f_n=1298</math> Hz</i></p> |  |
| <p><i>Fifth mode at <math>f_n=1686</math> Hz</i></p>  |  |

To have a closer look on the PCB vibration, the third mode shape is represented in Figure 36 with hidden covers. Natural frequency of the PCB is increased by 1.1% when it is mounted inside the box. Mode shape is not affected at maximum deflection points but around screw connections slight differences can be observed. This result can be attributed to the boundary conditions at screw connections. When modeling only the PCB, circumference of the screw holes are fixed. In the case of mounting PCB inside the box, screw connection provided more rigid boundary condition which results in increasing frequency and slight differences in mode shape.

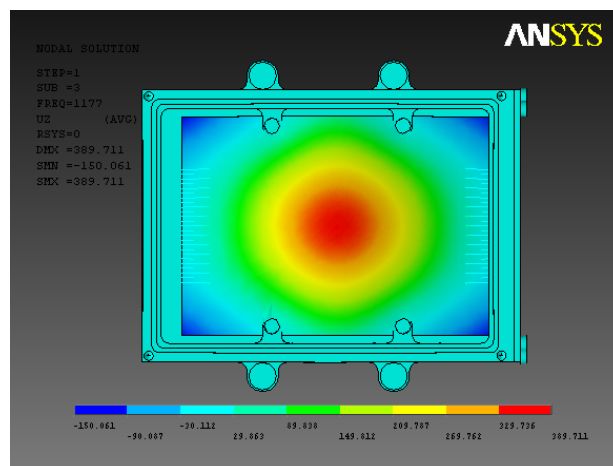


Figure 36. Fourth mode shape of the assembly-contour plot in z direction (front and top cover hidden)

### 3.3 Finite Element Vibration Analysis of Electronic Assembly

Until this point, vibration and finite element analysis techniques of the electronic box, the PCB and the components are studied in detail. Critical issues and important aspects of the subject are clarified and interpreted. In this section, these substructures are put together and analyzed as a whole. The significant points observed are presented here. Three different assembly configurations are formed. These

configurations differ in component modeling approaches which are lumped, merged and lead wired modeling. These assemblies are analyzed to obtain natural frequencies and mode shapes. Suitable modeling techniques are investigated by comparing these configurations.

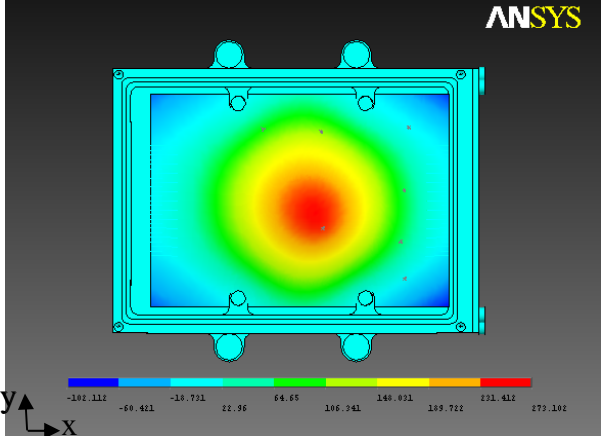
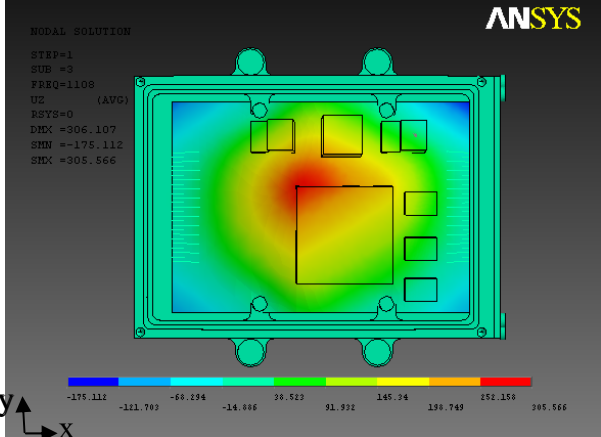
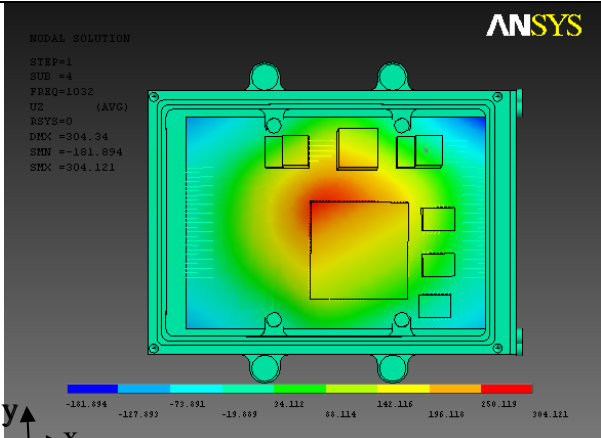
In the previous section, bare PCB was added to the box and besides the PCB mode, 4 natural frequencies are obtained related to top cover. Results of the analyses of the whole electronic assembly showed that these top cover frequencies and mode shapes remain the same. PCB modes are altered as expected because of the component addition. Therefore, only the modes of the PCB are presented for three configurations.

The same element types are used for the assembly parts, as in the previous sections. Natural frequencies and nodal displacements are obtained. Results show that mounting the PCB into the electronic box changes the natural frequency values of the PCB. The change in natural frequencies shows that PCB connection points on the box are not rigid. Flexibility at the connection points results in decrease in natural frequencies. First natural frequencies of the PCB with and without box attachment is given in Table 14 for comparison. Nodal displacements in z-direction are given in Table 15.

Table 14. First natural frequencies of PCB configurations

| Modeling type | PCB is not the box | PCB is in the box |
|---------------|--------------------|-------------------|
| Lumped        | 1294 Hz            | 801 Hz            |
| Merged        | 1287 Hz            | 1108 Hz           |
| Lead wired    | 1217 Hz            | 1032 Hz           |

Table 15. Natural frequencies and mode shapes of electronic assembly with different component modeling approaches

| Lumped mass model: Components are modeled as lumped masses |  |
|--|--|
| $f_n=801 \text{ Hz}$                                       |    |
| Merged model: Component bodies are merged to PCB           |  |
| $f_n=1108 \text{ Hz}$                                      |   |
| Lead wired model: Components are modeled exactly           |  |
| $f_n=1032 \text{ Hz}$                                      |  |

Yet, at this stage it can be concluded that PCB vibration is affected both by component addition and mounting into the box. First natural frequency of the PCB modeled with lumped components is decreased by 38% when it is mounted into the box. On the other hand, first natural frequencies of both PCBs modeled with merged and lead wired components are decreased by 15% when they are mounted into the box.

An important observation is that the mode shapes of the merged and lead wired models are close to each other, while the lumped model yields a different vibration mode shape. This is the inherent result of ignoring stiffening effect of the component body. It is not only the mode shapes, but also natural frequencies of the lumped model are also very different from those of the other models.

Another significant result is that lumped model gives two more modes in the range of 20 and 2000 Hz.

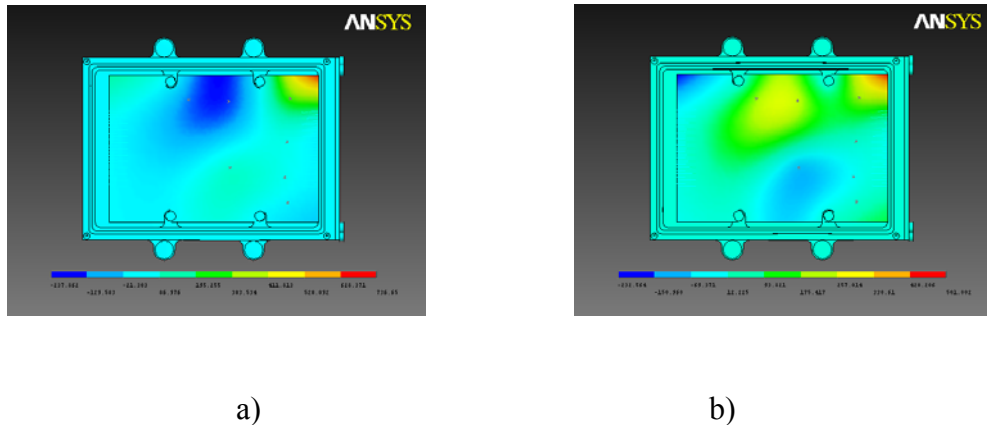


Figure 37. a) Second (1631 Hz) and b) third (1748 Hz) mode shapes of the PCB with lumped components (top cover hidden)

After evaluating these results, it can be concluded that merge modeling of components can be applicable during preliminary analyses. This will reduce

computational time required for modeling process when compared to those of lead wire modeling. On the other hand, lumped modeling of components may not lead to valid results because stiffening effect of components is disregarded.

## **CHAPTER 4**

### **EXPERIMENTAL ANALYSIS**

In this chapter, sine sweep testing of the electronic assembly is presented. First, the experimental setup is explained and experimental conditions are described. Then, the experiments on the electronic box without front and top covers are presented. Afterward, the experimental results for the box with front and top covers are given. Finally, the results of the experiments for the printed circuit board which is assembled into the box are presented. Since the PCB has electronic components on its surface, component effects are investigated by taking measurements on the largest component body.

The results obtained are studied in order to understand the vibration characteristics of the structure and to understand the effects of connections between electronic box and the PCB as well as those between the PCB and the electronic component. In order to make a meaningful comparison of the results obtained from experimental and finite element models, the mass effect of the accelerometer is also taken into consideration. A detailed comparison of finite element analyses and experimental results are given and possible reasons of variations are discussed.

#### **4.1 Experimental Setup**

Vibration experiments are performed in the Vibration and Modal Testing Facility of TÜBİTAK-SAGE. Vibration test system is composed of two shakers, a slip table (Figure 38) and a controller.

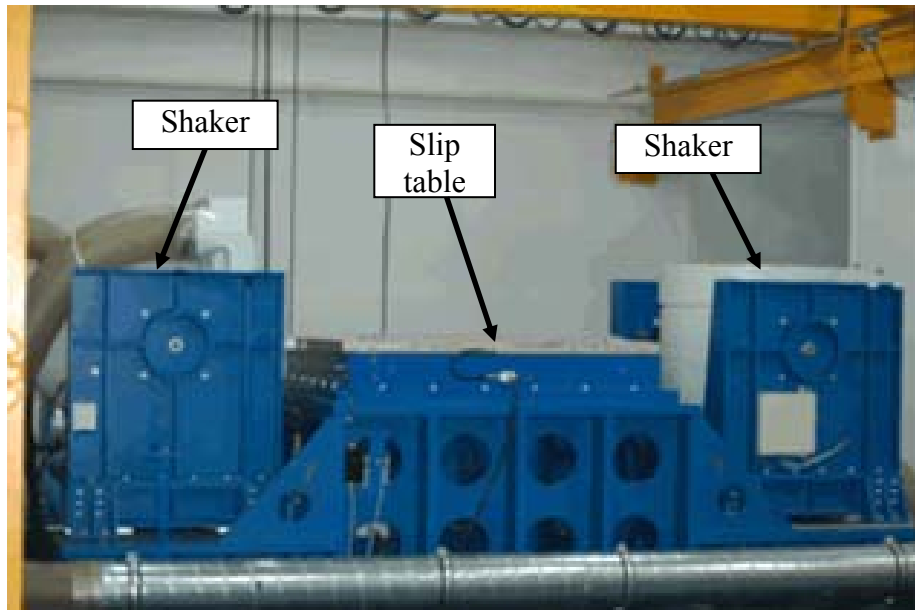


Figure 38. Shakers and slip table [41]

In experiments, the shaker which is positioned vertically is utilized. The shaker is driven by 16 channel LMS<sup>®</sup> SCADAS III data acquisition hardware (Figure 39) and LMS<sup>®</sup> Test.Lab software.



Figure 39. LMS<sup>®</sup> SCADAS III data acquisition hardware [41]

During the experiments two types of accelerometers are used. Control accelerometer is a single axis piezoelectric ICP<sup>®</sup> accelerometer (Model: PCB 352A56) and it is mounted on the fixture. Response accelerometer is a miniature single axis

piezoelectric ICP<sup>®</sup> accelerometer (Model: PCB JT352C34). Positions of response accelerometers are determined by using the finite element analysis results of individual cases.

The vibration excitation is applied in vertical direction (z-direction) in all experiments and vibrations are measured in this direction.

A test fixture is designed for the experiments. Before performing experiments, vibration characteristic of the fixture is examined by sine sweep tests. The results showed that between 5-2000 Hz the fixture has three natural frequencies at 1581 Hz, 1739 Hz and 1950 Hz which can be observed from Figure 40. Hence, it is concluded that, reliable measurements cannot be performed above 1500 Hz to observe the real behaviors of test items. Therefore, test results are interpreted by taking these frequencies into account. Transmissibility values of the fixture at its natural frequencies are given in Table 16.

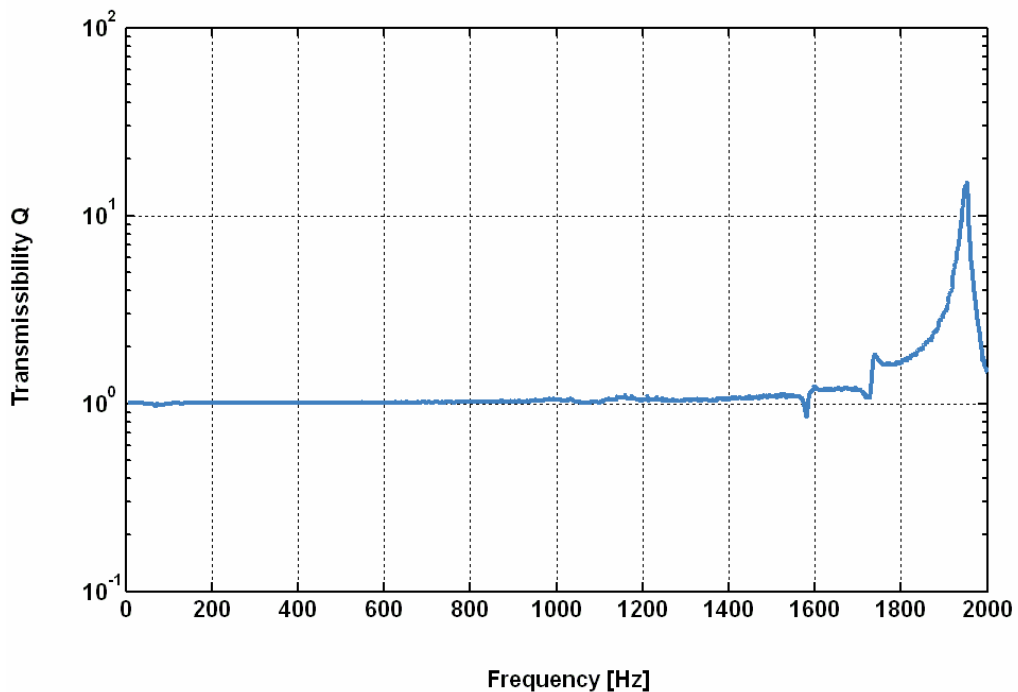


Figure 40. Transmissibility of the fixture

Table 16. Transmissibility of the fixture at natural frequencies

| Natural Frequency | Transmissibility |
|-------------------|------------------|
| 1581              | 1.3              |
| 1739              | 1.8              |
| 1950              | 15.0             |

All the tests are performed with the same acceleration amplitude, sweep rate and sweep mode. Sine sweep testing conditions are given in Table 17.

Table 17. Summary of sine sweep testing conditions

|                        |             |
|------------------------|-------------|
| Acceleration amplitude | 1g          |
| Sweep rate             | 4 oct/min   |
| Sweep mode             | Logarithmic |

Frequency range of the experiments is 5-2000 Hz except Experiment 1 and 4 whose range is between 5-2100 Hz. In these experiments maximum frequency level is altered in order to observe the natural frequency of the base.

Test items and accelerometer configurations are tabulated in Table 18. First three experiments are performed in order to understand the vibration behavior of the box base and to observe whether or not the PCB is affected by the base motion. Fourth experiment is performed to see top cover vibration. The last two experiments are related to PCB vibration.

Table 18. Summary of sine sweep testing configurations

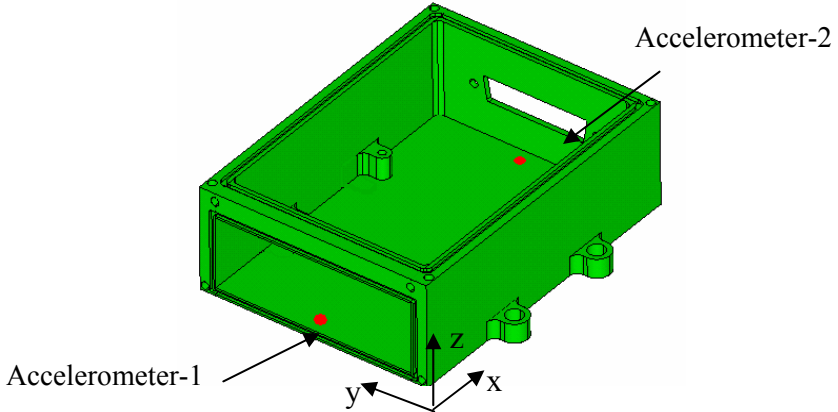
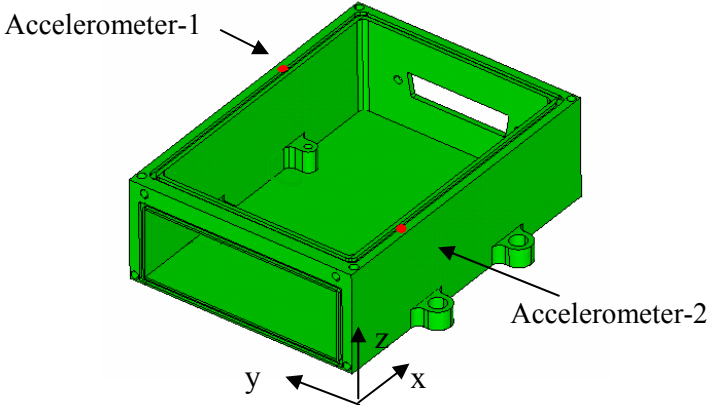
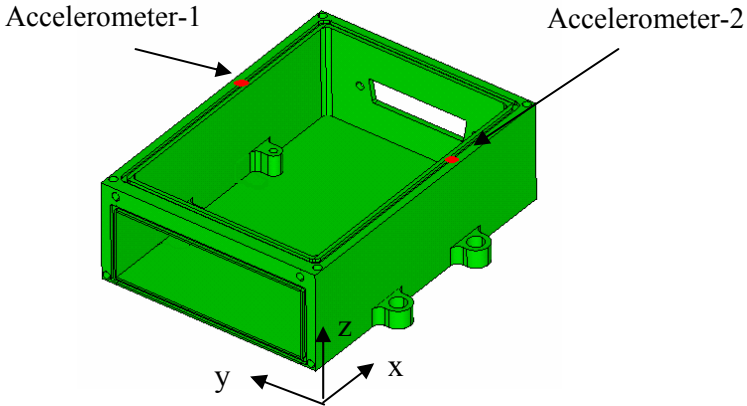
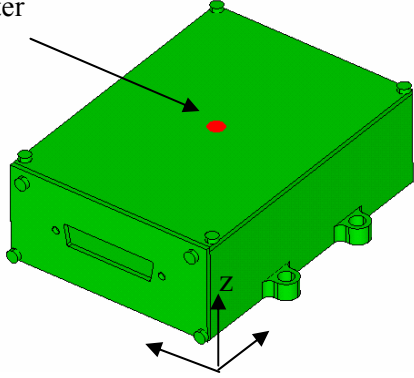
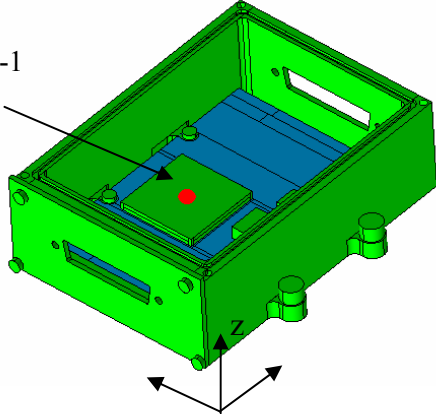
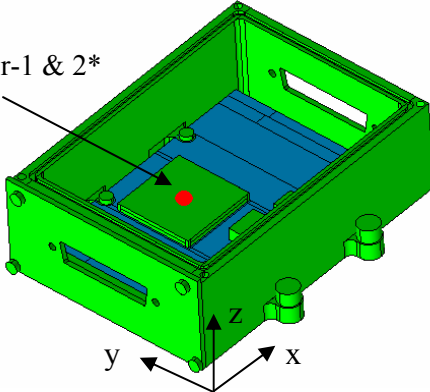
| Experiment number | Test item and accelerometer configuration   |
|-------------------|---|
| 1                 |  <p>Accelerometer-2</p> <p>Accelerometer-1</p> <p>x</p> <p>y</p> <p>z</p>   |
| 2                 |  <p>Accelerometer-1</p> <p>Accelerometer-2</p> <p>x</p> <p>y</p> <p>z</p>  |
| 3                 |  <p>Accelerometer-1</p> <p>Accelerometer-2</p> <p>x</p> <p>y</p> <p>z</p> |

Table18 (continued). Summary of sine sweep testing configurations

| Experiment number | Test item and accelerometer configuration   |
|-------------------|---|
| 4                 | <p data-bbox="577 434 756 461">Accelerometer</p>    |
| 5                 | <p data-bbox="539 945 740 972">Accelerometer-1</p>   |
| 6                 | <p data-bbox="555 1415 820 1442">Accelerometer-1 &amp; 2*</p>  <p data-bbox="504 1792 1382 1859">* Accelerometer-1 is on the component and accelerometer-2 is on the backside of the PCB.</p> |

## 4.2 Experiment 1

The electronic box is mounted to the fixture which is attached to the shaker. In order to observe base vibration behavior, two miniature accelerometers are attached to base of the electronic box (Table 18), and control accelerometer is attached on the fixture. A sine sweep test is performed between 5-2100 Hz. Transmissibility of two measurement points is obtained and given in Figure 41.

As mentioned before, the fixture where control accelerometer is attached does not have a rigid behavior between 5-2000 Hz. Therefore, it is expected to have the effect of the fixture dynamics on the test item response.

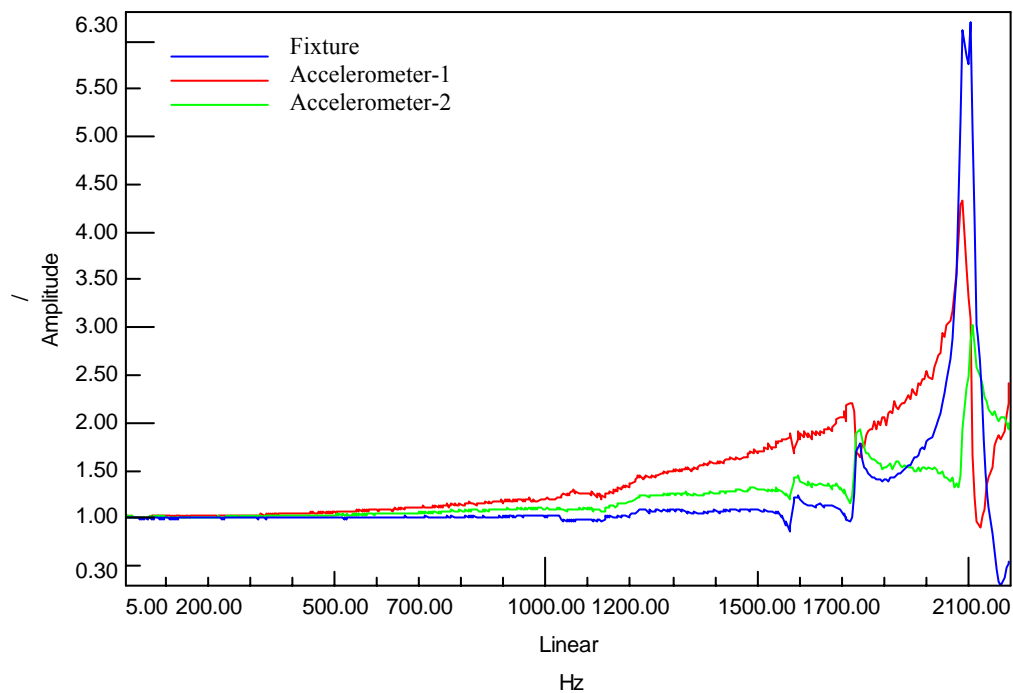


Figure 41. Transmissibility of the base of the box (Experiment 1)

It is observed that up to 1750 Hz, the response of second point, which is measured by accelerometer-2, follows the fixture motion. The response of the first measurement point, which is measured by accelerometer-1, is higher than the second measurement point. The difference between transmissibility until 1750 Hz is due to the fact that accelerometer-1 is attached to flexible part of the base. Thus, it measures higher transmissibility values.

After 1750 Hz, the fixture vibrations become considerably high. Therefore, it is difficult to have an exact conclusion on box behavior after 1750 Hz. Although it is not possible to decide on whether the peak points on the graph show natural frequency of the box; it is obvious that after 1950 Hz response of the box is lower in amplitude than the fixture. This observation shows that after 1950 Hz, box structure isolates the vibration loading.

### **4.3 Experiment 2**

After measuring response of bottom part of the base, side wall vibration is inspected. In this experiment, two miniature accelerometers are placed at the top of the box (Table 18). Control accelerometer is attached onto the fixture. Sine sweep test is performed between 5 and 2000 Hz. Transmissibility graph is given in Figure 42.

It is observed from the graph that until 1750 Hz, accelerometer-1 measures the same transmissibility values with the fixture. This shows that the point where accelerometer-1 is attached has rigid behavior up to 1750 Hz. On the other hand; after 1950 Hz, measurement of the accelerometer-2 starts following the fixture motion, which shows that up to 1950 Hz fixture vibrations are isolated at all frequencies.

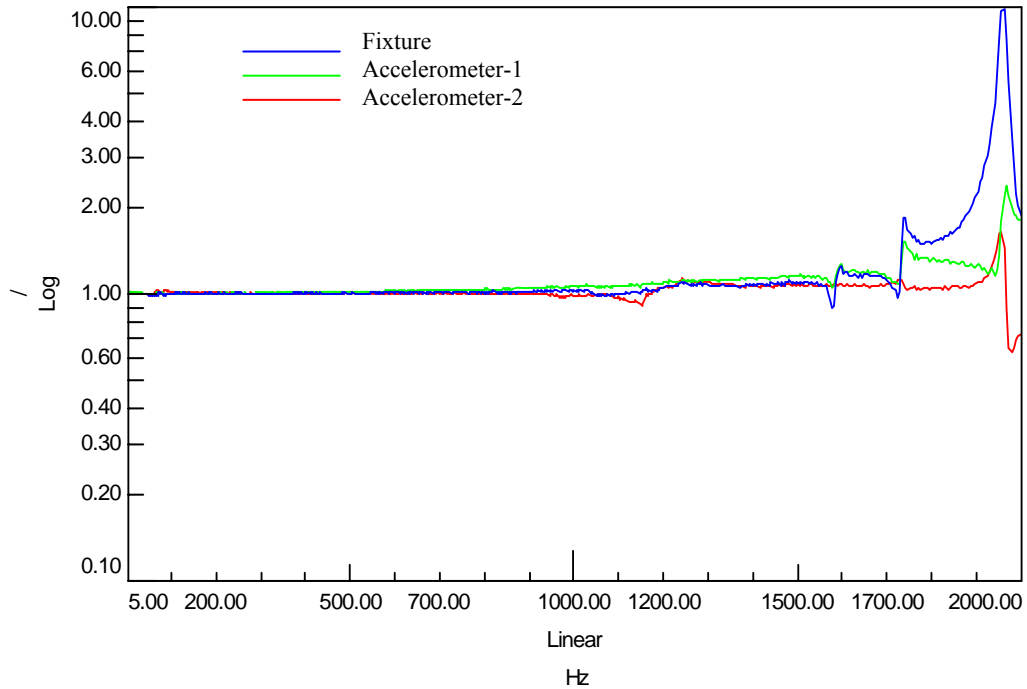


Figure 42. Transmissibility of the box (Experiment 2)

After 1750 Hz, the fixture vibration becomes too harsh. In spite the fact that the fixture vibrates in large amplitudes; accelerometer-1 and 2 measure lower transmissibility values than the fixture. Therefore, it is possible to conclude that box isolates the fixture vibration. Also, it may be possible to conclude that the peak values, which are read from response curves of the first and second accelerometer, are caused by fixture dynamics.

#### 4.4 Experiment 3

In this experiment another measurement configuration is used for the side wall vibration inspection. Again, two miniature accelerometers are placed at the top of the box (Table 18). Control accelerometer is attached on the fixture. Sine sweep test is performed between 5-2000 Hz. Transmissibility graph is given in Figure 43.

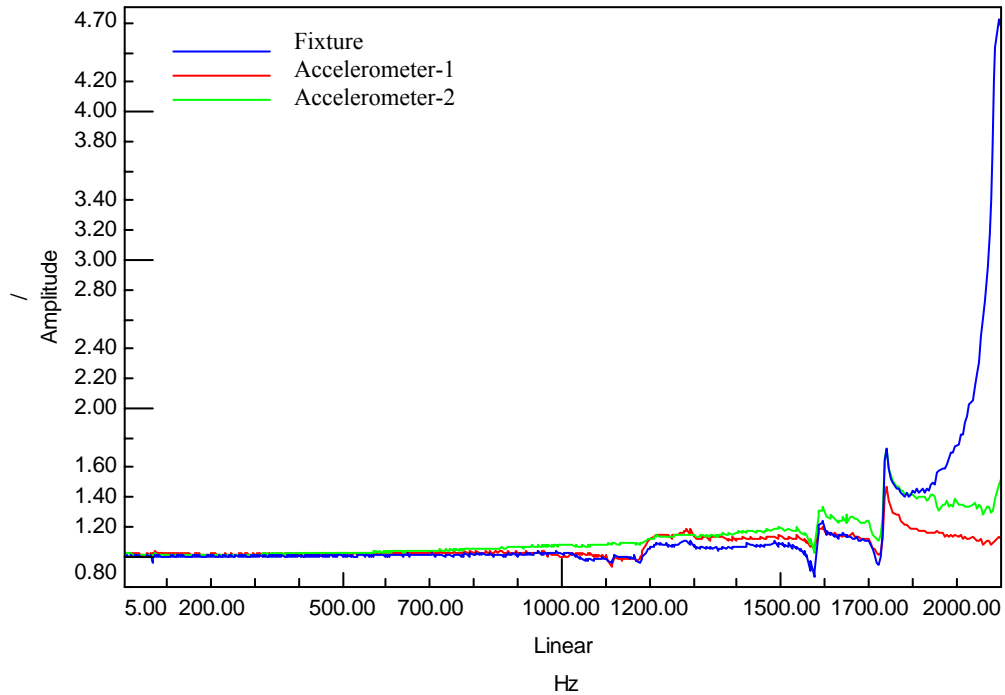


Figure 43. Transmissibility of base of the box (Experiment 3)

It is observed from the response graph that up to 1750 Hz, measurements of the accelerometer 1 and 2 follow the fixture motion. Therefore, it is possible to conclude that until 1750 Hz, box has a rigid behavior.

After that frequency, the fixture vibrates in larger amplitudes and it is not possible to comment on transmissibility values of the box. However, the most significant observation is that the box isolates the fixture vibration after 1750 Hz.

From experiments 1, 2 and 3 it can be concluded that the base of the box and side walls generally vibrate together as a rigid body up to 1750 Hz. However, after this frequency fixture vibration becomes too harsh and this condition results in fixture vibration with large amplitudes. Although the box is rigidly connected to the fixture, vibration of the fixture does not affect the box significantly. Therefore, it is possible to conclude that the box isolates the vibration at higher frequencies. This suppression effect is observed more in flexible parts of the box which is the front cover side.

## 4.5 Experiment 4

In this experiment top cover is added to the configuration of the previous experiment and it is aimed to observe top cover response. Measurement is done by the miniature accelerometer which is placed over the top cover (Table 18). Control accelerometer is attached on the fixture. Sine sweep test is performed between 5-2000 Hz. Transmissibility graph is given in Figure 44.

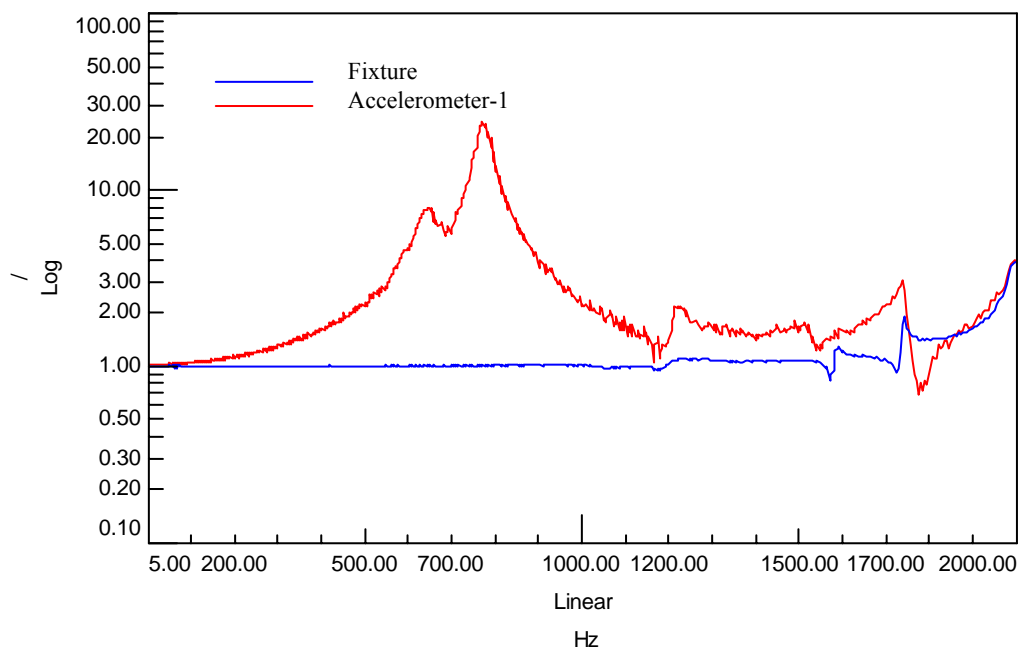


Figure 44. Transmissibility of the top cover (Experiment 4)

From the graph it is observed that two large peaks exist at 646 Hz and 773 Hz. It is possible to say that these peaks belong to top cover because up to 1580 Hz, the fixture behaves rigidly and has no effect on the box dynamics. There is one more peak observed in the response of the top cover at 1217 Hz where fixture has rigid behavior. The transmissibility at this frequency is 2.2 which is not as large as the first

two transmissibility values. Transmissibility values of these points are given in Table 19.

Table 19. Transmissibility of the top cover at natural frequencies - Experiment 4

| <i>Natural Frequency [Hz]</i> | <i>Transmissibility</i> |
|-------------------------------|-------------------------|
| 646                           | 8.0                     |
| 773                           | 24.0                    |
| 1217                          | 2.2                     |

After 1580 Hz, fixture vibration becomes apparent and it is not possible to comment on whether the peaks observed in the top cover response curve after this frequency occur as a result of fixture vibration or due to top cover dynamics.

As the top cover is a plate like structure fixed at four corners, it is expected to have distinct natural frequencies. From the study of the results it can be said that the first natural frequencies represent the first two elastic modes of the top cover.

#### **4.6 Experiment 5**

After completing experiments of the box; PCB with components on it, is mounted into the box and a miniature accelerometer is attached to the integrated circuit which is the largest component on the PCB (Table 18). The control accelerometer is attached on the fixture. Sine sweep test is performed between 5-2000 Hz. Transmissibility graph obtained is given in Figure 45.

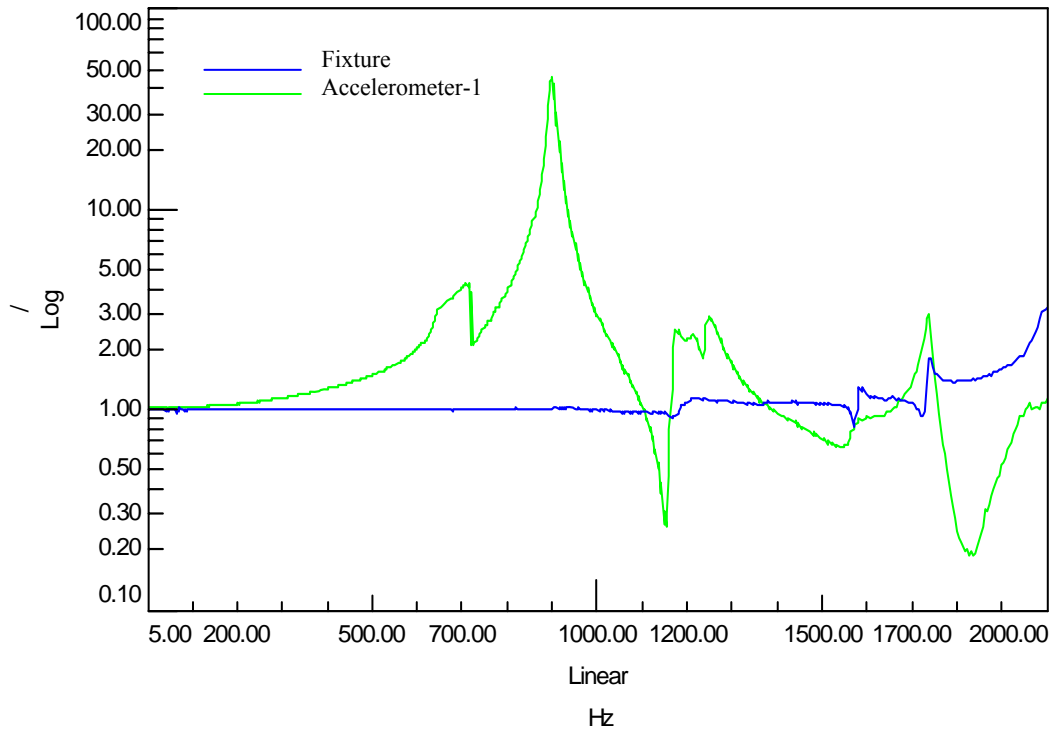


Figure 45. Transmissibility of the largest component (Experiment 5)

From the transmissibility graph of the component, four peak points are observed in the frequency range of interest, where PCB response is independent from the fixture dynamics. These peaks occur at 715 Hz, 903 Hz, 1177 Hz and 1251 Hz. Transmissibility values of these frequencies are tabulated in Table 20.

Table 20. Transmissibility of the largest component -Experiment 5

| <i>Natural Frequency [Hz]</i> | <i>Transmissibility</i> |
|-------------------------------|-------------------------|
| 715                           | 4.27                    |
| 903                           | 46.0                    |
| 1177                          | 2.5                     |
| 1251                          | 2.9                     |

From the graph it is observed that the first two natural frequencies are very distinct. The transmissibility is very large especially at the second natural frequency.

After 1580 Hz, fixture dynamics become too effective, again. Therefore, it may not be possible to observe the real behavior of the component from this measurement after 1580 Hz. Yet, it can be said that the component does not have a major resonance frequency in this range.

#### **4.7 Experiment 6**

In this experiment, it is aimed to observe the vibration behaviors of two points: one is on the component and the other is on the PCB at the same location. In order to perform such an experiment, one of the accelerometers is placed on the largest component as in the previous section, and the other accelerometer is attached at the same location but on the back side of the PCB (Table 18). As a result, the chance of observing PCB and component vibrations at the same location is obtained.

Control accelerometer is attached onto the fixture. Sine sweep test is performed between 5-2000 Hz. Transmissibility graph is given in Figure 46 for accelerometer-1 and accelerometer-2.

In Experiment-4 in which top cover response is measured, two obvious natural frequencies are obtained representing the elastic modes of the cop cover. In this experiment similar behavior is observed for the first two natural frequencies of the PCB which are very distinct. This similarity is due to the fact that both top cover and PCB are plate structures and they are nearly at the same size.

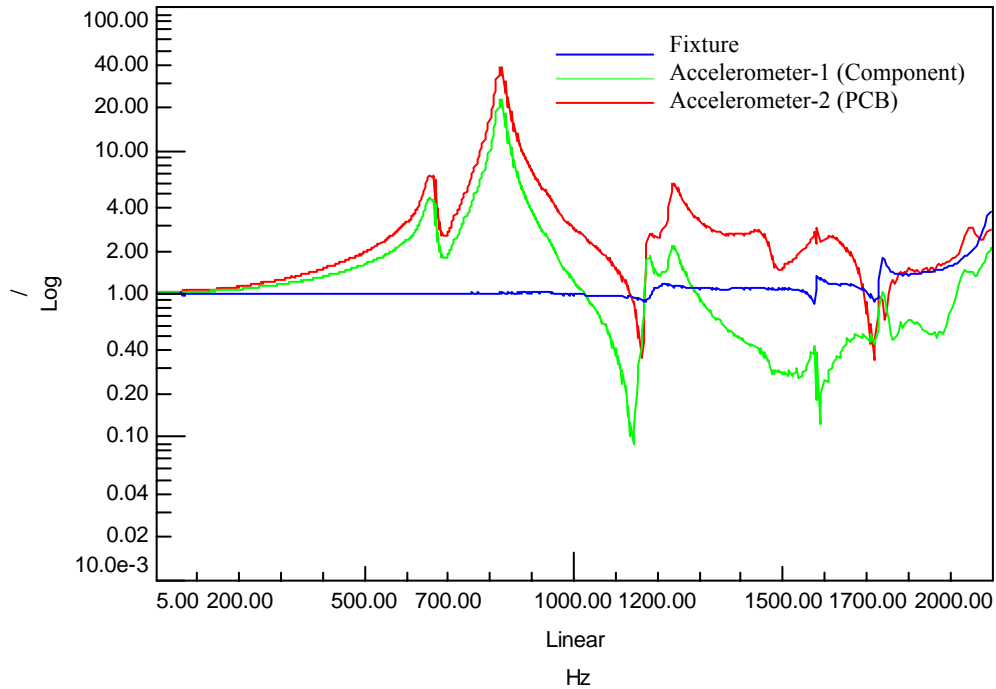


Figure 46. Transmissibility of the PCB and the largest component (Experiment 6)

From the graph it is also observed that both vibrations are very similar and have the same trend until 1500 Hz. Two very obvious peaks which occur at 657 Hz and 829 Hz are observed in the responses of both PCB and component. Two more peaks are seen near 1180 Hz and 1240 Hz, again for PCB and the component. It is possible to say that these four frequencies are natural frequencies of the PCB and component since they are observed in the frequency range where fixture has a rigid behavior. Transmissibility values and natural frequencies are given in Table 21.

After 1500 Hz, fixture dynamics become effective. Therefore it is not possible to comment on the responses after this frequency.

From these results, it can be concluded that vibration analysis of the PCB with electronic component can be performed by taking component as a lumped mass.

Table 21. Transmissibility of component and PCB at natural frequencies-  
Experiment 6

| <b>Accelerometer-1 (Component)</b> |                         |
|------------------------------------|-------------------------|
| <i>Natural Frequency [Hz]</i>      | <i>Transmissibility</i> |
| 657                                | 4.7                     |
| 829                                | 23.0                    |
| 1180                               | 1.8                     |
| 1237                               | 2.2                     |
| <b>Accelerometer-2 (PCB)</b>       |                         |
| <i>Natural Frequency [Hz]</i>      | <i>Transmissibility</i> |
| 657                                | 6.7                     |
| 826                                | 39.0                    |
| 1180                               | 2.7                     |
| 1241                               | 5.9                     |

#### 4.8 Comparison of Finite Element and Experimental Results

Up to here the vibration behavior of the electronic assembly is investigated by finite element modeling and experimentation. In this section the finite element results will be compared with experimental results.

Finite element solution shows that base of the box has a natural frequency of 2220 Hz. However, during the experiments the real behavior of the box can only be

observed up to 1750 Hz. Upto this frequency, the box has a rigid behavior and no natural frequency is observed.

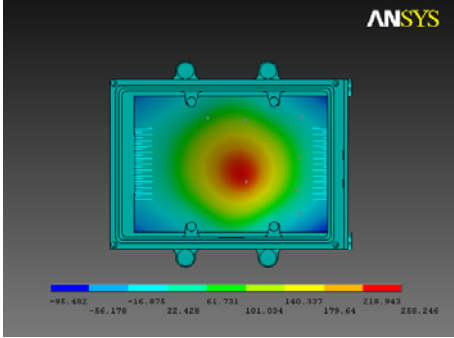
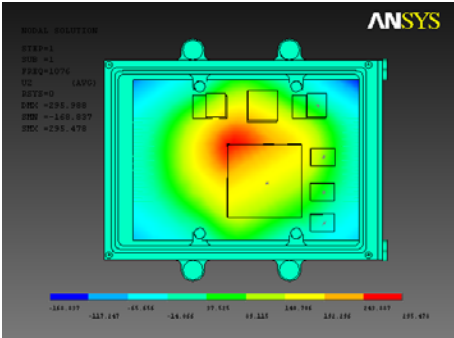
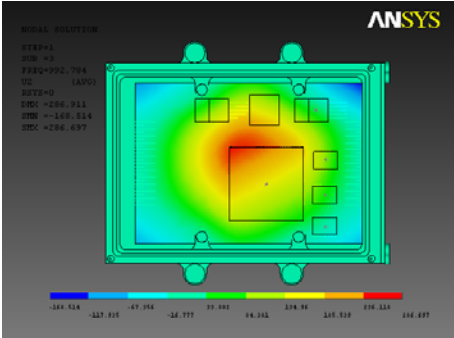
In the modal analysis performed by finite element program, for the box with the top cover four natural frequencies are obtained at 527 Hz, 980 Hz, 1217 Hz, and 1437 Hz. Results of the experiment of the top cover is affected from the fixture vibration after 1580 Hz. Therefore, after 1580 response of the top cover cannot be accurately read. However, up to 1580 Hz three natural frequencies were measured from the center of the top cover. These are 646 Hz, 773 Hz, and 1217 Hz. Consequently, it can be said that first three natural frequencies of the top cover are obtained in the experiment but the last one cannot be observed since it is in the frequency range where the fixture dynamics become apparent.

The last set of experiments was carried out with the whole assembly. However, in these experiments, top cover was not installed on the box, so that the accelerometers could attached to the PCB. Therefore, finite element analyses are also carried out for this configuration of the system. The first natural frequencies and mode shapes obtained for lumped, merged and lead wired components are presented in Table 22. The mass of the accelerometer is also included in these analyses as a lumped mass on the largest component, so that the comparison of theoretical and experimental results will be more meaningful.

Vibration measurements of the electronic assembly, which are taken over the largest component, depict four natural frequencies at 715 Hz, 903 Hz, 1177 Hz, and 1251 Hz. However, finite element solution gives only one mode for the assembly except the lumped mass model configuration.

The lumped component model configuration yields three natural frequencies in the frequency range of interest. The last two modes are shown in Figure 47.

Table 22. Natural frequencies and mode shapes of the test item with different component modeling approaches

| <p style="text-align: center;"><b>Lumped mass model: Components are modeled as lumped masses</b></p> |  |
|--|--|
| <p><i>First mode at</i><br/><math>f_n=755</math> Hz</p>  |    |
| <p style="text-align: center;"><b>Merged model: Component bodies are merged to PCB</b></p>           |  |
| <p><i>First mode at</i><br/><math>f_n=1076</math> Hz</p>   |   |
| <p style="text-align: center;"><b>Lead wired model: Components are modeled exactly</b></p>           |  |
| <p><i>First mode at</i><br/><math>f_n=993</math> Hz</p>  |  |

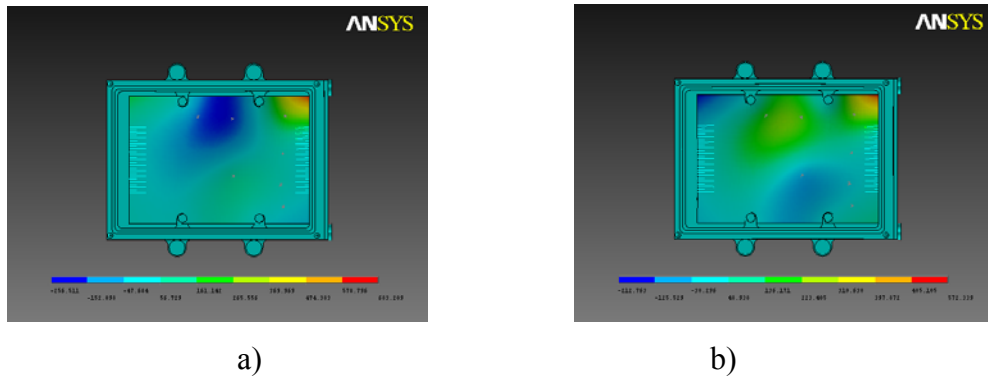


Figure 47. a) Second (1621 Hz) and b) third (1732 Hz) mode shapes of the PCB with lumped components in electronic box

Although the lumped configuration has the closest first natural frequency to the experiment results, the validity of this modeling shall be questioned. The shortcomings of the lumped component modeling are mentioned in previous sections. This approach disregards the stiffening effect of the component body. In addition to the stiffening effect, mass loading is applied to one point although it should be distributed over the board. The lack of stiffening effect and mass loading distribution probably leads to invalid results. Therefore, finite element solution of lumped configuration results in different vibration modes compared to those obtained from merged and lead wired configurations.

As a result, it is concluded that the best model for the electronic component on a PCB is the lead wired model. However, the finite element solution of the lead wired model only yields one natural frequency at 993 Hz. This natural frequency most probably corresponds to the second peak in the response graph of the PCB which occurs at 903 Hz in experiment 5. It can be said that most obvious mode in this experiment is the one that occurs at 903 Hz since it has a transmissibility value of 46.

To conclude, comparison of finite element results and experimentation revealed that, it is not always possible to obtain reliable results from the finite element analysis of a PCB in an electronic box. During design process finite element modeling can be used

to compare different approaches and design alternatives. Although it may not be easy to make an experimental study in each design and the experimental studies may also have their limitations, the necessity of experimentation should not be disregarded especially in complex designs.

## CHAPTER 5

### ANALYTICAL MODEL

In this chapter, analytical approaches to obtain vibration parameters and perform vibration analysis of electronic assemblies are proposed. First of all, electronic box is discussed briefly. Then, a discrete model representing first mode of the printed circuit board is introduced. Boundary conditions are specified for two different cases: (i) four edges fixed and (ii) four edges simply supported. Equivalent mass and equivalent spring constants are obtained for both boundary conditions. Next, two different component types are modeled in the same manner, and equivalent mass and equivalent spring constant representing the lead wires are calculated. After obtaining vibration parameters of electronic components, two degree of freedom spring mass models are suggested for PCB-component systems. These models are used to obtain natural frequencies and the response for a specific random vibration profile which belongs to jet aircraft store vibrations. Acceleration power spectral densities and root mean square values of acceleration are calculated. The finite element models of the same PCB-component configurations are also developed, and modal and spectral analyses are performed in ANSYS<sup>®</sup>. Finite element results are compared with those of the analytical solution and results are discussed.

#### 5.1 Electronic Box Vibration as a Rigid Body

From both finite element analyses and experimental results it was observed that the electronic box does not vibrate as a rigid body. Indeed, a simple model which consists of cap screws, which are used to mount box to the base, as elastic

connections and an equivalent mass representing the box yields very high natural frequencies which are far beyond the frequency range of interest. These frequencies are also much higher than the natural frequency of the box due to its plate like walls. Therefore, it is concluded that the vibration of the box as a rigid body is not important and will not be considered in the analytical model that will be developed.

## **5.2 Printed Circuit Board Vibration**

In this section, printed circuit board modeling is performed only for the first mode of vibration. A unit force is applied to the point which vibrates the most at the first mode and amount of static displacement is calculated for both fixed and simply supported boundaries. These displacements are used for calculating equivalent spring constants for both boundary conditions. Then, exact natural frequencies are calculated from natural frequency equations which can be found in literature. The natural frequency and spring constant are used for obtaining equivalent mass for fixed edge boundary condition. Equivalent mass of the simply supported printed circuit board is derived by assuming a velocity profile for the PCB displacement during vibration. The velocity profile is used for calculating corresponding kinetic energy from which the equivalent mass value is obtained.

The printed circuit board's natural frequencies calculated from a plate model will be compared with finite element solution results.

### **5.2.1 The Natural Frequency of a Plate**

Exact natural frequency formulations of continuous structures can be found in literature. Natural frequency formulation for a rectangular plate is given as follows [42]:

$$f_{ij} = \frac{\lambda_{ij}^2}{2 \cdot \pi \cdot a^2} \cdot \left[ \frac{E \cdot h^3}{12 \cdot \gamma \cdot (1 - \nu^2)} \right]^{1/2}; \quad i = 1, 2, 3, \dots, \quad j = 1, 2, 3, \dots, \quad (5.1)$$

where  $\lambda_{ij}$  is dimensionless parameter which is given as a function of the mode indices ( $i, j$ ), the plate geometry, and the boundary conditions,  $\nu$  is Poisson's ratio,  $\gamma$  is mass per unit area of the plate,  $a$  is the width of the plate and  $h$  is the thickness and  $E$  is the Young's Modulus.

### 5.2.2 Sandwich Plates

Sandwich plates consist of uniform layers of material which are glued together. Each layer is assumed to be homogenous and isotropic. The plate is symmetric about the mid-surface (Figure 48).

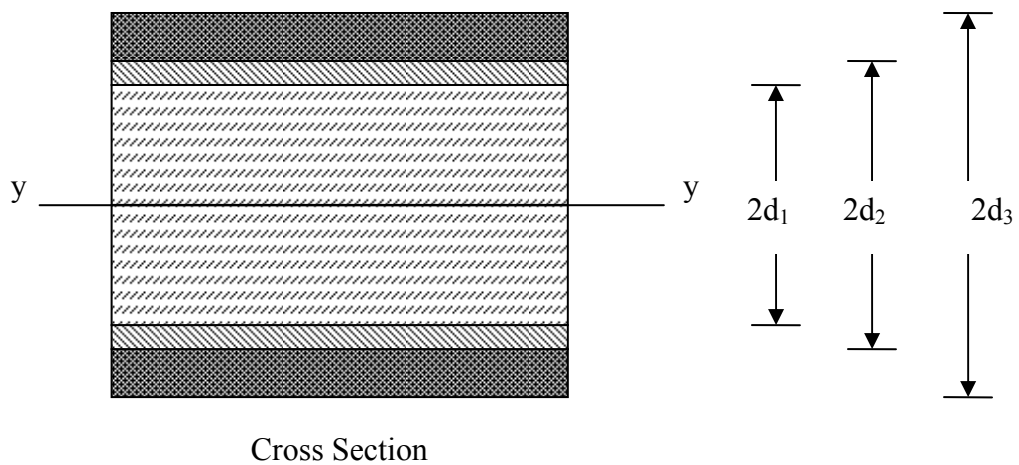


Figure 48. Sandwich plate [42]

If the sandwich plate is slender, that is, the thickness of the plate is small compared to typical lateral dimensions and to the distance between vibration nodes then it is reasonable to assume that normals to the mid-surface remain normal during vibration [42]. Using this assumption, the natural frequencies of slender sandwich plates can be computed by using the formulae developed for homogenous plates. The sandwich plate equivalent stiffness is expressed as [42]

$$\frac{E \cdot h^3}{12} = \frac{2}{3} \sum_{k=0,1,2,\dots} E_k \cdot (d_{k+1}^3 - d_k^3) \quad (5.2)$$

and equivalent mass per unit area can be calculated as [42],

$$\gamma = 2 \sum_{k=0,1,2,\dots} \mu_k \cdot (d_{k+1} - d_k) \quad (5.3)$$

where  $E_k$  and  $\mu_k$  are the modulus of elasticity and the density of the  $k$  layer.

Flexural rigidity of a plate is expressed as [43]

$$D = \frac{E \cdot h^3}{12 \cdot (1 - \nu^2)} \quad (5.4)$$

### 5.2.3 PCB Geometry and Material Properties

Printed circuit boards can be assumed as sandwich plates. The PCB which will be used in calculations is a 7 layered rectangular composite plate composed of copper and FR4 (Figure 49).

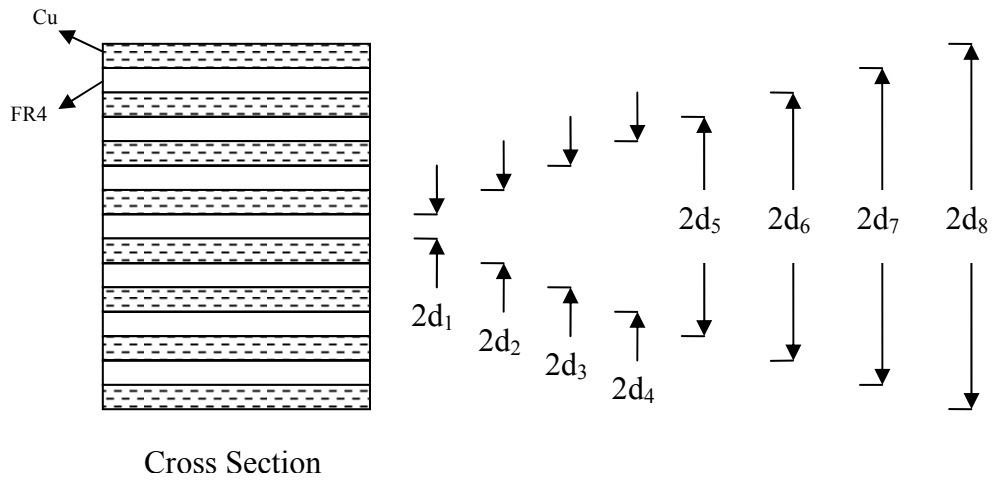


Figure 49. PCB layers

Geometric and material properties  $a$ ,  $b$ ,  $h$ ,  $E$ ,  $\nu$  and  $\mu$  are defined for the printed circuit board, representing length, width, thickness, Young's modulus, Poisson's ratio and mass density, respectively. The geometry is represented in Figure 50 and related dimensions are given in Table 23. Material properties of printed circuit board is taken from the manufacturer data and given in Table 24.

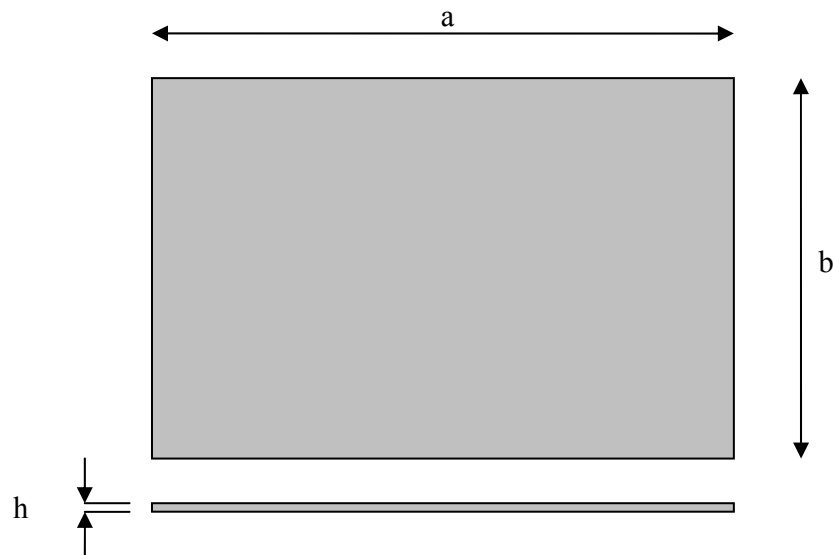


Figure 50. PCB geometry

Table 23. PCB dimensions

|                    | <b>Dimensions [mm]</b> |
|--------------------|------------------------|
| a                  | 100                    |
| b                  | 70                     |
| h                  | 1.60                   |
| Cu layer thickness | 0.035                  |

Table 24. Material properties of PCB laminas

|                              | <b>Copper</b> | <b>FR4</b> |
|------------------------------|---------------|------------|
| Modulus of Elasticity [MPa]  | 107900        | 18900      |
| Poisson's Ratio              | 0.3           | 0.3        |
| Density [kg/m <sup>3</sup> ] | 8900          | 1900       |

Flexural rigidity and mass per area of the printed circuit board is necessary for obtaining natural frequencies. For a sandwich plate, flexural rigidity is obtained from Equation (5.2) as

$$D = \frac{2}{3 \cdot (1 - \nu^2)} \cdot \left[ \begin{array}{l} E_{FR4} \cdot (d^3_1 - d^3_0) + E_{Cu} \cdot (d^3_2 - d^3_1) + E_{FR4} \cdot (d^3_3 - d^3_2) \dots \\ + E_{Cu} \cdot (d^3_4 - d^3_3) + E_{FR4} \cdot (d^3_5 - d^3_4) + E_{Cu} \cdot (d^3_6 - d^3_5) \dots \\ + E_{FR4} \cdot (d^3_7 - d^3_6) + E_{Cu} \cdot (d^3_8 - d^3_7) \end{array} \right] \quad (5.5)$$

where  $\nu$  is Poisson's ratio,  $E$  is Young's Modulus and  $d_i$  is thickness defined in Figure 49.

For a sandwich plate, mass per unit area can be calculated from Equation (5.3) as

$$\gamma = 2 \cdot \left[ \begin{array}{l} \mu_{FR4} \cdot (d_1 - d_0) + \mu_{Cu} \cdot (d_2 - d_1) + \mu_{FR4} \cdot (d_3 - d_2) + \mu_{Cu} \cdot (d_4 - d_3) \dots \\ + \mu_{FR4} \cdot (d_5 - d_4) + \mu_{Cu} \cdot (d_6 - d_5) + \mu_{FR4} \cdot (d_7 - d_6) + \mu_{Cu} \cdot (d_8 - d_7) \end{array} \right] \quad (5.6)$$

where  $\mu$  is mass density,  $E$  is Young's Modulus and  $d_i$  is thickness defined in Figure 49.

#### 5.2.4 Discrete Modeling of PCB

In order to develop a discrete model representing the first mode of a printed circuit board, equivalent mass and spring constants should be obtained. In this part, two cases with different boundary conditions are presented: fixed and simply supported boundary conditions.

##### 5.2.4.1 PCB with Fixed Edges

Consider the rectangular printed circuit board whose geometric and material properties are given above with fixed boundary conditions at four edges as shown in Figure 51. For equivalent stiffness and mass calculations, one should apply a unit force to the point of interest and obtain deformation which yields the stiffness value.

When force is applied to the center point of a rectangular plate with fixed edges maximum deflection value, which occurs at the center, is given as [43]

$$W_{\max} = c_1 \cdot \frac{P \cdot b^2}{D} \quad (5.7)$$

where  $c_1$  is a constant depending on  $a/b$  ratio and  $P$  is the applied force.

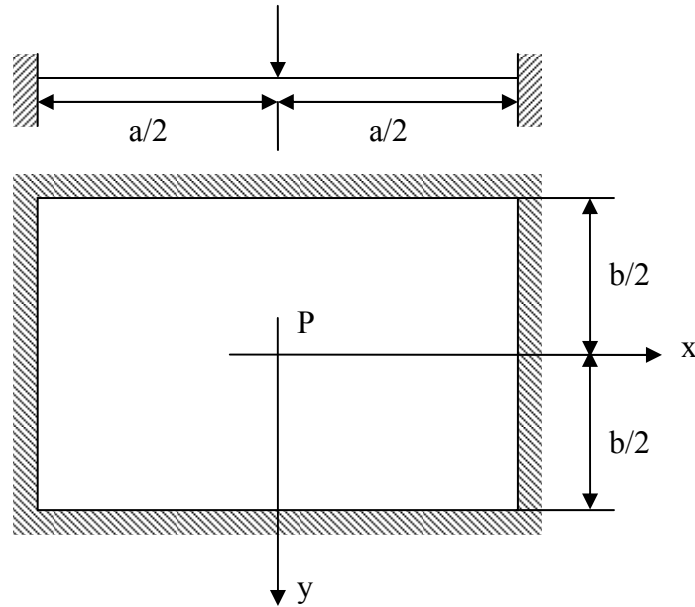


Figure 51. Point Load on the PCB with Fixed Edges

In the first mode, maximum deflection will occur at the center of the PCB with fixed edges. If a unit force is applied to the center point and deflection is calculated equivalent spring constant for the first mode of the PCB can be obtained. Equivalent spring constant for the first mode will be

$$k_{eq} = \frac{F}{w} \tag{5.8}$$

Now, if we calculate the exact natural frequency of PCB by using Equation 5.1, then the equivalent mass of the PCB can be calculated from

$$\omega_n = \sqrt{\frac{k_{eq}}{m_{eq}}} \tag{5.9}$$

For the fixed edged PCB, the equivalent stiffness, equivalent mass and first natural frequency values calculated by applying the procedure given here are tabulated in Table 25.

Table 25. First natural frequency and vibration parameter of PCB with fixed edges

| Equivalent stiffness<br>[N/m] | First natural frequency<br>[Hz] | Equivalent mass<br>[kg] |
|-------------------------------|---------------------------------|-------------------------|
| 412574                        | 1530                            | $4.47 \cdot 10^{-3}$    |

From these results it is observed that entire mass of the PCB does not contribute to the first mode. This is expected since PCB is a continuous plate structure and does not vibrate as a rigid body. The equivalent mass of the PCB is compared to the total PCB mass by obtaining entire mass of the printed circuit board:

$$m_{PCB} = \gamma \cdot a \cdot b \quad (5.10)$$

Then it is observed that the equivalent mass in the model representing the first mode is only 12.8% of the total mass:

$$m_{eq} = 0.128 \cdot m_{PCB} \quad (5.11)$$

#### 5.2.4.2 PCB with Simply Supported Edges

As a second case, consider a printed circuit board with the same geometry and material properties as defined above but with simply supported edges, as shown in Figure 52.

Deflection equation for a plate with simply supported edges is given by [43]

$$w(x,y) = \frac{4 \cdot P}{D \cdot \pi^4 \cdot a \cdot b} \sum_m \sum_n \frac{\sin\left(\frac{m\pi\xi}{a}\right) \cdot \sin\left(\frac{n\pi\eta}{b}\right) \cdot \sin\left(\frac{m\pi x}{a}\right) \cdot \sin\left(\frac{n\pi y}{b}\right)}{\left(\frac{m^2}{a^2} + \frac{n^2}{b^2}\right)^2} \quad (5.12)$$

where  $w$  is deflection,  $P$  is the force applied,  $D$  is flexural rigidity.  $\xi$  and  $\eta$  define the application point of the forcing.

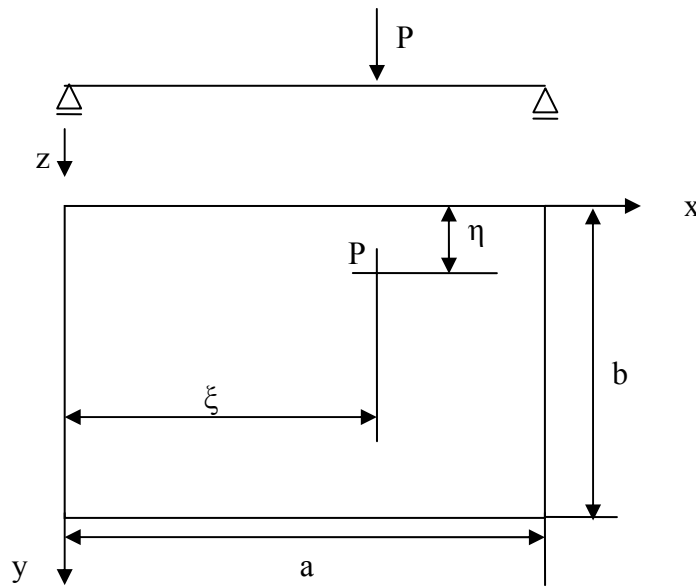


Figure 52. Point Load on the PCB with Simply Supported Edges

Since the center point will deflect the most in the first mode of vibration of a PCB with simply supported edges, a unit force will be applied to the center and deflection at this point of the PCB is calculated. This value is used to calculate equivalent stiffness of the printed circuit board as in the case of fixed boundary condition. Then, first natural frequency is calculated from Equation (5.1). Equivalent mass can be obtained from these calculated values as in the previous case. However, in this case equivalent mass is formulated with a different approach.

Inertia effect of a simply supported printed circuit board is formulated by assuming a velocity distribution during vibration the same as the static deflection curve.

The velocity profile which is assumed in the same form with the deflection curve given in Equation (5.12) can be written as:

$$\dot{w}(x, y) = C \cdot \sum_m \sum_n \frac{\sin\left(\frac{m\pi\xi}{a}\right) \cdot \sin\left(\frac{n\pi\eta}{b}\right) \cdot \sin\left(\frac{m\pi x}{a}\right) \cdot \sin\left(\frac{n\pi y}{b}\right)}{\left(\frac{m^2}{a^2} + \frac{n^2}{b^2}\right)^2} \quad (5.13)$$

Then, the velocity profile can be expressed in terms of the velocity of point P,  $\dot{w}(\xi, \eta) = \dot{w}_p$ , by first calculating the unknown constant C from

$$\dot{w}_p = C \cdot \sum_m \sum_n \frac{\sin^2\left(\frac{m\pi\xi}{a}\right) \cdot \sin^2\left(\frac{n\pi\eta}{b}\right)}{\left(\frac{m^2}{a^2} + \frac{n^2}{b^2}\right)^2} \quad (5.14)$$

as

$$C = \dot{w}_p \cdot \frac{1}{\sum_m \sum_n \frac{\sin^2\left(\frac{m\pi\xi}{a}\right) \cdot \sin^2\left(\frac{n\pi\eta}{b}\right)}{\left(\frac{m^2}{a^2} + \frac{n^2}{b^2}\right)^2}} \quad (5.15)$$

If Equation (5.15) is substituted into Equation (5.13), the velocity profile for the PCB with simply supported boundary conditions is obtained as:

$$\dot{w}(x, y) = \dot{w}_p \cdot \frac{1}{\sum_m \sum_n \frac{\sin^2(\frac{m\pi\xi}{a}) \cdot \sin^2(\frac{n\pi\eta}{b})}{\left(\frac{m^2}{a^2} + \frac{n^2}{b^2}\right)^2}} \cdot \sum_m \sum_n \frac{\sin(\frac{m\pi\xi}{a}) \cdot \sin(\frac{n\pi\eta}{b}) \cdot \sin(\frac{m\pi x}{a}) \cdot \sin(\frac{n\pi y}{b})}{\left(\frac{m^2}{a^2} + \frac{n^2}{b^2}\right)^2} \quad (5.16)$$

Now, the kinetic energy of the PCB with simply supported boundary conditions can be calculated by utilizing the velocity profile of the plate. Kinetic energy of incremental board area (dm) is given as:

$$dT_{PCB} = \frac{1}{2} \cdot dm \cdot [\dot{w}(x, y)]^2 \quad (5.17)$$

If the mass of the PCB is assumed as distributed uniformly through the PCB, the incremental board area (dm) is given as:

$$dm = \frac{m}{a \cdot b} \cdot dx \cdot dy \quad (5.18)$$

$$dm = \gamma \cdot dx \cdot dy \quad (5.19)$$

Total kinetic energy of the printed circuit board is obtained by integrating the incremental kinetic energy as follows:

$$T_{PCB} = \int dT_{PCB} = \int_0^a \int_0^b \frac{1}{2} \cdot \gamma \cdot [\dot{w}(x, y)]^2 \cdot dy \cdot dx \quad (5.20)$$

Since it is aimed to formulate the inertia effect with respect to point P, the equivalent kinetic energy is written as:

$$T_{PCB} = \frac{1}{2} \cdot m_{eq} \cdot \dot{w}_p^2 \quad (5.21)$$

From the equality of Equation (5.20) and (5.21), the equivalent mass of the printed circuit board can be formulated as:

$$m_{eq} = \frac{\gamma}{\left[ \sum_m \sum_n \frac{\sin^2\left(\frac{m\pi\xi}{a}\right) \cdot \sin^2\left(\frac{n\pi\eta}{b}\right)}{\left(\frac{m^2}{a^2} + \frac{n^2}{b^2}\right)^2} \right]^2} \cdot \int_0^a \int_0^b \left[ \sum_m \sum_n \frac{\sin\left(\frac{m\pi\xi}{a}\right) \cdot \sin\left(\frac{n\pi\eta}{b}\right) \cdot \sin\left(\frac{m\pi x}{a}\right) \cdot \sin\left(\frac{n\pi y}{b}\right)}{\left(\frac{m^2}{a^2} + \frac{n^2}{b^2}\right)^2} \right]^2 \cdot dy \cdot dx \quad (5.22)$$

This formulation can be used for obtaining the equivalent mass of the printed circuit board with simply supported boundary conditions for any  $\xi$ ,  $\eta$ ,  $a$  and  $b$  values.

Using the procedure described above the equivalent stiffness, equivalent mass and first natural frequency of the PCB with simply supported boundary conditions are calculated. The results obtained are tabulated in Table 26.

Table 26. The equivalent stiffness, equivalent mass and first natural frequency of PCB with simply supported edges

| Equivalent stiffness<br>[N/m] | Equivalent mass<br>[kg] | First natural frequency<br>[Hz] |
|-------------------------------|-------------------------|---------------------------------|
| 199203                        | $7.69 \cdot 10^{-3}$    | 810                             |

The natural frequencies calculated from the simple analytical model are compared with finite element results. Printed circuit board is modeled with shell element SHELL99 of ANSYS<sup>®</sup> and solved for both fixed and simply supported edges. Results are tabulated in Table 27.

Table 27. Analytical and finite element solution comparison of PCB natural frequencies

| Fixed Edges           |                         | Simply Supported Edges |                         |
|-----------------------|-------------------------|------------------------|-------------------------|
| Analytical Solution   | Finite Element Solution | Analytical Solution    | Finite Element Solution |
| 1529 Hz               | 1513 Hz                 | 810 Hz                 | 803 Hz                  |
| <i>Error = 1.05 %</i> |                         | <i>Error = 0.86 %</i>  |                         |

### 5.3 Discrete Modeling of Electronic Component

Vibration of electronic components is important in two main aspects: (i) they may have serious effects on vibration characteristics of PCB and (ii) they usually limit life of the electronic system due to fatigue failure of components. Therefore it is necessary to include electronic components in vibration analysis. In order to be able to study the vibration of a component itself, it is necessary to model the electronic component and its connection to the PCB. In case of leaded components, their stiffness coefficients can be calculated by analyzing lead wire deflection. Component body can be taken as a rigid body when its flexibility is compared with that of the lead wires. Then it will only have an inertia effect.

Component lead wires can be assumed as beam structures. Their equivalent stiffness coefficients can be obtained from beam deflections for transverse and longitudinal vibrations.

The ratio of the applied force to the deflection gives the equivalent spring constant for a cantilever beam in transverse vibrations as:

$$k = \frac{3 \cdot E \cdot I}{L^3} \quad (5.23)$$

In longitudinal vibrations; equivalent spring constant is expressed as:

$$k = \frac{E \cdot A}{L} \quad (5.24)$$

Equations (5.23) and (5.24) for equivalent spring constants will be used in following sections to construct a mathematical model for an oscillator and an integrated circuit, respectively.

### 5.3.1 Case Study I-An Oscillator

The methodology described in previous section is firstly used to model a leaded component which is mounted over the center of the PCB. The leaded component is an oscillator which is given in Figure 53. This oscillator is modeled as a mass and spring system. The component has four lead wires made of copper alloy. Properties are given in Table 28.

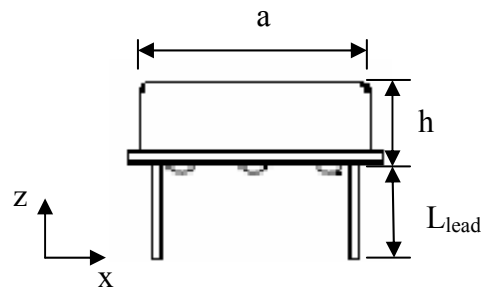


Figure 53. Oscillator front view

Table 28. Oscillator properties

|   |  |
|---|--|
| Modulus of elasticity (E) of lead wire                        | 131 GPa                                  |
| Mass of the component body ( $m_c$ )                          | 1.95 g                                   |
| Length of lead wire ( $L_{lead}$ )                            | 6.8 mm                                   |
| Cross sectional area of lead wire                             | 0.16 mm <sup>2</sup>                     |
| Width (a) and length of the component body                    | 12.9 mm                                  |
| Height of the component body (h)                              | 5.3 mm                                   |
| Area moment of inertia of component body ( $I_{xx}, I_{yy}$ ) | 31.61·10 <sup>-9</sup> kg.m <sup>2</sup> |

Under base excitation in z direction, component's lead wire stiffness should be calculated only in longitudinal direction. Equivalent stiffness coefficient for one lead wire is obtained from Equation (5.24). Stiffness values obtained are presented in Table 29.

Table 29. Oscillator properties

|                                  |       |
|----------------------------------|-------|
| Stiffness for 1 lead wire [N/m]  | 3064  |
| Stiffness for 4 lead wires [N/m] | 12256 |

After obtaining equivalent stiffness values of the lead wires, spring mass model of the component is constructed. Firstly, 3 degree of freedom model is constructed in

order to see whether tilt modes are important. Constructed model is given in Figure 58.

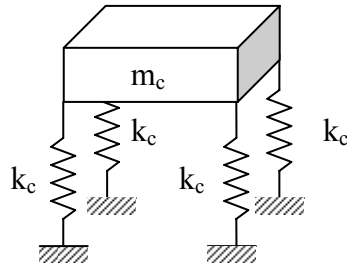


Figure 54. Three dof model of oscillator

Mass and stiffness matrices of the 3 dof model are given respectively as follows:

$$[M] = \begin{pmatrix} m_c & 0 & 0 \\ 0 & I_{xx} & 0 \\ 0 & 0 & I_{yy} \end{pmatrix} \quad (5.25)$$

$$[K] = \begin{pmatrix} k_c & 0 & 0 \\ 0 & 2.L.k_c & 0 \\ 0 & 0 & 2.L.k_c \end{pmatrix} \quad (5.26)$$

The natural frequency of the system can be obtained from the solution of the eigenvalue problem:

$$[K]\{u\} = \omega^2 [M]\{u\} \quad (5.27)$$

Solution of the eigenvalue problem gives the three natural frequencies of the system, which are tabulated in Table 30.

Table 30. Natural frequency values for integrated circuit

|            |           |
|------------|-----------|
| $f_1$      | 12615 Hz  |
| $f_2, f_3$ | 251605 Hz |

These results show that modeling the component as a three degree of freedom system is not necessary since the tilt modes are too high. Furthermore since even the first natural frequency is very high compared to the natural frequencies of the PCB, it can easily be seen that taking the component as a rigid body directly connected to the PCB is not a bad simplification. Yet, in order to see a possible coupling effect, the PCB and the component are modeled as a two degree of freedom system (Figure 55).

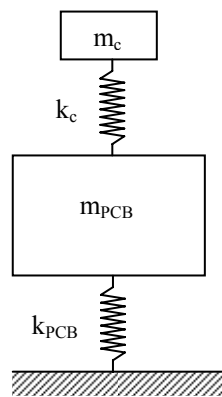


Figure 55. Discrete model of PCB and oscillator

Two degree of freedom model of PCB and oscillator is used to find the natural frequencies. Mass and stiffness matrices of the system are given as

$$[M] = \begin{pmatrix} m_{PCB} & 0 \\ 0 & m_c \end{pmatrix} \quad (5.28)$$

$$[K] = \begin{pmatrix} k_{PCB} + k_C & -k_C \\ -k_C & k_C \end{pmatrix} \quad (5.29)$$

Solution of characteristic equation yields the natural frequencies of the system which are tabulated both for fixed and simply supported edge conditions in Table 31.

Table 31. Natural frequency values for oscillator and PCB system

| Fixed BC <sup>s</sup> |            | Simply supported BC <sup>s</sup> |            |
|-----------------------|------------|----------------------------------|------------|
| $f_1$ [Hz]            | $f_2$ [Hz] | $f_1$ [Hz]                       | $f_2$ [Hz] |
| 1270                  | 15141      | 725                              | 14126      |

From Table 31 it is clearly observed that the second mode has a very high frequency and uncoupled from the first mode which represents PCB vibrations. If the component is taken as rigidly connected to PCB, the natural frequency of the system can be obtained by adding component's mass to the equivalent mass of the PCB ( $m_{PCB}$ ). Results for lumped mass assumption are given in Table 32.

$$f_n = \sqrt{\frac{k_{PCB}}{m_{PCB} + m_c}} \quad (5.30)$$

Table 32. First natural frequency values for integrated circuit and PCB system obtained by lumped mass model

| Fixed BC <sup>s</sup> | Simply supported BC <sup>s</sup> |
|-----------------------|----------------------------------|
| 1276 [Hz]             | 724 [Hz]                         |

Comparison of these results with those in Table 31 clearly shows that oscillator can easily be taken as rigidly fixed to the PCB in studying vibrations of the PCB.

### 5.3.2 Case Study II-An Integrated Circuit

As a second example, an integrated circuit given in Figure 56 is modeled as a mass-spring system and natural frequencies are obtained. The component has 60 pins at each edge. Lead wire material is C7025 [44], a copper alloy usually preferred as a pin material. Component lead wires are taken as beams and equivalent stiffness coefficients are calculated. Component body is taken as a lumped mass.

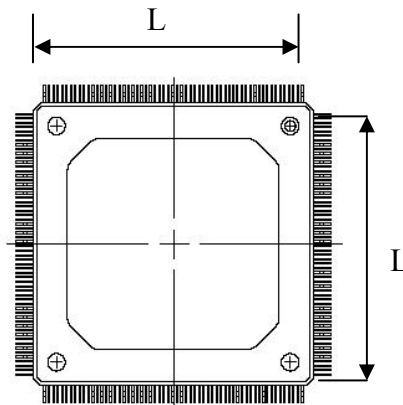


Figure 56. Integrated Circuit Top View [28]

Component lead wire geometry is given in Figure 57. As can be seen from the figure, the wire can be considered in two parts. Equivalent stiffness of part 1 is obtained by considering the transverse vibration of the wire, and equivalent stiffness of part 2 is obtained by considering longitudinal vibrations. These two beams are connected to each other in series. Geometric and material properties of lead wire are given in Table 33. Stiffness values are presented in Table 34.

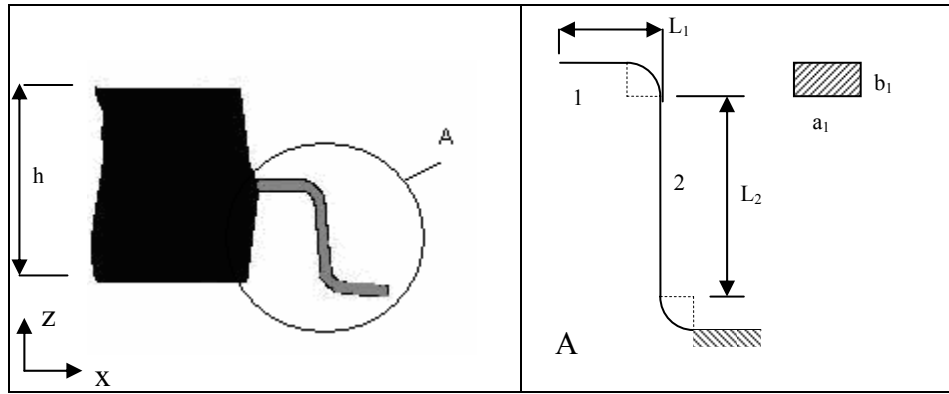


Figure 57. Lead wire geometry of the integrated circuit [44]

Table 33. Lead wire properties

|   |                                     |
|---|-------------------------------------|
| Modulus of Elasticity (E)                                 | 131 GPa                             |
| Mass of the component body                                | 7.31 g                              |
| Lead wire length ( $L_1$ )                                | 0.2 mm                              |
| Lead wire length ( $L_2$ )                                | 1.8 mm                              |
| $a_1$   | 0.27 mm                             |
| $b_1$   | 0.2 mm                              |
| Width and length of the component body (L)                | 32 mm                               |
| Height of the component body (h)                          | 3.4 mm                              |
| Area moment of inertia of component body $I_{xx}, I_{yy}$ | $6.31 \cdot 10^{-7} \text{ kg.m}^2$ |

Table 34. Spring constant for IC's lead wire

|                                    | Equivalent stiffness<br>in transverse<br>direction<br>[N/m] | Equivalent stiffness<br>in longitudinal<br>direction<br>[N/m] | Resultant Stiffness<br>[N/m] |
|------------------------------------|---|---|------------------------------|
| For 1 Lead<br>Wire                 | $262 \cdot 10^4$  | $393 \cdot 10^4$  | $1572 \cdot 10^3$            |
| For 1 Edge<br>(60 lead<br>wires)   | $15720 \cdot 10^4$  | $23580 \cdot 10^4$  | $9432 \cdot 10^4$            |
| For 4 Edges<br>(240 lead<br>wires) | $6288 \cdot 10^5$   | $9432 \cdot 10^5$   | $37728 \cdot 10^4$           |

Spring constants appeared to be too high compared to PCB's spring constant. It can be concluded that component will act as a rigid mass attached to PCB. However it can be useful to see components natural frequencies and PCB-component system vibration in order to justify the rigid connection assumption for a component.

Spring mass model of the component is given in Figure 58. Here, first three modes of the component will be determined.

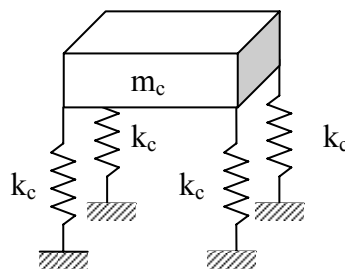


Figure 58. Three dof model of integrated circuit

Mass and stiffness matrices are given, respectively, as follows

$$[M] = \begin{pmatrix} m_c & 0 & 0 \\ 0 & I_{xx} & 0 \\ 0 & 0 & I_{yy} \end{pmatrix} \quad (5.31)$$

$$[K] = \begin{pmatrix} k_c & 0 & 0 \\ 0 & 2.L.k_c & 0 \\ 0 & 0 & 2.L.k_c \end{pmatrix} \quad (5.32)$$

From the solution of the resulting eigenvalue problem the natural frequencies of the first three modes can be calculated. The results are given in Table 35.

Table 35. Natural frequency values for integrated circuit

|            |           |
|------------|-----------|
| $f_1$      | 36157 Hz  |
| $f_2, f_3$ | 492263 Hz |

As in the oscillator example, integrated circuit results show that modeling component as a three degree of freedom system is not necessary because tilt modes are too high. In addition to this result, when the first natural frequency is compared to PCB natural frequencies it is observed that component can be taken as rigidly connected to the PCB for vibration analysis of the PCB. This can also be shown by modeling PCB and component as a two degree of freedom system. Furthermore, it should be noted that in this case it is not suitable to use equivalent stiffness and mass properties of PCBs since they are calculated for the maximum displacement point which is the center. The reason is that the integrated circuit is very large compared to the oscillator, and lead wire connection points are far away from the center of the PCB.

This condition results in different deformation in every lead wire which cannot be represented by previously presented mathematical model.

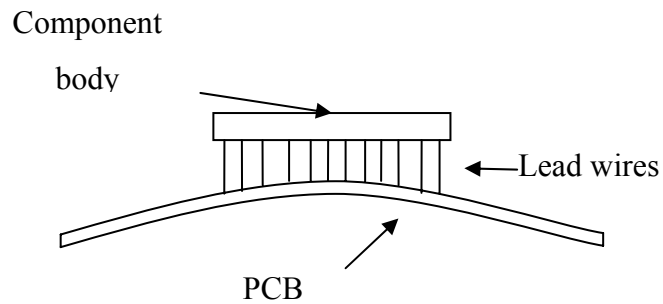


Figure 59. Side view of lead wire deflection for large components

#### 5.4 Random Vibration Analysis of the Analytical Model

Most of the military platforms create random vibration excitations. Therefore random vibration requirements should be met by the military systems which include electronic equipments.

In this section, random vibration analysis by using the analytical model is performed in order to obtain vibration response in real working environment.

Random vibration values corresponding to the input calculated from given specification for aircraft store equipment in MIL-STD-810F [45] are given in Figure 60.

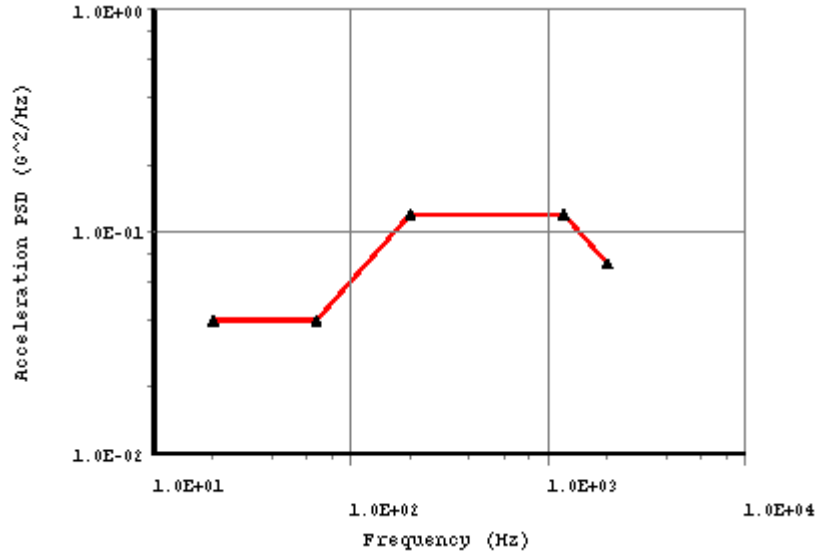


Figure 60. Random vibration input

#### 5.4.1 Transmission of Random Vibration

Transmission of random vibrations through stable linear systems causes change in characteristics of the input vibrations. This change can be observed from input/output relationship which is expressed below [46]:

$$S_y(\omega) = \sum_{r=1}^N \sum_{s=1}^N H_r^*(\omega) \cdot H_s(\omega) \cdot S_{x_r x_s}(\omega) \quad (5.33)$$

where  $S(\omega)$  is spectral density,  $H(\omega)$  is frequency response function, and  $*$  denotes complex conjugate.

In case of response to single input, expression (5.33) becomes:

$$S_y(\omega) = H^*(\omega) \cdot H(\omega) \cdot S_x(\omega) \quad (5.34)$$

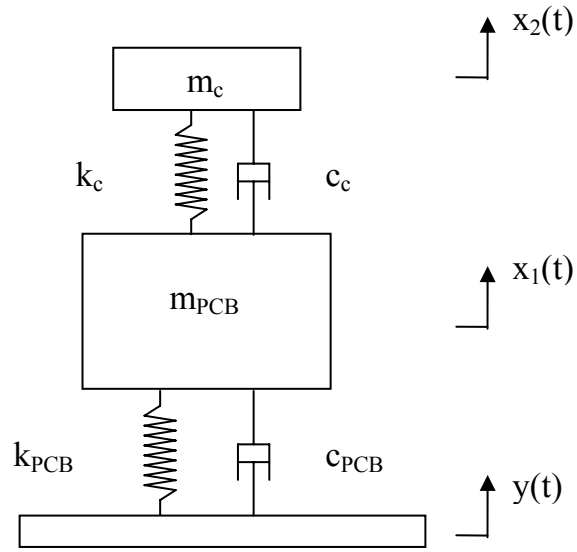


Figure 61. PCB and component 2 dof model

Mass, damping and stiffness matrices for two degree of freedom PCB-component model given in Figure 61, are given below:

$$[M] = \begin{pmatrix} m_{PCB} & 0 \\ 0 & m_c \end{pmatrix} \quad (5.35)$$

$$[C] = \begin{pmatrix} c_{PCB} & -c_c \\ -c_c & c_c \end{pmatrix} \quad (5.36)$$

$$[K] = \begin{pmatrix} k_{PCB} & -k_c \\ -k_c & k_c \end{pmatrix} \quad (5.37)$$

Equation of motion of the system in matrix form can be written as

$$[M] \cdot \{\ddot{x}\} + [C] \cdot \{\dot{x}\} + [K] \cdot \{x\} = \{F\} \quad (5.38)$$

Inserting mass, damping and stiffness matrices into Equation (5.38) gives

$$\begin{pmatrix} m_{PCB} & 0 \\ 0 & m_c \end{pmatrix} \begin{Bmatrix} \ddot{x}_1 \\ \ddot{x}_2 \end{Bmatrix} + \begin{pmatrix} c_{PCB} + c_c & -c_c \\ -c_c & c_c \end{pmatrix} \begin{Bmatrix} \dot{x}_1 \\ \dot{x}_2 \end{Bmatrix} + \begin{pmatrix} k_{PCB} + k_c & -k_c \\ -k_c & k_c \end{pmatrix} \begin{Bmatrix} x_1 \\ x_2 \end{Bmatrix} = \begin{Bmatrix} c_1 \dot{y} + k_1 y \\ 0 \end{Bmatrix} \quad (5.39)$$

$$m_{PCB} \cdot \ddot{x}_1 + (c_{PCB} + c_c) \cdot \dot{x}_1 - c_c \cdot \dot{x}_2 + (k_{PCB} + k_c) \cdot x_1 - k_c \cdot x_2 = c_1 \dot{y} + k_1 y \quad (5.40)$$

$$m_c \cdot \ddot{x}_2 - c_c \cdot \dot{x}_1 + c_c \cdot \dot{x}_2 - k_c \cdot x_1 - k_c \cdot x_2 = 0 \quad (5.41)$$

Transmissibility between PCB and the component is calculated as

$$H_1(\omega) = \frac{k_2 + i \cdot \omega \cdot c_2}{(k_2 - \omega^2 \cdot m_2) + i \cdot \omega \cdot c_2} \quad (5.42)$$

Transmissibility between base and the component is calculated as

$$H_2(\omega) = \frac{(k_1 + i \cdot \omega \cdot c_1) \cdot (k_2 + i \cdot \omega \cdot c_2)}{\left\{ [-\omega^2 \cdot m_1 + i \cdot \omega \cdot (c_1 + c_2) + (k_1 + k_2)](k_2 - \omega^2 \cdot m_2 + i \cdot \omega \cdot c_2) - (k_2 + i \cdot \omega \cdot c_2)^2 \right\}} \quad (5.43)$$

These equations are used to calculate random vibration response of oscillator-PCB system with zero damping and results obtained for the PCB with fixed edges and the PCB with simply supported edges are given in Figure 62 and Figure 63, respectively.

Peak values in the graphs which occur at natural frequencies, are tabulated in Table 36.

Power spectral density graphs have large peaks at natural frequencies since the system is solved for an undamped case.

Table 36. Natural frequency result of analytical model

|           |                      |
|-----------|----------------------|
| Fixed PCB | Simply supported PCB |
| 1274 Hz   | 723 Hz               |

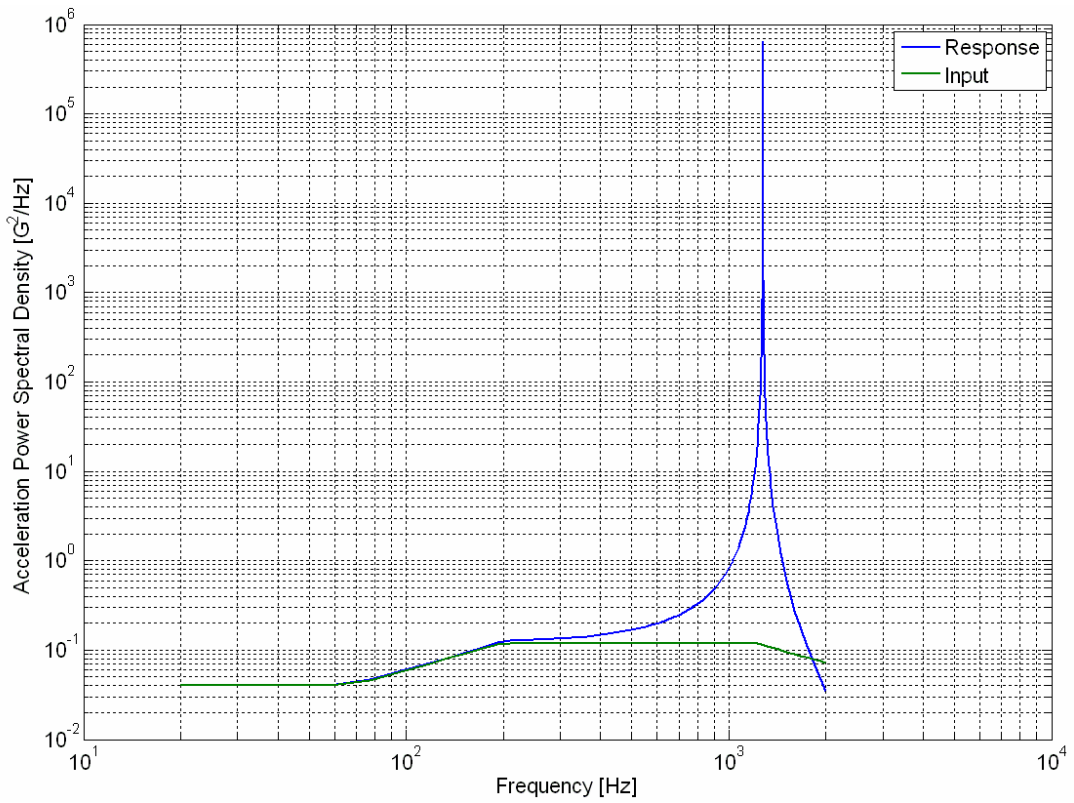


Figure 62. Random vibration response of oscillator bonded over fixed PCB

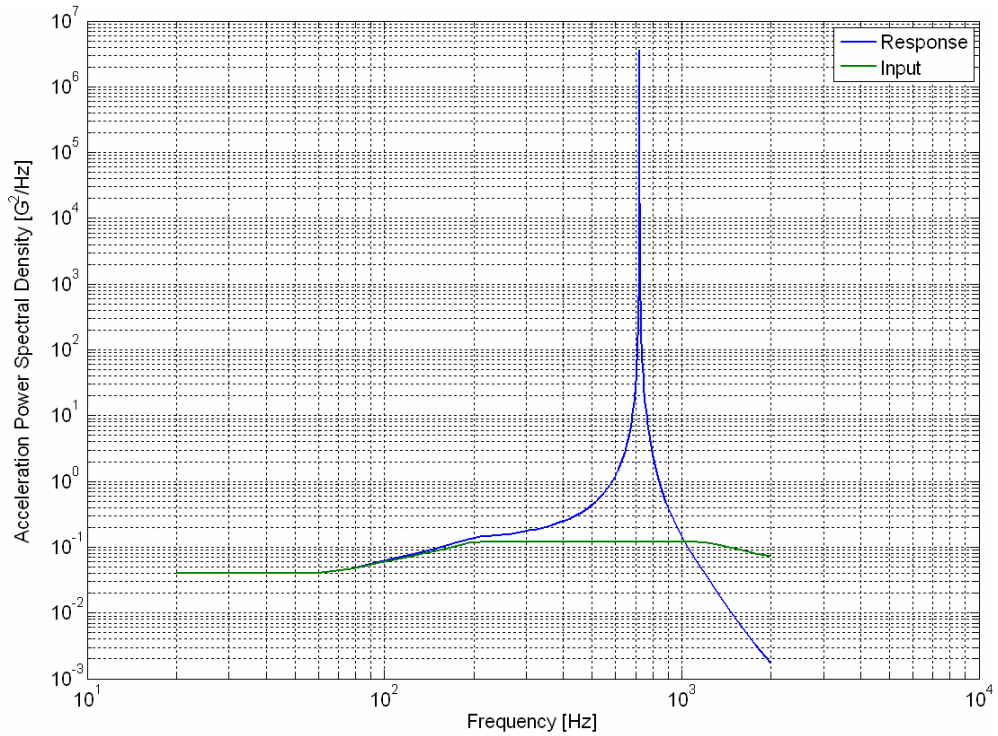


Figure 63. Random vibration response of oscillator bonded over simply supported PCB

## 5.5 Validation of the Model

The validity of the model is checked by finite element analysis. The same printed circuit board and oscillator is modeled in ANSYS<sup>®</sup>. The PCB is modeled with shell element SHELL99, lead wires are modeled with beam element BEAM188 and component body is modeled as a rigid structure with SOLID92 element of ANSYS<sup>®</sup>. Modal analysis and spectral analysis are performed. Natural frequency and  $g_{rms}$  values are obtained. First mode shape of the PCB assembly is given in Figure 64.

One important point about the finite element solution is that the spectral analysis requires a damping value in order to have a solution. However, damping value of the system is not known. Therefore, damping values given in literature are studied and a loss factor of 0.01 is used [20].

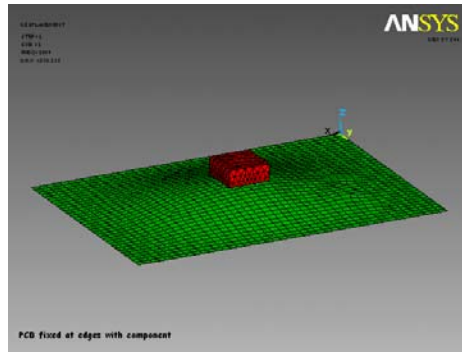


Figure 64. Finite element model of oscillator bonded over PCB

Power spectral density graphs are given in Figure 65 for PCB with fixed edges and in Figure 66 for PCB with simply supported edges, respectively.

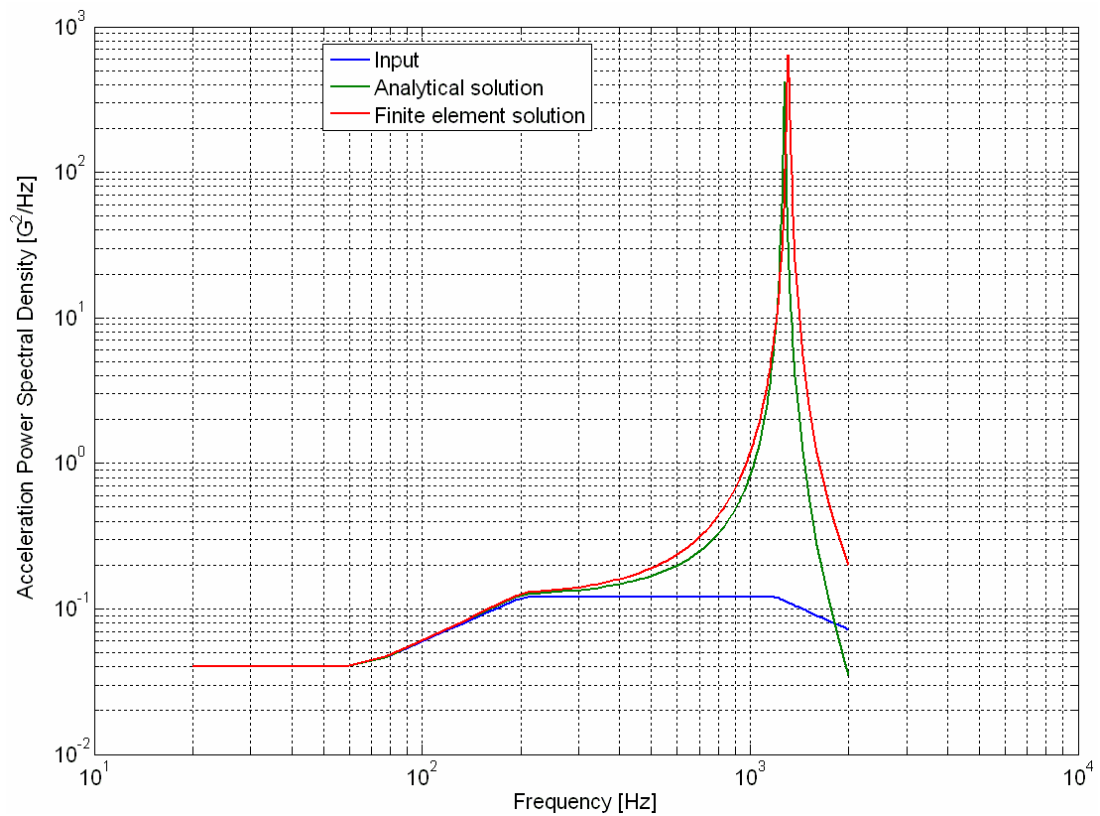


Figure 65. Oscillator response comparison of analytical model and finite element solution for fixed PCB

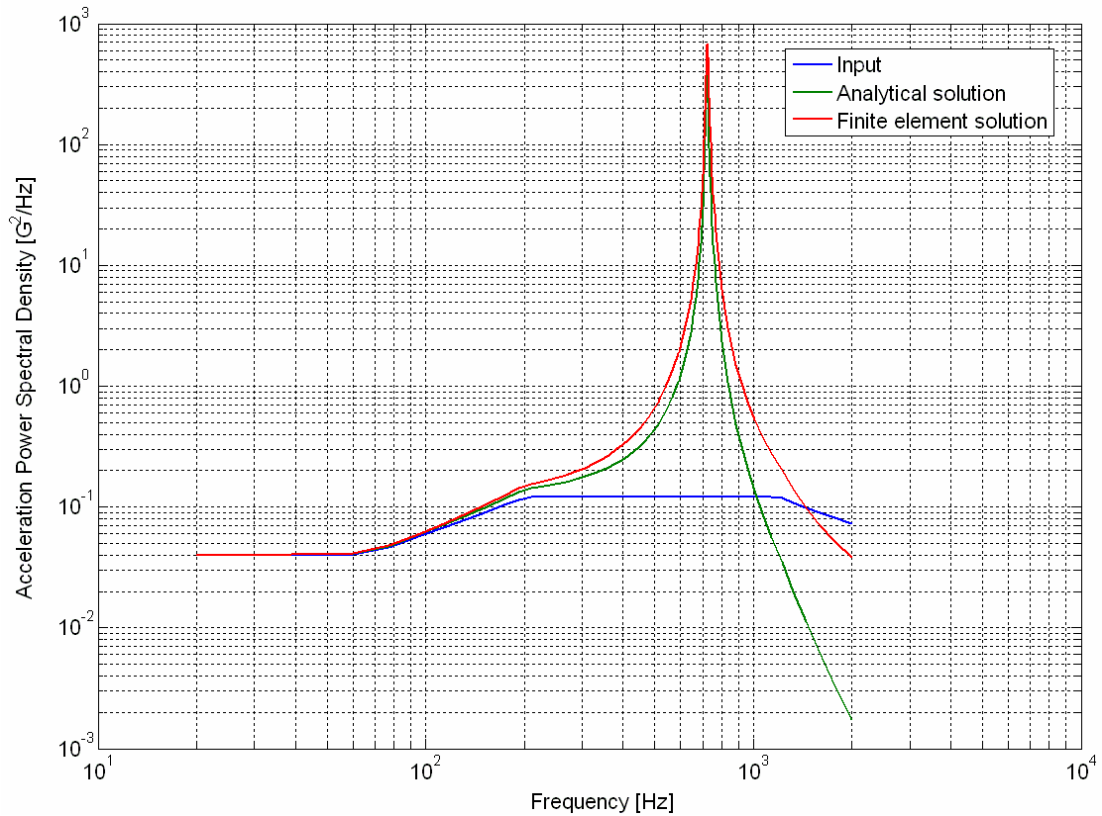


Figure 66. Oscillator response comparison of analytical model and finite element solution for simply supported PCB

The graphs in Figure 65 and Figure 66 show acceleration input and response of the system which is obtained by finite element model and analytical model.

It is observed from these graphs that natural frequencies are very close to each other and power spectral density values have a reasonable match, except at frequencies higher than 1000 Hz. Natural frequencies are given in Table 37 for comparison.

Table 37. Natural frequency comparison between analytical and finite element solution

| <i>PCB with Fixed Edges</i>            |                       |                                       |
|--|-----------------------|---------------------------------------|
| Analytical result                      | Finite element result | Difference from finite element result |
| 1270 Hz                                | 1309 Hz               | 2.7 %                                 |
| <i>PCB with Simply Supported Edges</i> |                       |                                       |
| Analytical result                      | Finite element result | Difference from finite element result |
| 725 Hz                                 | 725 Hz                | 0.3 %                                 |

In addition to natural frequency values, response acceleration values are also important. Therefore  $g_{rms}$  values of the responses are compared. It is observed from the graphs that the analytical model solution is in good agreement with the finite element solution up to the natural frequency. At higher frequencies, the acceleration PSD obtained by analytical model deviates from finite element solution which results in difference between  $g_{rms}$  values. The comparison of  $g_{rms}$  values is given in Table 38.

Table 38. Acceleration PSD comparison between analytical and finite element solution

|                                 | Difference from finite element result |
|---------------------------------|---------------------------------------|
| PCB with Fixed Edges            | 27 %                                  |
| PCB with Simply Supported Edges | 29 %                                  |

As a summary, it can be said that the natural frequencies obtained from the analytical model suggested in this thesis are very accurate compared to the finite element analysis results. Furthermore, response to random input can be obtained quite accurately until and at resonance, but the agreement between two solutions is not so good at higher frequencies. Therefore, the  $g_{rms}$  values are obtained from the analytical model deviate from those of the finite element model as much as 29%. Considering the very simple nature of the analytical model, it can be concluded that the analytical model can successfully be used in preliminary vibration analysis of PCBs.

## CHAPTER 6

### SUMMARY AND CONCLUSIONS

In this thesis, vibration analyses of electronic devices are performed considering military environmental conditions. First of all finite element modeling and an experimental study are performed in order to understand the vibratory behavior of a selected electronic system. Then, an analytical model for a rectangular printed circuit board with simply supported and fixed edges is developed. Furthermore, analytical models for specific types of electronic components, which are connected to PCB by lead wires are suggested. These models can be used in natural frequency calculations of PCBs and electronic components, as well as in response predictions to random input.

#### 6.1 Finite Element Modeling

An electronic assembly composed of electronic box, printed circuit board and components are modeled using reliable commercial finite element software, ANSYS<sup>®</sup>. Natural frequencies and mode shapes are obtained from these analyses.

Effect of design and mounting of the electronic box is investigated. Importance of box rigidity in terms of vibration transmission to the PCB is observed. The effects of cover in electronic box design are examined and the effect of cover mounting on the dynamics of the system is presented. It is observed that vibration of front cover may affect PCB indirectly by lead wires of the connector.

An important item in electronic devices is the connector. It is found in the analyses that connectors may act like elastic supports and cannot be treated as rigid connections. Therefore, boundary conditions on the connector mounted edges should be analyzed in detail in order to have a valid modeling.

One of the most important issues in finite element modeling of printed circuit boards is defining boundary conditions. The identification of PCB edge condition is very critical to have a reliable solution. Another important issue about PCB vibrations is component addition. Depending on vibration modes of a PCB, the location of component may affect the dynamics of the PCB. Especially, addition of large and heavy components may alter the dynamics, and therefore such cases should be analyzed in detail. Finite element solutions showed that attaching a component on a PCB decreases natural frequency and increases stiffness of the board in that region. Also, it is observed that small components may have very little effect on PCB dynamics depending on their location. Therefore, they can be ignored which results in simplification in modeling. Electronic component modeling can be performed in many different ways. In this study, three possible modeling approaches are used (i) lumped, (ii) merged and (iii) lead wired. Lead wire modeling is also important in finite element modeling of the electronic component. In this study, it is concluded that using solid elements in lead wire modeling is not necessary. Beam elements represent the lead wire structure accurately enough.

The finite element study of the vibratory behavior of the complete box and PCB assembly showed that the vibrations of the PCB are mainly due to its plate modes.

## **6.2 Experimental Study**

The electronic assembly analyzed with finite element modeling is also analyzed experimentally. Several experiments are carried out: First only the electronic box is

tested, then the box with addition of the front cover, top cover and then with the printed circuit board, in turn, are tested.

From experimental results of the box, it can be concluded that the base and the side walls of the box generally vibrate together, in the frequency range where fixture behavior is rigid. Therefore it can be said that the vibratory behavior of the box is almost rigid in this frequency range.

Experimental results of the PCB showed that vibratory behavior of the PCB is dominated by its plate modes. Transmissibility values of these modes are very large compared to box transmissibility values.

The study of the vibratory behavior of the complete box PCB assembly showed that the vibration of the PCB is mainly due to its plate modes, and the contribution of the transmissibility of the box and connections can be neglected compared to the transmissibility of the PCB itself.

Comparison of experimental results with finite element solutions revealed that finite element vibration analysis may not always give the vibratory behavior of a PCB mounted in a box accurately, as the system is rather complex and it may be difficult to model several connections precisely.

### **6.3 Analytical Model**

Finite element and experimental results showed that PCB vibrations are mainly due to its elastic plate modes. Transmissibility values of the plate at these modes are experimentally observed to be very high compared to box transmissibility values. Therefore, it may be possible to ignore the box dynamics in the study of the PCB vibration. In addition to that, the PCB considered has only one plate mode in the

frequency range of interest. Hence, a single degree of freedom model of the PCB can be obtained to represent the first plate mode.

Analytical model of the components showed that their natural frequencies are very high but in order to observe the relative motion between the PCB and component a two degree of freedom model is developed. From the two dof model solution, it is observed that in vibration analysis of the PCB with electronic component added, the component can be taken as a lumped mass if the PCB vibration is investigated.

The natural frequency results of the analytical model are found to be in good agreement with finite element vibration analysis results. Also, response to random vibration input can be obtained quite accurately by using the analytical model until the frequencies right after the resonance.

From these results it can be concluded that the analytical model can successfully be used in preliminary vibration analysis of PCBs. During preliminary design, mounting types and locations of PCBs can be determined by using this model. Also, component locations on the PCB can be arranged to obtain desired natural frequencies.

The most widely used analytical models for vibration analysis of PCBs are developed by Steinberg [13,17]. These models are based on empirical formulations. The reliability of these models is questionable. Although not presented in this thesis, it is observed in this study that these empirical results do not agree with experimental and FE results obtained. Furthermore, these models may not be applicable to today's complex electronic systems which are products of high technology materials. It is believed that the analytical model proposed in this thesis is a very good alternative to the empirical models of Steinberg.

## 6.4 Design Guidelines

The detailed analyses made in this study revealed several important features of PCB vibrations. Several results obtained in this study may be used to set some design rules.

Electronic box design is based on protection of internal components from environmental conditions. In case of vibration loading, the electronic box should provide structural integrity of the system.

Electronic box design has many important issues resulting from vibration loading such as mounting and isolation of the box, connector fixing to the box, attachment of PCB inside the box and cover mounting. Among these issues, connectors, covers and PCB are studied in this thesis and important results are obtained.

Although connectors seem to be rigidly fixed to PCB, analyses revealed that they act as elastic supports. Therefore assuming connector region fixed will probably lead to incorrect results. In order to avoid misleading results a detailed analysis should be performed and connector dynamics should be understood. If possible, elastic properties should be obtained and used in modeling; otherwise valid assumptions should be made.

Covers are inevitable parts of electronic boxes. Their dynamic properties are very important especially when a PCB or a connector is mounted to a cover. In box design, it is not preferred to mount PCB directly to the cover, instead they are indirectly connected if a connector is to be attached to a cover. Covers are plate like structures compared to the base of the box, and commonly mounted to the base with screws. Therefore, it is easier to excite covers compared to the base of the box. Having connector on such a cover may affect PCB dynamics. The worst case may occur if the natural frequencies of the cover where the connector is mounted and those of the printed circuit board coincide. Then the vibration amplitudes will be

higher which will result in higher stresses in the structure. Consequently, coincident natural frequencies should be avoided during the design.

Component addition on a PCB has a significant effect on the structural dynamics of the PCB. This effect will depend on component location on the board, component mass and size. Mounting type of a component on a PCB is also important. Therefore, extreme care is to be shown in component addition.

The most important result of this thesis is the analytical model developed for vibration analysis of PCBs and electronic components. The models suggested are very simple; however they will reduce the computational time and effort in preliminary design stage. By using this model, evaluations can be made on design alternatives based on vibration behavior of the PCB-component system. These design alternatives include different PCB geometries and materials, PCB mounting types and locations, component locations on the PCB, etc.

## **6.5 Suggestions for Future Research**

Experimental verification of the analytical model proposed in this thesis can be investigated further. Also, the suitability of the proposed model for analyzing relative vibration between PCB and component can be investigated. In addition to that, the proposed analytical model can be used in fatigue life prediction of PCBs and electronic components.

## REFERENCES

- [1] C. T. Robertson, Printed Circuit Board Designer's Reference: Basics, Prentice Hall, 2003
- [2] Linkwitz Lab Web Site, <http://www.linkwitzlab.com/Pluto/supplies.htm>, Last access date February 2008
- [3] DMS-Tech Web Site, <http://www.dms-tech.com/te/pcb>, Last access date February 2008
- [4] L. Marks, J. A. Caterina, Printed Circuit Board Assembly Design, Mcraw-Hill, 2000
- [5] AP Labs Web Site, [http://www.aplabs.com/atr\\_conduction.html](http://www.aplabs.com/atr_conduction.html), Last access date February 2008
- [6] Printing Web International, Inc. Web Site, [http://www.printweb.com.tw/P03\\_Chassis](http://www.printweb.com.tw/P03_Chassis), Last access date February 2008
- [7] Series 225 “Card-Lok” Retainer Data Sheet, Calmark Corp.
- [8] Southco<sup>®</sup> NY Standoff Quarter-Turn Data Sheet, Southco<sup>®</sup> Company
- [9] Gelmec Web Site, <http://www.gelmec.co.uk/GelmecBroadTemperatureGrommet>, Last access date February 2008

- [10] Gelmec Web Site, <http://www.gelmec.co.uk/GelmecPCBMountingElements> Page, Last access date February 2008
- [11] Parvus Corp. Web Site, <http://www.parvus.com/products/>, Last access date February 2008
- [12] Elma-Mektron Web Site, <http://www.elma-mektron.co.uk/product>, Last access date February 2008
- [13] D. S. Steinberg., Preventing Thermal Cycling and Vibration Failures in Electronic Equipment, John Wiley & Sons, Inc.2001
- [14] Workshop on Reliability, Center for Microelectronics Assembly and Packaging, University of Toronto, 2001
- [15] Espec Technology Report No.17, Espect Corp., 2004
- [16] D.Barker, A. Dasgupta., B. Han, M. Osterman, CALCE Pb-free Solder Interconnect Reliability Modeling Activities, University of Maryland, 2005
- [17] D. S. Steinberg, Vibration Analysis for Electronic Equipment, John Wiley & Sons, Inc., 2000
- [18] McKeown, Mechanical Analysis of Electronic Packaging Systems, Marcel Dekker, Inc., 1999
- [19] A.M. Veprik, Vibration Protection of Critical Components of Electronic Equipment in Harsh Environmental Conditions, Journal of Sound and Vibration, 2003, v.259 (1), p.161-175
- [20] A.M. Veprik, V.I. Babitsky, Vibration protection of Sensitive Electronic Equipment from Harsh Harmonic Vibration

- [21] V.C. Ho, A.M. Veprik, V.I. Babitsky, Ruggedizing Printed Circuit Boards Using a Wideband Dynamic Absorber, *Shock and Vibration* 10 (2003) 195-210
- [22] Jung, Park, Seo, Han, Kim, Structural Vibration Analysis of Electronic Equipment for Satellite under Launch Environment, *Key Engineering Materials* Vols. 270-273 (2004) pp.1440-1445
- [23] B Esser, D. Huston, Active Mass Damping of Electronic Circuit Boards, *Journal of Sound and Vibration*.
- [24] M.A. Zampino, Vibration Analysis of an Electronic Enclosure Using Finite Element Method
- [25] A. O. Cifuentes, A. Kalbag, Dynamic Behavior of Printed Wiring Boards: Increasing Board Stiffness by Optimizing Support Locations, *IEEE*, 1993
- [26] A. O. Cifuentes, Estimating the Dynamic Behavior of Printed Circuit Boards, *IEEE Transactions on Components, Packaging, and Manufacturing Technology-Part B: Advanced Packaging*, Vol.17, No.1, 1994
- [27] J. M. Pitarresi, Modeling of Printed Circuit Cards Subject to Vibration, *IEEE Proceedings of the Circuits and Systems Conference*, New Orleans, LA, May 3-5, 1990, pp. 2104-2107
- [28] G. S. Aglietti, C. Schwingshackl, Analysis of Enclosures and Anti Vibration Devices for Electronic Equipment for Space Applications, *Proceedings of the 6th International Conference on Dynamics and Control of Systems and Structures in Space 2004*.
- [29] M. XIE, D. Huang, T. Zhang, L. Lu, Dynamic Analysis of Circuit Boards in ANSYS, *Proceedings of the IEEE, International Conference on Mechatronics and Automation*, 2006

- [30] E. Suhir, Predicting Fundamental Vibration Frequency of a Heavy Electronic Component Mounted on a Printed Circuit Board, *Journal of Electronic Packaging*, 2000
- [31] L. Salvatore, D. Followell, Vibration Fatigue of Surface Mount Technology (SMT) Solder Joints, *Proceedings Annual Reliability and Maintainability Symposium*, 1995
- [32] A. Schaller, Finite Element Analysis of Microelectronic Systems – State of the art, *IEEE*, 1988
- [33] A. C Chiang, D. B. Barker, J. G. Krolewski, M. J. Cushing, Electronic Box-level Reliability Assessment Using Computer Modeling and Simulation, *Proceedings of Annual Reliability and Maintainability Symposium*, 1995
- [34] X. He, R. Fulton, Modeling and Simulation of the Dynamic Response of the Electronic Packaging, *Electronic Components and Technology Conference*, 2000
- [35] E. G. Veilleux, Vibration Control of Printed-Circuit Boards in a Dynamic Environment, *IEEE Transactions on Parts, Materials, and Packaging*, Vol. PMP-6, No. 3, 1970
- [36] J. H. Lau, C. A. Keely, Dynamic Characterization of Surface-Mount Component Leads for Solder Joint Inspection, *IEEE Transaction on Components, Hybrids, and Manufacturing Technology*, Vol. 12, No.4, 1989
- [37] S. J. Ham, S. B. Lee, Experimental Study for Reliability of Electronic Packaging under Vibration, *Journal of Experimental Mechanics*, Vol. 36, No. 4, 1996
- [38] A. Perkins, S. K. Sitaraman, Vibration-Induced Solder Joint Failure of a Ceramic Column Grid Array (CCGA) Package, *Electronic Components and Technology Conference, IEEE-CMPT and EIA*, 2004

- [39] Q. J. Yang, H. L. J. Pang, Z. P. Wang, G. H. Lim, F. F. Yap, R. M. Lin, Vibration Reliability Characterization of PBGA Assemblies, Microelectronics Reliability, Vol. 40, p. 1097-1107, 2000
- [40] C. Genç, Mechanical Fatigue and life Estimation Analysis of Printed Circuit Board Components, METU, 2006
- [41] TÜBİTAK-SAGE Web Site [http://www.sage.tubitak.gov.tr/altyapilar\\_titresimodaltest.asp](http://www.sage.tubitak.gov.tr/altyapilar_titresimodaltest.asp) , Last access date February 2008
- [42] R.D. Blevins, Formulas for Natural Frequency and Mode Shape, Krieger Publishing Company, 1995
- [43] R. Szilard, Theory and Analysis of Plates, Prentice Hall Inc., 1974
- [44] The Programmable Logic Data Book, Xilinx<sup>®</sup> Inc, 1996
- [45] MIL-STD-810F, “Environmental Engineering Considerations and Laboratory Tests”, Department of Defense Test Method Standard, USA, 2000.
- [46] D. E. Newland, Random Vibrations, Spectral and Wavelet Analysis, Longman, 1993